NASA Contractor Report 201674

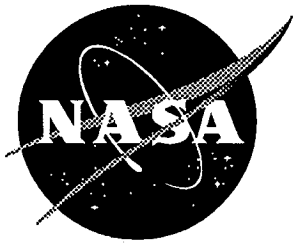

A Higher-Order Bending Theory for Laminated Composite and Sandwich Beams

Geoffrey M. Cook
George Washington University
Joint Institute for Advancement of Flight Sciences
Hampton, Virginia

Cooperative Agreement NCC1-208

March 1997

National Aeronautics and
Space Administration
Langley Research Center
Hampton, Virginia 23681-0001

Abstract

A higher-order bending theory is derived for laminated composite and sandwich beams. The recent {1,2}-order theory is extended to include higher-order axial effects without introducing additional kinematic variables. This is accomplished by assuming a special form for the axial and transverse displacement expansions. An independent expansion is also assumed for the transverse normal stress, improving the transverse strain and stress predictive capability of the theory. Appropriate shear correction factors based on energy considerations are used to adjust the shear stiffness, thereby improving the transverse displacement response. A set of transverse normal correction factors is introduced, leading to significant improvements in the transverse normal strain and stress for laminated composite and sandwich beams. A closed-form solution to the cylindrical bending problem is derived, demonstrating excellent correlation to the corresponding exact elasticity solutions for a wide range of beam aspect ratios and commonly used material systems. Accurate shear stresses for a wide range of laminates, including the challenging unsymmetric composite and sandwich laminates, are obtained using an original corrected integration scheme. For application of the theory to a wider range of problems, guidelines for finite element approximations are presented.

Table of Contents

List of Figures

List of Tables

Nomenclature

A	cross-sectional area of beam
A_{ij}	membrane beam rigidities
b	beam width
B_{ij}	membrane-bending coupling beam rigidities
$C_{ij}^{(k)}$	elastic stiffness coefficients for k^{th} ply
D_{ij}	bending beam rigidities
E_{ij}	Young's moduli
F_k	Heaviside unit function for k^{th} ply
G	shear rigidity
G_{ij}	shear moduli
$2h$	beam thickness
h_k , h_{k-1}	distances from midplane to bottom and top surfaces k^{th} of ply
k	shear correction factor
(k)	ply index for laminate
k_{z0}, k_{z1}	transverse correction factors
L	beam span
M	number of 0° plies in laminate
M_x, M_z, M_H	axial, transverse, and higher-order bending moment resultants
$\overline{M}_{i0}$, $\overline{M}_{iL}$	prescribed end moment resultants
N	number of plies in laminate
N_x, N_z, N_H	axial, transverse, and higher-order membrane force resultants
$\overline{N}_{x0}$, $\overline{N}_{xL}$	prescribed end force resultants
p_i, r_i, P_i, R_i	constants for transverse normal strain thickness distributions
q^+, q^-	normal pressure loads on the top and bottom surfaces of beam
Q_x	transverse shear force resultant
$\overline{Q}_{i0}$, $\overline{Q}_{iL}$	prescribed end shear force resultants
S^+, S^-	top and bottom surfaces of beam
$S_{ij}^{(k)}$	elastic compliance coefficients for k^{th} ply
t^k	thickness of k^{th} ply
T_{x0}, T_{xL}, T_{z0}, T_{zL}	arbitrary stress components prescribed at ends of beam

$[T_\sigma], [T_\varepsilon]$	stress and strain transformation matrices
u	midplane displacement along x-axis
u_x, u_z	axial and transverse displacement components
u_0, u_1, u_2, u_3	coefficients for axial displacement expansion
U_{shear}	shear strain energy per unit length
w, w_1, w_2	transverse displacement components
α	tracer for shear stress error correction
β	orientation of principle material axis within each ply
δ	variational operator
ε_{xx}	axial strain
ε_{zz}	transverse normal strain
$\varepsilon_{x0}, \varepsilon_{z0}, \varepsilon_H$	axial, transverse, and higher-order strain measures
ϕ_i	through the thickness distribution functions
γ	shear angle
γ_{xz}	transverse shear strain
γ_{xz0}	shear strain measure
$\kappa_{x0}, \kappa_{z0}, \kappa_H$	axial, transverse, and higher-order curvatures
ν_{ij}	Poisson ratios
θ	rotation of normal about y-axis
σ_{xx}	axial stress
σ_{zz}	transverse normal stress
σ_{zn}	coefficients for transverse normal stress expansion
τ_{xz}	transverse shear stress
τ_k	shear stress error function for k^{th} ply
$\psi_i^{(k)}$	transverse normal strain thickness distributions for k^{th} ply
ζ	dimensionsless thickness coordinate

1. Introduction

The high performance aircraft and spacecraft currently being considered for the next generation of aerospace vehicles require the use of strong yet lightweight materials. Laminated composites, such as graphite fiber reinforced epoxy, are commonly used for spacecraft and aircraft where weight is critical. While composite laminates provide higher stiffness, strength, and reduce weight over conventional metallic structures, sandwich structures can further reduce the structural weight and improve thermal performance without sacrificing stiffness and strength. A sandwich structure typically consists of two laminated composite or metallic face sheets with a core of foam, metallic honeycomb, or other lightweight material. The face sheets provide axial stiffness while the core acts as a shear web to carry the transverse shear load. Core materials are typically lighter and several orders of magnitude more compliant than the face sheet materials. This presents an analytical challenge with respect to the prediction of strain and stress distributions through the thickness. The knowledge of accurate, detailed strains and stresses is critical to the design of lightweight aerospace structures. Without accurate strain and stress predictions, higher factors of safety are often used, thereby increasing the weight and cost while reducing performance.

Numerous bending theories to analyze the response of beam, plate, and shell structures have been proposed. Many of the significant developments in elastic theory are summarized in review papers by Reissner (1985), Reddy (1989), and Noor and Burton (1989). The following discussion reviews the most pertinent developments in beam theory, and also makes comparisons to similar plate and shell theories.

Classical Bernoulli-Euler beam theory is the earliest and simplest approximation used for analysis of homogeneous beams. It dates back to 1705 and precedes the theory of elasticity by over 100 years (Love,1952). In the classical bending theory of beams, the beam cross section is assumed to be much smaller than the length of the beam and the displacements are small compared to the thickness of the beam. The transverse normal

and shear strains are assumed to be negligible. As a result, the cross section to the midplane is assumed to maintain a constant thickness and remain straight and normal to the midplane after deformation. While this approximation is appropriate for thin, homogenous beams, neglecting transverse shear deformation causes the deflection of the beam to be underpredicted for thick beams. To remedy this deficiency, several theories have been developed which account for transverse shear deformation.

The first beam theory to include transverse shear deformation was proposed by Timoshenko (1921). The cross section is no longer restricted to remain normal to the midplane. The cross section is assumed to remain plane as in classical theory, but transverse shearing is permitted to occur. By accounting for shear deformation, the theory provides more accurate response predictions for thin and moderately thick homogeneous beams. Reissner (1945) and Mindlin (1951) later extended Timoshenko theory, also known as first-order shear deformation theory, to the analysis of homogeneous elastic plates. Since then, numerous displacement-based, stress-based, and mixed formulation bending theories have been developed, with more recent emphasis on the analysis of laminated composite and sandwich structures.

Although classical and Timoshenko beam theories were originally developed for homogenous beams, they can also be extended to the analysis of heterogeneous beams. This is accomplished by modeling the laminate using either (1) a layer-wise theory or (2) a single layer theory. Both theories assume the laminate to be an assembly of homogeneous, anisotropic plies perfectly bonded at the ply interfaces. For layer-wise theories, the displacement components are assumed to be piece-wise smooth through the thickness. This implies that the function is continuous through the thickness of the beam, but at the ply interfaces, the slope of the function may not be continuous. These theories are especially useful for the analysis of moderately thick to thick laminates with span to thickness ratios ranging from 10 to 4. In single layer theories, the laminate is treated as an equivalent single layer, where the displacement assumptions represent some weighted average distribution through the thickness. Although layer-wise theories are capable of

accurate modeling of laminated composites and sandwiches, the number of independent variables is directly proportional to the number of plies in the laminate. Solutions to these equations can become computationally expensive and intractable as the number of layers in the laminate increases (Reddy and Liu,1987). The single layer theories are found to be the most computationally efficient and will provide the background for the present higher-order theory.

For single layer, displacement-based theories, the displacement approximations are assumed to take on a particular polynomial form through the laminate thickness. Each term in the expansion adds an additional power of the thickness coordinate, while the expansion coefficients are functions of the x coordinate only. These approximations are the basis for the development of the strain and stress quantities, and hence will govern the complexity and accuracy of the theory. The axial displacements are expanded with a polynomial of degree, m, while the transverse displacement may be of a different degree, n. Thus, the notation {m,n} may be used to distinguish between the different order single layer theories (Tessler and Saether,1991).

One of the most commonly used approximations for single layer displacement-based theories is {1,0}(or first-order) shear deformation theory, i.e., having a linear axial displacement and a constant transverse displacement. With the advent of advanced composite materials, there has been a great deal of work in the development of plate theories which extend the Timoshenko beam theory and Reissner-Mindlin plate theory to the analysis of laminated, heterogeneous structures. Stavsky (1959) is apparently the first to develop such a theory, and improvements upon this theory have been made by Yang, *et al.* (1966) and Whitney and Pagano (1970). Even with modifications to the theory, the detailed stress distributions show little improvement over the classical theory for moderately thick heterogeneous beams. Although the transverse shear stresses are included in these theories, the transverse normal stresses are neglected. Both transverse shear and transverse normal stresses become significant for moderately thick to thick laminated composite and sandwich beams. They often contribute to delaminations of the

plies and subsequent structural failure. Thick composites and sandwiches generally exhibit nonlinear displacement and strain distributions through the thickness which cannot be predicted using linear displacement assumptions. Because of the inadequacies of the first-order shear deformation theories, higher-order theories have been developed which attempt to predict more accurately the response of heterogeneous structures.

Higher-order theories in this context refer to the class of theories, for either beams, plates, or shells, in which the polynomial expansions of the displacement field are of higher order than {1,0} approximations. While the {1,0} Timoshenko beam theory includes transverse shear deformation, the transverse normal strains are still assumed negligible. Essenburg (1975) proposed a {1,2}-order beam theory which includes transverse normal effects, and a similar plate theory has been proposed by Whitney and Sun (1974). Lo, *et al.* (1977) developed a {3,2} laminated plate theory which produces adequate predictions for inplane displacement and stress distributions. The theory has a higher degree of complexity having eleven kinematic variables, and its predictive capability for the transverse normal and shear stresses is rather poor.

As a compromise between accuracy and computational efficiency, Reddy (1984) developed a {3,0}-order theory. By taking a special form for the inplane displacement components, the theory contains the same number of kinematic variables as the first-order shear deformation theory. This special displacement form also results in the parabolic distribution of the shear strain through the thickness. The shear stresses satisfy the traction-free boundary conditions on the surfaces of the plate, an important physical condition which previous theories did not enforce. Phan and Reddy (1985) investigated solutions to the aforementioned theory, showing improvements over classical theory.

Tessler and coworkers (1991-1995) developed a {1,2}-order theory for beam, plate, and shell analyses. The theory assumes a special form for the transverse displacement to obtain the 'average', parabolic shear strain distribution and shear traction free surface conditions. The theory is novel in that the transverse strains are not directly derived from the strain-displacement relations. The transverse normal and shear strains are assumed as

independent polynomial expansions. They are required to be least squares compatible, through the laminate thickness, to the strains obtained directly from the strain-displacement relations. The resulting thickness distributions for the transverse stresses and strains show adequate correlation with results given by elasticity theory, an improvement over previous higher-order theories. Tessler (1993a) improved the theory further for application to composites by introducing an independent polynomial assumption for the transverse normal stress in place of the transverse normal strain. The improved theory results in a more accurate representation of transverse normal stresses and strains, and is further substantiated by solutions given by Schleicher (1994). The {1,2} theory retains the simplicity of the first-order shear deformation theory as far as the engineering boundary conditions are concerned. Furthermore, the theory gives rise to finite element formulations that are compatible with the first-order shear deformation elements.

Application of the {1,2} theory generally results in excellent predictions for thin and moderately thick homogeneous and laminated beams, but the theory has some deficiencies in modeling the response of sandwich beams. The linear axial displacement assumption cannot model the nonlinear thickness distributions of the axial displacement and strain. In thick laminates, this generally results in underestimation of the axial stress, typically the largest stress which governs the design of the structure. The other deficiency is the transverse normal stress violation of traction conditions on the top and bottom surfaces of sandwich beams.

The main objective of this report is to expand upon Tessler's {1,2} theory by proposing a higher-order theory of order {3,2} which includes nonlinear axial effects. The theory is expected to model accurately the nonlinear axial displacement and strain through the thickness of the beam, resulting in a more accurate axial stress prediction. A special form for the cubic axial displacement field is used such that no additional kinematic variables are introduced into the theory. This enables the present higher-order theory to retain the simplicity of the {1,2} theory while improving predictions of the axial response

of the beam. The transverse normal stress and transverse shear stress predictive capability will also be improved for sandwich beams.

In Section 2, the mathematical formulation of a higher-order theory is presented. The {3,2}-order displacement field is assumed. These displacement approximations account for the nonlinear variations of stress and strain quantities typically present in thick composite and sandwich structures. As in the {1,2}-order theory, a special form of the quadratic transverse displacement is assumed. An independent expansion is also assumed for the transverse normal stress, as in Tessler (1993a). However, the shear strain is computed directly from the strain-displacement relations. Because of the special form for the axial displacement assumption, the traction-free shear stress boundary conditions are satisfied exactly. The principle of virtual work is used to derive the equilibrium equations and boundary equations for the theory. The hierarchical form of the {3,2}-order displacement approximations permits a straightforward reduction to lower-order beam theories of Tessler and Timoshenko.

In Section 3, transverse shear and transverse normal correction factors are determined from the energy and traction equilibrium considerations. Furthermore, accurate piece-wise smooth shear stresses are determined by integrating the two-dimensional equilibrium equation of elasticity theory. A correction procedure is also developed to improve the accuracy of this approach for unsymmetric and sandwich laminates.

In Section 4, an analytic solution to the cylindrical bending problem is presented. Numerical results are presented for commonly used aerospace material systems. Comparisons are made to the {1,2} theory and three-dimensional elasticity solutions. In Section 5, guidelines for finite element formulation and implementation based on the {3,2} theory are presented. Finally, Section 6 presents conclusions and recommendations for future work.

2. Mathematical Formulation

This section discusses the derivation of a higher-order bending theory for heterogeneous beams. A displacement field of order {3,2} is assumed and the strains, stresses, equilibrium equations, and boundary conditions are derived.

2.1 Higher-Order Theory for Laminated Beams

Consider a straight, linearly elastic beam laminated with N orthotropic plies subject to the loading shown in Figure 2.1. The beam has a span L and a rectangular cross-section of thickness 2h and width b. The orthotropic plies are stacked from the bottom face (z=-h) such that the material properties, in general, are functions of the z coordinate. The loadings q^+ and q^- are stresses applied normal to the top and bottom faces of the beam and may vary in the x coordinate. T_{i0} and T_{iL} (i=x,z) are arbitrary stress components prescribed at the ends of the beam.

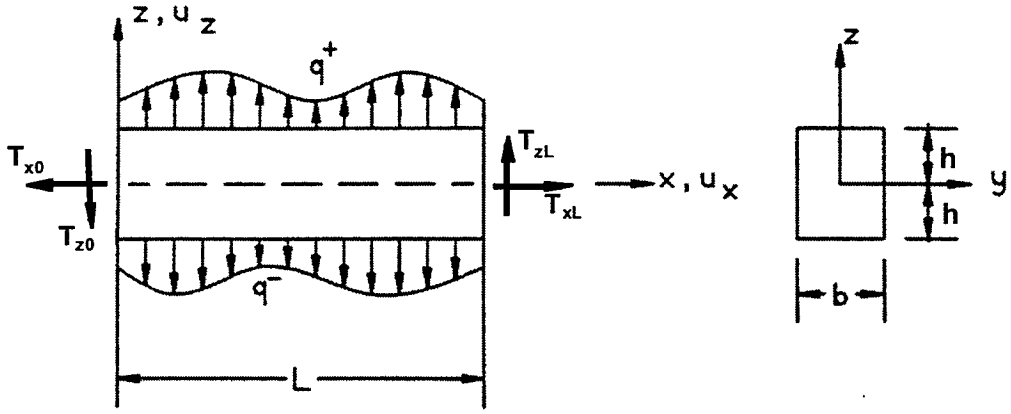

Figure 2.1 Sign Convention for Beam

2.1.1 Kinematic Displacement Assumptions

The first step in developing a displacement-based theory is to introduce kinematic assumptions for the displacements. These assumptions are made by first choosing a polynomial form for the displacement components. For thick laminated composite and sandwich beams, the displacement components are piece-wise smooth and nonlinear through the thickness. This contrasts with the predominantly linear displacement distributions for thin beams. To capture these higher-order deformation effects, a cubic polynomial is assumed for the axial displacement u_x and a quadratic distribution is assumed for the transverse displacement u_z, i.e.

$$\begin{aligned} u_x(x,z) &= u_0(x) + u_1(x)\zeta + u_2(x)\zeta^2 + u_3(x)\zeta^3 \\ u_z(x,z) &= w(x) + w_1(x)\zeta + w_2(x)\left(\zeta^2 + C\right) \end{aligned} \tag{2.1}$$

where $\zeta = \frac{z}{h} \in [-1,1]$ is the dimensionless thickness coordinate such that $\zeta = 0$ defines the midplane of the beam. The four u_i coefficients in the axial displacement expression are independent unknowns to be determined. The w_i coefficients in the transverse displacement are kinematic variables identical to those defined by Tessler (1991). The constant C is included in the transverse displacement equation to allow w(x) to represent a weighted average transverse displacement.

Three conventional kinematic variables are introduced and defined, as in Reissner (1945), as weighted average quantities through the thickness, such that

$$u(x) = \frac{1}{2h}\int_{-h}^{h} u_x(x,z)\, dz$$

$$\theta(x) = \frac{3}{2h^3}\int_{-h}^{h} u_x(x,z)\, z\, dz \qquad (2.2)$$

$$w(x) = \frac{3}{4h}\int_{-h}^{h} u_z(x,z)\,(1-\zeta^2)\, dz$$

where $u(x)$ is the midplane displacement along the x axis, $\theta(x)$ is the rotation of the normal about the y axis, and $w(x)$ is the weighted average of the transverse displacement. To determine the constant C which satisfies the weighted average displacement distribution through the thickness, the transverse displacement expansion from (2.1) is substituted into the expression for w(x) in equation (2.2) to yield

$$w(x) = \frac{3}{4h}\int_{-h}^{h}\left[w(x) + w_1(x)\,\zeta + w_2(x)\left(\zeta^2 + C\right)\right](1-\zeta^2)\, dz \qquad (2.3)$$

from which C is found to be equal to $-\frac{1}{5}$. Similarly, the expressions for $u(x)$ and $\theta(x)$ from (2.2) are used to determine two of the four coefficients for the axial displacement distribution:

$$u(x) = \frac{1}{2h}\int_{-h}^{h}\left[u_0(x) + u_1(x)\zeta + u_2(x)\zeta^2 + u_3(x)\zeta^3\right]dz$$

$$\theta(x) = \frac{3}{2h^3}\int_{-h}^{h}\left[u_0(x) + u_1(x)\zeta + u_2(x)\zeta^2 + u_3(x)\zeta^3\right]z\, dz \qquad (2.4)$$

From the above equations, the coefficients u_2 and u_3 are calculated to be

$$u_2(x) = 3\left(u(x) - u_0(x)\right), \qquad u_3(x) = \frac{5}{3}\left(h\,\theta(x) - u_1(x)\right) \qquad (2.5)$$

The remaining coefficients are determined by using the condition that the shear stress at the top and bottom faces of the beam must vanish, i.e. $\tau_{xz}(x,z=\pm h)=0$. Because of the direct relationship between stress and strain in beam theory, $\tau_{xz} = C_{55}\gamma_{xz}$, the shear strains at the top and bottom faces must also vanish:

$$\gamma_{xz}(x,\ z=\pm h)=0 \tag{2.6}$$

Using the strain-displacement relation for the transverse shear strain, $\gamma_{xz} = u_{x,z} + u_{z,x}$, and equation (2.5) yields

$$\begin{aligned}\gamma_{xz}(x,z) \ = \ & w(x)+\frac{u_1(x)+w_1(x)\,z}{h}+\frac{6\left(u(x)-u_0(x)\right)z}{h^2} \\ & +\frac{5\left(h\,\theta(x)-u_1(x)\right)z^2}{h^3}+w_2(x)\left(\frac{z^2}{h^2}-\frac{1}{5}\right)\end{aligned} \tag{2.7}$$

where a comma (,) denotes partial differentiation. After enforcing the two boundary conditions from (2.6), the coefficients u_0 and u_1 are found to be

$$u_0(x) = u(x)+\frac{h\,w_1(x)_{,x}}{6}, \qquad u_1(x) = \frac{h\left(25\,\theta(x)+5\,w(x)_{,x}+4\,w_2(x)_{,x}\right)}{20} \tag{2.8}$$

Substitution of the coefficients u_0, u_1, u_2, u_3, and the constant C into equation (2.1) yields the final form of the displacement components:

$$\begin{aligned}u_x(x,z) &= u+h\zeta\theta-\tfrac{1}{6}\left(3\zeta^2-1\right)h\,w_{1,x}-h\zeta\left(\tfrac{1}{3}\zeta^2-\tfrac{1}{5}\right)\gamma \\ u_z(x,z) &= w+\zeta\,w_1+\left(\zeta^2-\tfrac{1}{5}\right)w_2\end{aligned} \tag{2.9}$$

with the shear angle γ defined as

$$\gamma(x) = \tfrac{5}{4}\left[\theta(x) + w_{,x}(x)\right] + w_{2,x}(x) \tag{2.10}$$

The kinematic variables u, θ, w, w_1, and w_2 are functions of the x coordinate only. Note that although the displacement assumptions in (2.1) contain seven independent variables, the resulting displacements given in (2.9) are in terms of only five kinematic variables, which are identical to those given in {1,2}-order theory proposed by Tessler (1991). The terms $u(x)$, $\theta(x)$, and $w(x)$ are the conventional Reissner variables defined as weighted averages in equation (2.2). The higher-order terms for the transverse displacement, $w_1(x)$ and $w_2(x)$, account for the extension of the beam through the thickness.

The quadratic transverse displacement component u_z is identical to that of Tessler (1991). The cubic axial displacement u_x has an hierarchical form such that if the higher-order terms $w_{1,x}$ and γ are eliminated, the displacement field is reduced to the {1,2}-order theory with a linear axial displacement distribution. The further reduction of this theory to lower-order theories will be discussed in Section 2.2.

The displacements given in (2.9) are the two-dimensional form of the {3,2}-order plate displacement field proposed by Tessler (1993b). Tessler did not formulate a {3,2}-order theory but proposed the use of these displacements for a hierarchical recovery of the {1,2} results using {3,2}-order displacement, strain, and stress approximations. This concept will be discussed in Section 6 as a future application of this theory.

2.1.2 Reduced Stress-Strain Relations

Two sets of reduced constitutive relations have been developed for a beam with arbitrary material orientations: one for plane strain and the other for plane stress. For the development of the theory, the following notation will be utilized so that the theory is independent of the two-dimensional approximation employed:

$$\overline{C}_{ij}^{(k)} = \begin{cases} \hat{C}_{ij}^{(k)} & \text{for plane strain} \\ \\ \tilde{C}_{ij}^{(k)} & \text{for plane stress} \end{cases} \tag{2.11}$$

with the stress-strain relations expressed in the more general form

$$\begin{Bmatrix} \sigma_{xx} \\ \sigma_{zz} \\ \tau_{xz} \end{Bmatrix}_g^{(k)} = \begin{bmatrix} \overline{C}_{11} & \overline{C}_{13} & 0 \\ \overline{C}_{13} & \overline{C}_{33} & 0 \\ 0 & 0 & \overline{C}_{55} \end{bmatrix}_g^{(k)} \begin{Bmatrix} \varepsilon_{xx} \\ \varepsilon_{zz} \\ \gamma_{xz} \end{Bmatrix}_g^{(k)} \tag{2.12}$$

A complete derivation of the constitutive relations can be found in Appendix D.

2.1.3 Strain-Displacement Relations

Two methods are used to determine the strain-displacement relations for the beam. The axial strain ε_{xx} and transverse shear strain γ_{xz} are found in the usual fashion from the strain-displacement relations of elasticity theory. The derivation of the transverse normal strain departs from the conventional method. The transverse normal strain ε_{zz} is found by assuming a cubic stress field through the thickness for the transverse normal stress σ_{zz}, solving for the coefficients, and using the constitutive relations to obtain ε_{zz}. The strain-displacement expressions are summarized here along with the of the derivation of the transverse normal strain.

The axial strain is obtained from the strain-displacement relations of linear elasticity, i.e.,

$$\varepsilon_{xx} = u_{x,x} = \varepsilon_{x0} + \kappa_{x0}\,\phi_1 + \varepsilon_H\,\phi_2 + \kappa_H\,\phi_3 \tag{2.13}$$

where the strain measures and curvature variables, that are functions of the x coordinate, and the thickness distributions are defined as

$$\begin{aligned}
\left[\varepsilon_{x0},\ \varepsilon_H\right] &= \left[u_{,x},\ h\,w_{1,xx}\right] \\
\left[\kappa_{x0},\ \kappa_H\right] &= \left[\theta_{,x},\ \tfrac{5}{4}(w_{,xx} + \theta_{,x}) + w_{2,xx}\right] \\
\left[\phi_1, \phi_2, \phi_3\right] &= \left[h\zeta,\ \left(\tfrac{1}{6} - \tfrac{\zeta^2}{2}\right),\ h\left(\tfrac{\zeta}{5} - \tfrac{\zeta^3}{3}\right)\right]
\end{aligned} \tag{2.14}$$

The transverse shear strain is obtained from the linear strain-displacement relations of elasticity with the additional inclusion of a shear correction factor k:

$$\gamma_{xz}^{corr} = k\gamma_{xz} = k\left(u_{x,z} + u_{z,x}\right) = k\gamma_{xz0}\,\phi_{xz} \tag{2.15}$$

where

$$\left[\gamma_{xz0},\ \phi_{xz}\right] = \left[\theta + w_{,x},\ \tfrac{5}{4}\left(1 - \zeta^2\right)\right] \tag{2.16}$$

The shear correction factor is introduced here in anticipation of correction of the shear stiffness of the beam. The calculation of the shear correction factor is addressed in Section 3.

The transverse normal strain ε_{zz} is not determined directly from the strain-displacement relations. The strain-displacement relations give rise to ε_{zz} which is

continuous through the thickness, resulting in a discontinuous σ_{zz} through the thickness for heterogeneous beams. Analytically, the opposite is true: σ_{zz} is always continuous through the thickness and ε_{zz} is discontinuous. For most cases, σ_{zz} is closely approximated by a cubic polynomial. As in Tessler (1993), the transverse normal stress is assumed to have a cubic expansion through the thickness:

$$\sigma_{zz} = \sum_{n=0}^{3} \sigma_{zn} \zeta^n \tag{2.17}$$

which leaves four coefficients σ_{zn} to be determined. Two of the coefficients are found using the equilibrium equation of elasticity theory, i.e.,

$$\tau_{xz,x} + \sigma_{zz,z} = 0 \tag{2.18}$$

Since the transverse shear stress satisfies traction-free boundary conditions on the top and bottom surfaces of the beam, i.e. $\tau_{xz}(x,\pm h) = 0$, the derivatives of the shear stress $\tau_{xz,x}$ at the top and bottom faces must vanish. To satisfy the equilibrium equation, the derivatives of the transverse normal stress must also vanish on the top and bottom surfaces:

$$\sigma_{zz,z}(x,\pm h) = 0 \tag{2.19}$$

These boundary conditions reduce the transverse stress approximation to the form

$$\sigma_{zz} = \sigma_{z0} + \sigma_{z1} \phi_5 \tag{2.20}$$

where

$$\phi_5 = \left(\zeta - \zeta^3 / 3\right) \tag{2.21}$$

The remaining two coefficients are found by forcing the $\varepsilon_{zz}^{(k)}$ strain field to be least-squares compatible with the "corrected" strain derived from the strain-displacement relation:

$$\text{minimize} \int_{-h}^{h} \left(\varepsilon_{zz}^{(k)} - u_{z,z}^{corr}\right)^2 dz \tag{2.22}$$

with the "corrected" linear strain-displacement relation from elasticity theory given as

$$u_{z,z}^{corr} = k_{z0}\,\varepsilon_{z0} + 2\,k_{z1}\,\kappa_{z0}\,\phi_1 \tag{2.23}$$

where k_{z0} and k_{z1} are transverse correction factors. A method for obtaining these factors is presented in Section 3. The transverse strain measure and curvature in equation (2.23) are defined as

$$\left[\varepsilon_{z0}, \kappa_{z0}\right] = \left[w_1 / h,\ w_2 / h^2\right] \tag{2.24}$$

At this point, $\varepsilon_{zz}^{(k)}$ must be obtained from the constitutive relations, equation (2.12), and is found to be

$$\varepsilon_{zz}^{(k)} = 1 / \overline{C}_{33}^{(k)} \left(\sigma_{zz} - \overline{C}_{13}^{(k)}\,\varepsilon_{xx}\right) \tag{2.25}$$

The difference between the strains defined in equations (2.25) and (2.23) is expressed as

$$\Delta = \varepsilon_{zz}^{(k)} - u_{z,z}^{corr}$$
$$= \frac{\sigma_{z0} + \sigma_{z1}\,\phi_5 - \overline{C}_{13}^{(k)}\left(\varepsilon_{x0} + \kappa_{x0}\,\phi_1 + \varepsilon_H\,\phi_2 + \kappa_H\,\phi_3\right)}{\overline{C}_{33}^{(k)}} - \left(k_{z0}\,\varepsilon_{z0} + 2\,k_{z1}\,\kappa_{z0}\,\phi_1\right) \tag{2.26}$$

Minimizing $\int \Delta^2 dz$ with respect to the undetermined coefficients, σ_{z0} and σ_{z1}, results in the two equations:

$$Z_0 = \int_{-h}^{h} \Delta_{,\sigma_{z0}}\,\Delta\,dz = 0\ , \quad Z_1 = \int_{-h}^{h} \Delta_{,\sigma_{z1}}\,\Delta\,dz = 0 \tag{2.27}$$

To simplify the equations for Z_0 and Z_1, they are expressed in terms of p and r constants

$$\begin{aligned} Z_0 &= \varepsilon_{x0}\,p_1 + \varepsilon_{z0}\,p_2 + \varepsilon_H\,p_3 + \kappa_{x0}\,p_4 + \kappa_{z0}\,p_5 + \kappa_H\,p_6 + \sigma_{z0}\,p_7 + \sigma_{z1}\,p_8 = 0 \\ Z_1 &= \varepsilon_{x0}\,r_1 + \varepsilon_{z0}\,r_2 + \varepsilon_H\,r_3 + \kappa_{x0}\,r_4 + \kappa_{z0}\,r_5 + \kappa_H\,r_6 + \sigma_{z0}\,r_7 + \sigma_{z1}\,r_8 = 0 \end{aligned} \tag{2.28}$$

where the p_i and r_i constants are defined in Appendix A. Equations (2.28) are solved simultaneously for σ_{z0} and σ_{z1} with the results substituted into equation (2.20). Equation (2.25) is then simplified to yield the final expression for the transverse normal strain

$$\varepsilon_{zz}^{(k)} = \varepsilon_{x0}\psi_1^{(k)} + k_{z0}\,\varepsilon_{z0}\psi_2^{(k)} + \varepsilon_H\psi_3^{(k)} + \kappa_{x0}\psi_4^{(k)} + k_{z1}\,\kappa_{z0}\psi_5^{(k)} + \kappa_H\psi_6^{(k)} \tag{2.29}$$

where the thickness distributions $\psi_i^{(k)}$ are defined in Appendix A.

In contrast to the linear distribution of $u_{z,z}^{corr}$, equation (2.23), $\varepsilon_{zz}^{(k)}$ has the capability of being discontinuous at the ply interfaces and is piece-wise cubic through the thickness.

This form will significantly improve the transverse strain and stress distributions through the thickness of the beam.

2.1.4 Variational Principle

The principle of virtual work is used to derive the equilibrium equations and boundary conditions for the beam. These equations can then be solved to obtain the five kinematic displacement variables which satisfy the natural boundary conditions. Neglecting body forces, the two-dimensional variational statement is written as

$$\begin{aligned}
&\int_V \left(\sigma_{xx}^{(k)}\,\delta\varepsilon_{xx} + \sigma_{zz}\,\delta\varepsilon_{zz}^{(k)} + \tau_{xz}^{(k)}\,\delta\gamma_{xz}\right)dA\,dx \\
&\quad - \int_{S^+}\left(q^+\,\delta u_z(x,h)\right)dx\,dy + \int_{S^-}\left(q^-\,\delta u_z(x,-h)\right)dx\,dy \\
&\quad + \int_A\left[T_{x0}\,\delta u_x(0,z) + T_{z0}\,\delta u_z(0,z)\right]dA \\
&\quad - \int_A\left[T_{xL}\,\delta u_x(L,z) + T_{zL}\,\delta u_z(L,z)\right]dA = 0
\end{aligned} \tag{2.30}$$

where δ is the variational operator. A is the cross-sectional area of the beam and S^+ and S^- denote the top and bottom surfaces of the beam, which, respectively, are subject to the normal pressure loads q^+ and q^-. The first term is the volume integral representing the virtual work done by the stresses. The surface integrals denote the virtual work done by the external surface tractions.

The strain-displacement relations and the displacement assumptions are substituted into equation (2.30) to express the virtual work principle in terms of the strains and kinematic variables. After integrating through the thickness and grouping terms associated with each virtual displacement, the variational statement may be written in terms of force and moment resultants as

$$
\begin{aligned}
&\int_0^L \Big[N_x \delta\varepsilon_{x0} + N_z \delta\varepsilon_{z0} + N_H \delta\varepsilon_H + M_x \delta\kappa_{x0} + M_z \delta\kappa_{z0} + M_H \delta\kappa_H + Q_x \delta\gamma_{xz0} \\
&\quad - b\left(q^+ - q^-\right)\delta w - b\left(q^+ + q^-\right)\delta w_1 - b\tfrac{4}{5}\left(q^+ - q^-\right)\delta w_2 \Big] dx \\
&\quad + \overline{N}_{x0}\,\delta u(0) + \overline{M}_{x0}\,\delta\theta(0) + \overline{M}_{10}\,\delta w_{1,x}(0) + \overline{M}_{20}\,\delta\left\{\tfrac{5}{4}\left[\theta(0) + w_{,x}(0)\right] + w_{2,x}(0)\right\} \\
&\quad + \overline{Q}_{x0}\,\delta w(0) + \overline{Q}_{10}\,\delta w_1(0) + \overline{Q}_{20}\,\delta w_2(0) \\
&\quad - \overline{N}_{xL}\,\delta u(L) - \overline{M}_{xL}\,\delta\theta(L) - \overline{M}_{1L}\,\delta w_{1,x}(L) - \overline{M}_{2L}\,\delta\left\{\tfrac{5}{4}\left[\theta(L) + w_{,x}(L)\right] + w_{2,x}(L)\right\} \\
&\quad - \overline{Q}_{xL}\,\delta w(L) - \overline{Q}_{1L}\,\delta w_1(L) - \overline{Q}_{2L}\,\delta w_2(L) = 0
\end{aligned}
\tag{2.31}
$$

The beam stress resultants N, M, and Q along with the prescribed end force and moment resultants $\overline{N}$, $\overline{M}$, and $\overline{Q}$ are defined in Appendix B.

Since the strains and curvatures within the remaining integral are in terms of derivatives of the kinematic displacement variables, the stress resultants and virtual displacements are integrated by parts to yield

$$
\begin{aligned}
&\int_0^L \Big[\left(N_{x,x}\right)\delta u + \left(Q_x - M_{x,x} - \tfrac{5}{4}M_{H,x}\right)\delta\theta + \left(\tfrac{5}{4}M_{H,xx} - Q_{x,x} - \overline{q}_1\right)\delta w \\
&\quad + \left(N_z/h + hN_{H,xx} - \overline{q}_2\right)\delta w_1 + \left(M_z/h^2 + M_{H,xx} - \tfrac{4}{5}\overline{q}_1\right)\delta w_2 \Big] dx \\
&\quad + \left[\overline{N}_{x0} - N_x(0)\right]\delta u(0) + \left[\overline{M}_{x0} - M_x(0)\right]\delta\theta(0) + \left[\overline{M}_{10} - hN_H(0)\right]\delta w_{1,x}(0) \\
&\quad + \left[\overline{M}_{20} - M_H(0)\right]\delta\left\{\tfrac{5}{4}\left[\theta(0) + w_{,x}(0)\right] + w_{2,x}(0)\right\} \\
&\quad + \left[\overline{Q}_{x0} - Q_x(0)\right]\delta w(0) + \left[\overline{Q}_{10} - hN_{H,x}(0)\right]\delta w_1(0) + \left[\overline{Q}_{20} - M_{H,x}(0)\right]\delta w_2(0) \\
&\quad - \left[\overline{N}_{xL} - N_x(L)\right]\delta u(L) - \left[\overline{M}_{xL} - M_x(L)\right]\delta\theta(L) - \left[\overline{M}_{1L} - hN_H(L)\right]\delta w_{1,x}(L) \\
&\quad - \left[\overline{M}_{2L} - M_H(L)\right]\delta\left\{\tfrac{5}{4}\left[\theta(L) + w_{,x}(L)\right] + w_{2,x}(L)\right\} \\
&\quad - \left[\overline{Q}_{xL} - Q_x(L)\right]\delta w(L) - \left[\overline{Q}_{1L} - hN_{H,x}(L)\right]\delta w_1(L) - \left[\overline{Q}_{2L} - M_{H,x}(L)\right]\delta w_2(L) = 0
\end{aligned}
\tag{2.32}
$$

where $\overline{q}_1$ and $\overline{q}_2$ are defined as

$$
\overline{q}_1(x) = b\left[q^+(x) - q^-(x)\right], \qquad \overline{q}_2(x) = b\left[q^+(x) + q^-(x)\right] \tag{2.33}
$$

2.1.5 Equilibrium Equations and Boundary Conditions

Equilibrium equations and boundary conditions are obtained from the principle of virtual work, equation (2.32). The expressions associated with the arbitrary kinematic variations must vanish independently, resulting in the following equilibrium equations:

$$\begin{aligned}
&(\delta u): && N_{x,x} = 0 \\
&(\delta w_1): && N_z/h + hN_{H,xx} - \overline{q}_2 = 0 \\
&(\delta w): && \tfrac{5}{4}M_{H,xx} - Q_{x,x} - \overline{q}_1 = 0 \\
&(\delta \theta): && Q_x - M_{x,x} - \tfrac{5}{4}M_{H,x} = 0 \\
&(\delta w_2): && M_z/h^2 + M_{H,xx} - \tfrac{4}{5}\overline{q}_1 = 0
\end{aligned} \tag{2.34}$$

where the higher-order transverse equilibrium equations are associated with the δw_1 and δw_2 variations.

Similarly, the boundary conditions are determined by requiring that each term outside of the integral vanish independently. This is accomplished by either prescribing tractions or displacements at the ends of the beam, such that

@ x = 0:			**@ x = L:**		
$\overline{N}_{x0} = N_x(0)$	or	$\delta u(0) = 0$	$\overline{N}_{xL} = N_x(L)$	or	$\delta u(L) = 0$
$\overline{M}_{x0} = M_x(0)$	or	$\delta \theta(0) = 0$	$\overline{M}_{xL} = M_x(L)$	or	$\delta \theta(L) = 0$
$\overline{M}_{10} = hN_H(0)$	or	$\delta w_{1,x}(0) = 0$	$\overline{M}_{1L} = hN_H(L)$	or	$\delta w_{1,x}(L) = 0$
$\overline{M}_{20} = M_H(0)$	or	$\delta \gamma(0) = 0$	$\overline{M}_{2L} = M_H(L)$	or	$\delta \gamma(L) = 0$
$\overline{Q}_{x0} = Q_x(0)$	or	$\delta w(0) = 0$	$\overline{Q}_{xL} = Q_x(L)$	or	$\delta w(L) = 0$
$\overline{Q}_{10} = hN_{H,x}(0)$	or	$\delta w_1(0) = 0$	$\overline{Q}_{1L} = hN_{H,x}(L)$	or	$\delta w_1(L) = 0$
$\overline{Q}_{20} = M_{H,x}(0)$	or	$\delta w_2(0) = 0$	$\overline{Q}_{2L} = M_{H,x}(L)$	or	$\delta w_2(L) = 0$

(2.35)

2.1.6 Beam Constitutive Relations

The stress resultants which are defined in Appendix B, equation (B1), are expanded using the constitutive relations of equation (2.12) and the expressions for the strains: equations (2.13), (2.15), and (2.29). The terms are grouped according to their associated quantity and expressed in terms of the beam constitutive matrix:

$$\begin{Bmatrix} N_x \\ N_z \\ N_H \\ M_x \\ M_z \\ M_H \\ Q_x \end{Bmatrix} = \begin{bmatrix} A_{11} & k_{z0}A_{12} & A_{13} & B_{11} & k_{z1}B_{12} & B_{13} & 0 \\ k_{z0}A_{12} & k_{z0}^2A_{22} & k_{z0}A_{23} & k_{z0}B_{21} & k_{z0}k_{z1}B_{22} & k_{z0}B_{23} & 0 \\ A_{13} & k_{z0}A_{23} & A_{33} & B_{31} & k_{z1}B_{32} & B_{33} & 0 \\ B_{11} & k_{z0}B_{21} & B_{31} & D_{11} & k_{z1}D_{12} & D_{13} & 0 \\ k_{z1}B_{12} & k_{z1}k_{z0}B_{22} & k_{z1}B_{32} & k_{z1}D_{12} & k_{z1}^2D_{22} & k_{z1}D_{23} & 0 \\ B_{13} & k_{z0}B_{23} & B_{33} & D_{13} & k_{z1}D_{23} & D_{33} & 0 \\ 0 & 0 & 0 & 0 & 0 & 0 & k^2G \end{bmatrix} \begin{Bmatrix} \varepsilon_{x0} \\ \varepsilon_{z0} \\ \varepsilon_H \\ \kappa_{x0} \\ \kappa_{z0} \\ \kappa_H \\ \gamma_{xz0} \end{Bmatrix} \quad (2.36)$$

where A_{ij}, B_{ij}, D_{ij}, and G are the membrane, membrane-bending coupling, bending, and shear rigidities. These coefficients are defined in Appendix C. To complete the theory, the shear correction factor, k, and the transverse correction factors, k_{z0} and k_{z1}, need to be determined for each material system investigated. The procedure for determining these factors is discussed in Section 3, and their numerical values are presented in Section 4.

2.1.7 Equilibrium Equations in Terms of Displacements

To solve the beam equilibrium equations given in (2.34), the equations must be expressed in terms of the five basic kinematic variables. To accomplish this, the strain measures and curvatures must be expressed in terms of the kinematic variables of the theory, i.e.,

$$\begin{Bmatrix} \varepsilon_{x0} \\ \varepsilon_{z0} \\ \varepsilon_{H} \\ \kappa_{x0} \\ \kappa_{z0} \\ \kappa_{H} \\ \gamma_{xz0} \end{Bmatrix} = \begin{bmatrix} \frac{\partial}{\partial x} & 0 & 0 & 0 & 0 \\ 0 & \frac{1}{h} & 0 & 0 & 0 \\ 0 & h\frac{\partial^2}{\partial x^2} & 0 & 0 & 0 \\ 0 & 0 & 0 & \frac{\partial}{\partial x} & 0 \\ 0 & 0 & 0 & 0 & \frac{1}{h^2} \\ 0 & 0 & \frac{5}{4}\frac{\partial^2}{\partial x^2} & \frac{5}{4}\frac{\partial}{\partial x} & \frac{\partial^2}{\partial x^2} \\ 0 & 0 & \frac{\partial}{\partial x} & 1 & 0 \end{bmatrix} \begin{Bmatrix} u \\ w_1 \\ w \\ \theta \\ w_2 \end{Bmatrix} \tag{2.37}$$

Substituting the stress resultants from equation (2.36) and the strain measures and curvatures from (2.37) into equations (2.34), the equilibrium equations in terms of the kinematic variables are given as

$$(\delta u): \quad A_{11}u_{x,xx} + \frac{k_{z0}A_{12}}{h}w_{1,x} + hA_{13}w_{1,xxx} + B_{11}\theta_{,xx} + \frac{k_{z1}B_{12}}{h^2}w_{2,x} + B_{13}\left[\frac{5}{4}\left(\theta_{,xx} + w_{,xxx}\right) + w_{2,xxx}\right] = 0 \tag{2.38}$$

$$(\delta w_1): \quad h\left\{A_{13}u_{,xxx} + \frac{k_{z0}A_{23}}{h}w_{1,xx} + hA_{33}w_{1,4x} + B_{31}\theta_{,xxx} + \frac{k_{z1}B_{32}}{h^2}w_{2,xx} + B_{33}\left[\frac{5}{4}\left(\theta_{,xxx} + w_{,4x}\right) + w_{2,4x}\right]\right\} + \frac{1}{h}\left\{k_{z0}A_{12}u_{,x} + \frac{k_{z0}^2A_{22}}{h}w_1 + hk_{z0}A_{23}w_{1,xx} + k_{z0}B_{21}\theta_{,x} + \frac{k_{z0}k_{z1}B_{22}}{h^2}w_2 + k_{z0}B_{23}\left[\frac{5}{4}\left(\theta_{,x} + w_{,xx}\right) + w_{2,xx}\right]\right\} - \overline{q}_2 = 0 \tag{2.39}$$

$$(\delta w): \quad \frac{5}{4}\left\{B_{13}u_{,xxx} + \frac{k_{z0}B_{23}}{h}w_{1,xx} + hB_{33}w_{1,4x} + D_{13}\theta_{,xxx} + \frac{k_{z1}D_{23}}{h^2}w_{2,xx} + D_{33}\left[\frac{5}{4}\left(\theta_{,xxx} + w_{,4x}\right) + w_{2,4x}\right]\right\} - k^2G\left(\theta_{,x} + w_{,xx}\right) - \overline{q}_1 = 0 \tag{2.40}$$

$$
\begin{aligned}
(\delta\theta): \quad & B_{11}u_{,xx} + \frac{k_{z0}B_{21}}{h}w_{1,x} + hB_{31}w_{1,xxx} + D_{11}\theta_{,xx} + \frac{k_{z1}D_{12}}{h^2}w_{2,x} + \\
& D_{13}\left[\tfrac{5}{4}\left(\theta_{,xx} + w_{,xxx}\right) + w_{2,xxx}\right] + \tfrac{5}{4}\left\{B_{13}u_{,xx} + \frac{k_{z0}B_{23}}{h}w_{1,x} + \right. \\
& hB_{33}w_{1,xxx} + D_{13}\theta_{,xx} + \frac{k_{z1}D_{23}}{h^2}w_{2,x} + \\
& \left. D_{33}\left[\tfrac{5}{4}\left(\theta_{,xx} + w_{,xxx}\right) + w_{2,xxx}\right]\right\} - k^2 G\left(\theta + w_{,x}\right) = 0
\end{aligned}
\tag{2.41}
$$

$$
\begin{aligned}
(\delta w_2): \quad & B_{13}u_{,xxx} + \frac{k_{z0}B_{23}}{h}w_{1,xx} + hB_{33}w_{1,4x} + D_{13}\theta_{,xxx} + \frac{k_{z1}D_{23}}{h^2}w_{2,xx} + \\
& D_{33}\left[\tfrac{5}{4}\left(\theta_{,xxx} + w_{,4x}\right) + w_{2,4x}\right] + \frac{1}{h^2}\left\{k_{z1}B_{12}u_{,x} + \frac{k_{z1}k_{z0}B_{22}}{h}w_1 + \right. \\
& k_{z1}hB_{32}w_{1,xx} + k_{z1}D_{12}\theta_{,x} + \frac{k_{z1}k_{z0}D_{22}}{h^2}w_2 + \\
& \left. k_{z1}D_{23}\left[\tfrac{5}{4}\left(\theta_{,x} + w_{,xx}\right) + w_{2,xx}\right]\right\} - \tfrac{4}{5}\bar{q}_1 = 0
\end{aligned}
\tag{2.42}
$$

where $w_{,4x} = w_{,xxxx}$.

Equations (2.38) - (2.42), subject to the boundary conditions given in (2.35), can now be solved simultaneously to determine the five kinematic variables and subsequent displacement, strain, and stress distributions in the beam.

2.2 Reduction of Present Theory to Lower-Order Theories

The hierarchical structure of the present {3,2}order theory permits a straightforward reduction to several lower-order theories. By eliminating the higher-order displacement terms $w_{1,x}(x)$ and $\gamma(x)$ from equation (2.9), the displacement field reduces to the {1,2} form given by Tessler (1991):

$$u_x(x,z) = u + h\zeta\theta$$
$$u_z(x,z) = w + \zeta w_1 + \left(\zeta^2 - \tfrac{1}{5}\right)w_2 \qquad (2.43)$$

By reducing the axial displacement to a linear approximation, the higher-order strain and curvature terms, ε_H and κ_H, are eliminated from the theory. This results in the simplification of the equilibrium equations, boundary conditions, and stress resultants, given in equations (2.34), (2.35), and (2.36) respectively, such that all of the terms with a subscript $_H$ are eliminated. This feature will be utilized to compare the present {3,2} theory to the {1,2} results in Section 4.

The {1,2} displacement theory can be further reduced to Timoshenko theory by neglecting the coupling between the axial and transverse stretching of the beam and by enforcing the inextensibility of the beam's cross section. This is accomplished by setting $\nu_{13} = 0$ and $E_3 = \infty$. While this simplifies the equilibrium equations, the boundary conditions for Timoshenko theory are the same as in the {1,2} theory. The results of Timoshenko theory can be further reduced to those of classical beam theory by setting the transverse shear rigidity to be infinite, i.e., $G = \infty$.

3. Adjustments to Theory

3.1 Shear Correction Factors

The implementation of shear correction factors is a commonly used technique to correct the shear stiffness of an approximate theory. Timoshenko (1921) and Mindlin (1951) employed shear correction factors for the analysis of isotropic beams and plates, respectively. More recently, Whitney and Pagano (1970) and Reddy (1984) presented shear-deformable plate theories in which correction factors were applied to laminated

plate analysis. The aforementioned theories are based on kinematic approximations which tend to underestimate shear deformation, which results in an underestimation of the transverse displacement. The shear correction factors compensate, in a gross sense, for these deficiencies and bring the transverse displacement results closer to those expected from exact elasticity theory.

The shear correction factor concept is introduced in the present {3,2}-order theory to improve the response of laminated composite and sandwich beams. For the case of a homogenous beam, a shear correction factor is not needed due to the higher-order displacement approximations. The resulting parabolic shear stress field matches closely that obtained from elasticity theory. For laminated beams of arbitrary material layup, the shear distribution is only piece-wise smooth through the thickness. This implies that adjustment of the shear stiffness may be necessary and can be achieved with an appropriate value of a shear correction factor.

To determine the shear correction factor within the present theory, a straightforward energy matching method is employed. The approach is to match the transverse shear energy of the present theory with that of elasticity theory for a particular "benchmark" problem. Since it is reasonable to expect that in the thin limit, an approximate theory should produce correct shear stiffness, the matching is performed for very thin beams ($L/2h = 1000$). The cylindrical bending problem, for which an exact elasticity solution is available, serves as our "benchmark" problem (see Section 4). Vlachoutsis (1992) and others have shown that, for all practical purposes, these correction factors are independent of the loading and boundary conditions. The correction is therefore considered a function of the material system used in the analysis. This implies that once the correction factor is determined for a particular material system, it may be applied to any other analysis using that same system. Hence, it is sufficient to determine the shear correction factors from the cylindrical bending problem and the factors may be applied to other problems without loss of generality.

Factoring the shear correction factor from the {3,2} theory shear energy expression and equating it to the exact shear energy yields:

$$U_{shear}^{exact} = \frac{1}{k^2} U_{shear}^{uncorrected} \tag{3.1}$$

where $U_{shear}^{uncorrected}$ is the uncorrected shear strain energy of the present theory. Both $U_{So}^{uncorrected}$ and U_{shear}^{exact} are computed numerically. The parameter k is computed directly by computing the ratio of the shear strain energies. Note that the transverse correction factors k_{z0} and k_{z1} are also set to unity when calculating the shear correction factor as these factors are still unknown parameters.

It is noted that for laminated beams, the corresponding shear correction factors are dependent on the material properties and layup of the plies. For each material system, a new shear correction factor must be computed. In Section 4.4, shear correction factors are computed for several material systems and layups.

3.2 Transverse Correction Factors

Similar to the manner by which shear correction factors improve the gross transverse displacement response, the transverse correction factors are used to improve the thickness stretch response. Mindlin and Medick (1958) showed that with each thickness stretch mode, i.e. constant and linear, corresponding correction factors can be specified to improve the transverse normal response of plates. Tessler (1995) used transverse correction factors for problems pertaining to the vibration of elastic plates. These factors were used to rectify the neglect of inertial effects in the transverse normal equations.

While previous theories utilized correction factors to improve the dynamic response of plates, the present theory will extend the application of transverse normal correction factors to the static analysis of laminated beams. It was noted earlier that the {3,2}-order

theory without the use of transverse correction factors can yield up to 50 % error for the following transverse normal stress boundary conditions

$$\sigma_{zz}(x,+h) = q^{+}, \qquad \sigma_{zz}(x,-h) = q^{-} \tag{3.2}$$

These transverse normal stress boundary conditions are not explicitly enforced in the present theory. Because of this, the transverse stress distributions may deviate from the exact solution. For sandwiches with large variations in the elastic moduli through the thickness, these errors become even more pronounced. This error is illustrated in Figure 3.1 for a sandwich beam in cylindrical bending in which the core properties are more than three orders of magnitude softer than the face sheets. The uncorrected curve (i.e., without the use of transverse corrections) shows the large error in the transverse normal stress on the top surface.

Similar to the shear correction factors, the transverse correction factors are dependent on the material system, so a set of values for k_{z0} and k_{z1} must be found for each layup. To calculate the transverse correction factors, it is convenient to introduce an alternate form for the beam constitutive relations, equation (2.36), relating the force and moment resultants to the corresponding strain measures and curvatures, i.e.

$$\begin{Bmatrix} \mathbf{N} \\ \mathbf{M} \end{Bmatrix} = [k_z][E_0][k_z]\begin{Bmatrix} \varepsilon \\ \kappa \end{Bmatrix} \tag{3.3}$$

where

$$[E_0] = \begin{bmatrix} A_{11} & A_{12} & A_{13} & B_{11} & B_{12} & B_{13} \\ A_{12} & A_{22} & A_{23} & B_{21} & B_{22} & B_{23} \\ A_{13} & A_{23} & A_{33} & B_{31} & B_{32} & B_{33} \\ B_{11} & B_{21} & B_{31} & D_{11} & D_{12} & D_{13} \\ B_{12} & B_{22} & B_{32} & D_{12} & D_{22} & D_{23} \\ B_{13} & B_{23} & B_{33} & D_{13} & D_{23} & D_{33} \end{bmatrix}, \quad [k_z] = \begin{bmatrix} 1 & 0 & 0 & 0 & 0 & 0 \\ 0 & k_{z0} & 0 & 0 & 0 & 0 \\ 0 & 0 & 1 & 0 & 0 & 0 \\ 0 & 0 & 0 & 1 & 0 & 0 \\ 0 & 0 & 0 & 0 & k_{z1} & 0 \\ 0 & 0 & 0 & 0 & 0 & 1 \end{bmatrix},$$

$$\{N\}^T = \{N_x, N_z, N_H\}, \quad \{M\}^T = \{M_x, M_z, M_H\},$$

$$\{\varepsilon\}^T = \{\varepsilon_{x0}, \varepsilon_{z0}, \varepsilon_H\}, \quad \{\kappa\}^T = \{\kappa_{x0}, \kappa_{z0}, \kappa_H\}$$

The initial step is to obtain a solution for the case where $[k_z]$ is an identity matrix, i.e. $k_{z0} = k_{z1} = 1$. As before, the cylindrical bending problem is analyzed in the very thin regime (L/2h=1000), with the appropriate shear correction factor implemented. The stress resultants which are obtained from this analysis are defined as $\{N_0, M_0\}^T$. Substitution of these stress resultants into equation (3.3) and solving for the strain measures and curvatures gives rise to

$$\begin{Bmatrix} \varepsilon \\ \kappa \end{Bmatrix} = [k_z]^{-1}[E_0]^{-1}[k_z]^{-1} \begin{Bmatrix} N_0 \\ M_0 \end{Bmatrix} \tag{3.4}$$

such that the strain measures and curvatures are expressed in terms of the uncorrected computed quantities $[E_0]$, $\{N_0\}$, and $\{M_0\}$ and the undetermined corrections factors k_{z0} and k_{z1}. Substituting equation (3.4) into the expressions for the axial strain (2.13) and the transverse normal strain (2.29) and using the stress-strain relations (2.12), the transverse normal stress boundary conditions can now be enforced via the transverse correction factors, i.e.,

$$\begin{Bmatrix} \sigma_{zz}(x,+h) \\ \sigma_{zz}(x,-h) \end{Bmatrix} = \begin{bmatrix} \overline{C}_{13}^{+} & \overline{C}_{33}^{+} \\ \overline{C}_{13}^{-} & \overline{C}_{33}^{-} \end{bmatrix} \begin{Bmatrix} \varepsilon_{xx}(k_{z0}, k_{z1}) \\ \varepsilon_{zz}^{(k)}(k_{z0}, k_{z1}) \end{Bmatrix} = \begin{Bmatrix} q^+ \\ q^- \end{Bmatrix} \tag{3.5}$$

where the (+) and (-) superscripts denote the top and bottom surfaces of the beam, and the ε_{xx} and $\varepsilon_{zz}^{(k)}$ strains are now functions of k_{z0} and k_{z1}. Solving these equations

simultaneously for k_{z0} and k_{z1} results in the numerical values for the correction factors that fulfill correct traction boundary conditions. By satisfying equation (3.5), the distribution of the transverse normal stress through the thickness closely follows that of elasticity theory, with correct traction conditions enforced on the surfaces. Figure 3.1 illustrates this improvement for a sandwich beam in cylindrical bending subject to the normal tractions: $q^+ = 1.0$, $q^- = 0.0$ (refer to Section 4, Case D, L/2h = 100 for a detailed description of the problem).

This procedure is followed such that a set of correction factors is produced for each material system investigated. A table of transverse correction factors for the material systems examined in this report can be found in Section 4.4.

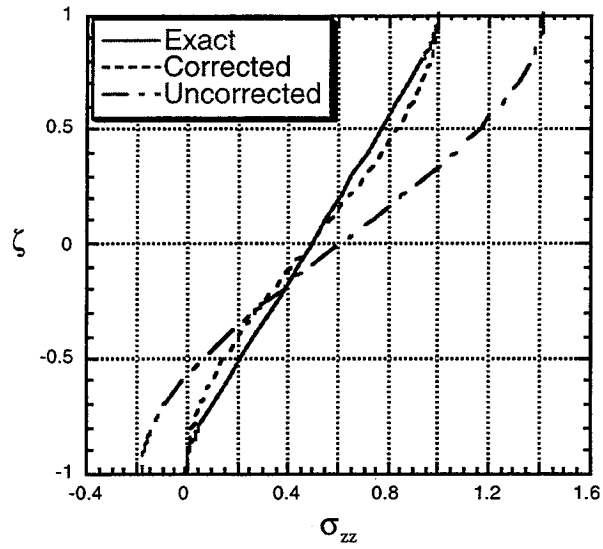

Figure 3.1 Transverse Correction for a Sandwich Beam

3.3 Integrated Interlaminar Shear Stress

The present theory approximates the transverse shear strain γ_{xz}, equation (2.15), as a continuous parabolic function through the thickness. This allows accurate modeling of shear strain and stress through the thickness for homogeneous beams. While the parabolic strain satisfies the traction-free boundary conditions, the actual shear strain distribution in

laminated beams is often discontinuous at the ply interfaces. The parabolic approximation for the shear strain yields erroneous shear stress, as demonstrated in Figure 3.2 for an unsymmetric cross-ply graphite/epoxy laminate (refer to Section 4, Case C, L/2h = 100). Here, the shear stress for the present higher-order theory (HOT) is obtained directly from Hooke's law using equation (2.12), resulting in a discontinuous shear stress distribution. For the exact solution, the opposite is true, i.e., the shear stress is continuous at the ply interfaces while the shear strain is discontinuous.

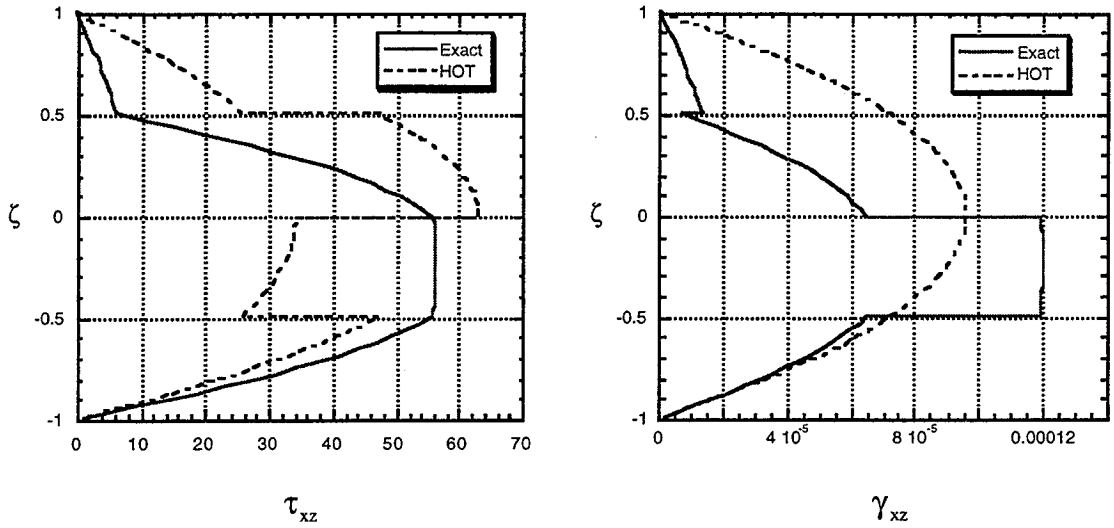

Figure 3.2 Comparison of Shear Stress and Strain for an Unsymmetric Laminate

To improve the transverse shear stress and strain predictions, the two-dimensional equilibrium equation of elasticity theory

$$\sigma^{(k)}_{xx,x} + \tau^{(k)}_{xz,z} = 0 \tag{3.6}$$

is integrated to recover the transverse shear stress. The axial normal stress is differentiated, then integrated piece-wise through the thickness, such that the resulting shear stress takes the form

$$\tau_{xz}^{(k)} = -\int_{-h}^{z} \sigma_{x,x}^{(k)} \, dz \tag{3.7}$$

The shear strain is then obtained directly from Hooke's law:

$$\gamma_{xz}^{(k)} = \tau_{xz}^{(k)} / \overline{C}_{55}^{(k)} \tag{3.8}$$

The above integration scheme is a well-established approach which generally produces adequate results (refer to Whitney (1972) and Reddy (1984)). However, for unsymmetric and sandwich laminates, the integration approach by itself yields rather inaccurate shear stresses. For such laminates, the integrated shear stresses do not satisfy the top boundary condition even though the shear stress on the bottom surface is explicitly set to zero for integration. The comparison of the integrated shear stress to that of the exact solution leads to the conclusion that error is accumulated as a result of the shear stress integration through the 0° plies. The axial stretching of the midplane, a characteristic of unsymmetric laminates and soft-core sandwiches, introduces an error in these plies. The "integrated" curve in Figure 3.3 represents the integrated shear stress according to equation (3.7). The results are for the same material system as in Figure 3.2.

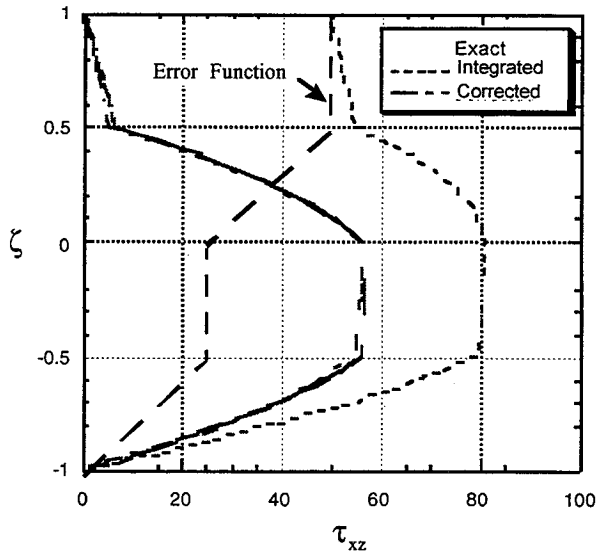

Figure 3.3 Integration Errors Caused by Stretching of the Midplane

For the unsymmetric and sandwich laminates examined, the integration errors are distributed linearly through the 0° plies, while in the 90° plies and the core material the error is constant. To correct for these errors, an automated procedure is developed in which the total error at the top of the beam is divided into equal increments based on the number of 0° plies. The error is subtracted from the integrated stress curve as linear functions through the 0° plies, and as a constant function through the 90° plies, as depicted in the "Error Function" curve in Figure 3.3. Using this modified integration scheme, the corrected shear stresses are computed as

$$\tau_{xz}^{corr} = \tau_{xz}^{(k)} - \tau_{xz}^{error} \tag{3.9}$$

where $\tau_{xz}^{(k)}$ is the integrated shear stress obtained using equation (3.7) and the error function is expressed analytically as

$$\tau_{xz}^{error} = \sum_{k=1}^{N} F_k(z)\, \tau_k(z) \tag{3.10}$$

where N is the total number of plies in the laminate and F_k is expressed in terms of Heaviside functions as

$$F_k(z) = H(z - h_{k-1}) - H(z - h_k) \tag{3.11}$$

The shear stress error function within the ply is defined as

$$\tau_k(z) = \tau_{k-1} + \alpha \frac{\tau_{error}^{+}}{M} \left(\frac{z - h_{k-1}}{h_k - h_{k-1}} \right) \tag{3.12}$$

where τ_{k-1} is the value of the error function at the bottom ply interface, and is initially set to zero ($\tau_0 = 0$) at the bottom surface of the laminate. τ_{error}^{+} is the magnitude of the error

at the top surface of the beam, M is equal to the number of 0° plies in the laminate, and α is a tracer which takes the form

$$\alpha = \begin{cases} 1, & \beta = 0° \\ 0, & \beta = 90° \text{ or core} \end{cases} \tag{3.13}$$

where β is the rotation angle of the ply, as per Figure 2.2. The thickness of the ply is defined as $t^k = h_k - h_{k-1}$, where h_k is the distance from the midplane to the top surface of the ply and h_{k-1} is the distance from the midplane to the bottom surface of the ply. The variables used in equation (3.12) are depicted in Figure 3.4 for an unsymmetric composite beam with the lamination sequence $[0/90/0/90]_T$.

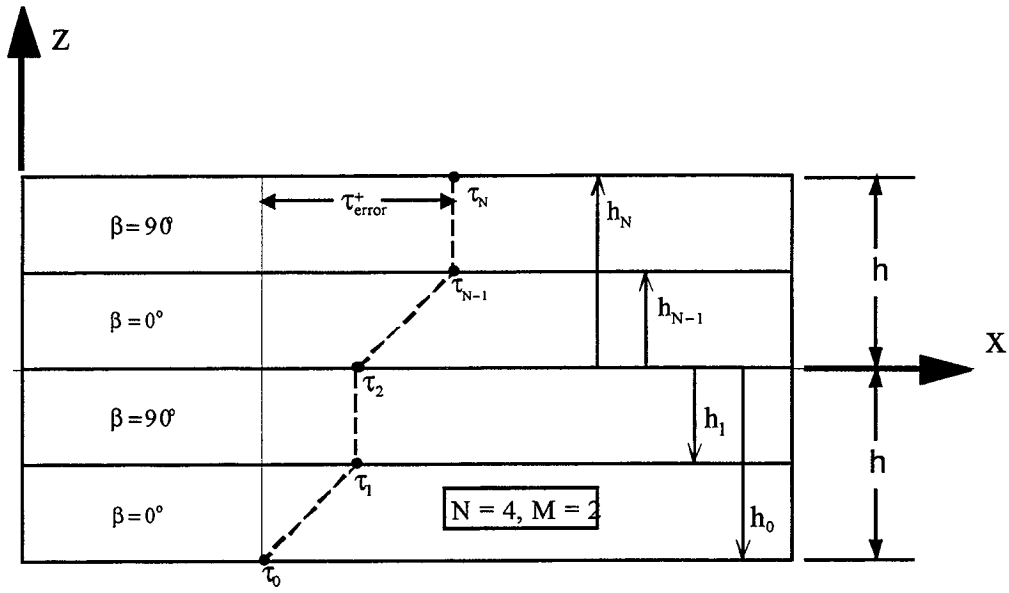

Figure 3.4 Error Function and Lamination Notation

As a result of this correction, the traction free boundary conditions are satisfied on the top and bottom surfaces, and the through the thickness distributions are in close agreement with the elasticity solution, as evident by the "corrected" curve in Figure 3.3.

Although not shown, the corrected shear strain is computed using equation (3.8), and excellent correlation to the exact solution is achieved. The shear stress distributions for the cases investigated in this report are in close agreement with corresponding elasticity solutions (refer to Section 4.5 for additional examples). Note that due to limitations in the exact solution, Burton and Noor (1994), only cross-ply laminates were considered for the cases investigated in this report. The present theory is capable of handling arbitrary angle-ply orientations, but the effect of these orientations on the integration scheme has not been investigated.

With the exception of the homogeneous case, equation (3.9) will be used for the recovery of the transverse shear stress for the results presented in Section 4. It should be noted that the modified stresses may not exactly satisfy the original beam equilibrium equations. Since the modified shear stresses yield significant improvements for thick laminates and sandwich beams, this constraint is relaxed in order to achieve a more meaningful recovery of the transverse shear quantities.

4. Cylindrical Bending Problem

4.1 Closed-Form Solution

To assess the capability of the {3,2}-order theory, a closed-form solution to the cylindrical bending problem is formulated and compared to the corresponding exact elasticity solution. Cylindrical bending is a special case of plate bending in which a sine load is applied to the top surface of the plate, as shown in Figure 4.1. The depth of the plate is infinite in the y-direction and the ends of the plate at $y = 0$ and $y = \infty$ are constrained by smooth, rigid planes such that a state of plane strain is achieved in the x-z plane. The plate is simply supported at the ends $x = 0$ and $x = L$ such that the resulting deformation is uniformly cylindrical in shape. Because each cross section in the x-z plane deforms identically, a beam theory in a state of plane strain may be used to determine solutions which are identical to those obtained from plate theory.

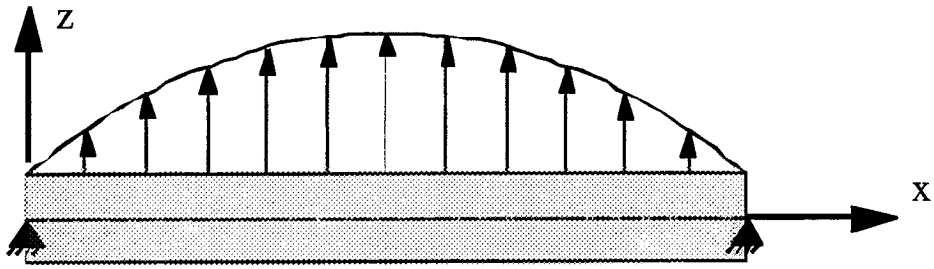

Figure 4.1 Cylindrical Bending Problem

Pagano (1969) first published elasticity solutions for unidirectional (0°) and bi-directional (0°-90°) composite laminates in cylindrical bending. Burton and Noor (1994) developed three-dimensional elasticity solutions for laminated and sandwich rectangular plates. As a special case, the Burton-Noor formulation yields an exact solution for the cylindrical bending problem. The exact Burton-Noor solutions are used for comparison in the present study.

For the cylindrical bending problem, the loadings on the top and bottom surfaces of the plate are defined as

$$q^{+}(x) = q_o \sin(\pi x / L)$$
$$q^{-}(x) = 0 \tag{4.1}$$

where q_o is the amplitude of the loading. For the solutions presented here, a unit amplitude will be considered. To solve the equilibrium equations derived for the present theory, equations (2.39) - (2.43), the kinematic displacement variables are assumed to have the form

$$u = U \cos(\pi x/L), \quad \theta = \Theta \cos(\pi x/L)$$
$$w = W \sin(\pi x/L), \quad w_1 = W_1 \sin(\pi x/L), \quad w_2 = W_2 \sin(\pi x/L) \tag{4.2}$$

The nature of these assumptions is such that the boundary conditions at the ends of the beam, equation (2.36), are all satisfied and take the form

@ x = 0:	**@ x = L:**
$\overline{N}_{x0} = N_x(0)$	$\overline{N}_{xL} = N_x(L)$
$\overline{M}_{x0} = M_x(0)$	$\overline{M}_{xL} = M_x(L)$
$\overline{M}_{10} = N_H(0)$	$\overline{M}_{1L} = N_H(L)$
$\overline{M}_{20} = M_H(0)$	$\overline{M}_{2L} = M_H(L)$
$\delta w(0) = 0$	$\delta w(L) = 0$
$\delta w_1(0) = 0$	$\delta w_1(L) = 0$
$\delta w_2(0) = 0$	$\delta w_2(L) = 0$

(4.3)

Using the displacement assumptions in (4.2), the equilibrium equations are simplified such that the trigonometric functions factor out in each equation, leaving only the

amplitudes U, Θ, W, W_1, and W_2, as unknowns. Once the displacement amplitudes are determined, the kinematic variables are completely defined, giving rise to the strain measures and curvatures. The strains, stresses, and displacements are then calculated and plotted through the thickness for comparison to the elasticity solution.

4.2 Material Properties

An extended range of commonly used aerospace material systems will be investigated. These include a homogeneous case, such as aluminum, fiber reinforced graphite / epoxy composites for symmetric and unsymmetric bi-directional laminates, and sandwich beams composed of stiff graphite/epoxy face sheets with soft core materials. Two core materials are used for the sandwich cases: isotropic polyvinyl chloride foam, the most commonly used core material (Zenkert,1995), and titanium honeycomb, which can be modeled as an equivalent orthotropic material. Titanium honeycomb sandwiches are currently being considered by NASA for use on the High Speed Civil Transport (HSCT). The material properties are summarized in Table 4.1.

Aluminum (**Al**):	E = 10.8 Msi,	ν = 0.33,	G = 4.06 Msi
Graphite / Epoxy (**Gr/Ep**):	E_L = 22.9 Msi,	ν_{LT} = 0.32,	G_{LT} = 0.86 Msi,
	E_T = 1.39 Msi	ν_{TT} = 0.49,	G_{TT} = 0.468 Msi
Polyvinyl Chloride (**PVC**):	E = 15.08 ksi,	ν = 0.3,	G = 5.80 ksi
Titanium Honeycomb (**Ti**):	E_1 = 62.36 psi,	ν_{13} = 5.6x10^{-5},	G_{13} = 75.1x10^3 psi,
	E_2 = 41.27 psi,	ν_{23} = 3.7x10^{-5},	G_{23} = 56.7x10^3 psi,
	E_3 = 345x10^3 psi,	ν_{12} = 1.23,	G_{12} = 1140 psi
	L = Longitudinal Direction (fiber), T = Transverse 1,2, & 3 = principle material directions		

Table 4.1 Material Properties

4.3 Test Case Definition

Six test cases are investigated using the material systems given in Table 4.2. While isotropic materials have identical material properties regardless of the orientation in the coordinate frame, orthotropic materials, like graphite/epoxy, are commonly oriented in various directions in the x-y plane to achieve the desired stiffness characteristics. The layup column in Table 4.2 gives the order of lamination, beginning with the bottom ply at $z = -h$, and the angular orientation of the longitudinal fiber direction for the Gr/Ep plies with respect to the x axis. The S subscript denotes symmetry with respect to the midplane of the beam. For unsymmetric laminates, the total layup must be given and is denoted by the T subscript. The unsymmetric cases will test the coupling effect between the stretching and bending modes of the beam. Because of the theoretical restrictions on

the exact elasticity cylindrical bending solution, only bi-directional 0° and 90° orientations are used in the analysis.

Case	Material	Layup
A :	Al	Homogeneous
B :	Gr/Ep	$[\ 0_2/90_2/0_2/90_2\ ]_S$
C :	Gr/Ep	$[\ 0_4/90_4/0_4/90_4\ ]_T$
D :	Gr/Ep - PVC	$[\ 0_4/90_2/0_4/90_2/0_4/$ PVC Core $]_S$
E :	Gr/Ep - Ti	$[\ 0_4/90_2/0_4/90_2/0_4/$ Ti Core $]_S$
F :	Gr/Ep - PVC	$[\ 0_4/90_2/0_4/90_2/0_4/$ PVC Core $/90_4/0_2/90_4/0_2/90_4\ ]_T$

Table 4.2 Definition of Test Cases and Corresponding Ply Layup

The ply thickness, t^k, for each graphite/epoxy lamina is set equal to 0.00625 in. This is a reasonable assumption for the actual thickness used in the manufacturing of composite laminates. The total thickness of the beam for the isotropic Case A and the sandwich Cases D, E, and F is 1.0 inch. The cores for the sandwich cases comprise 80% of the total thickness of the beam. For the composite laminate, Cases B and C, the total thickness is equal to 0.1 inch. The length of the beam will be varied to achieve the desired span to thickness ratio.

4.4 Correction Factors

The analytic solutions of the {3,2} theory rely on the use of appropriate shear and transverse correction factors. Following the procedure in Section 3, the correction factors are calculated for very thin beams (span to thickness ratio L/2h = 1000) and are summarized in Table 4.3.

Case	k^2	k_{z0}	k_{z1}
A	1.0	1.0	1.0
B	0.91056	1.0	0.96494
C	0.76187	1.21668	1.01975
D	0.30666	1.24326	1.59569
E	0.85883	1.14298	1.26431
F	0.33811	1.24914	1.59787

Table 4.3 {3,2} Theory Correction Factors

Note that the unsymmetric Cases, C and F, require a significant amount of shear correction as compared to the symmetric cases. This is because non-symmetry causes a coupling effect between the stretching and bending modes of the beam, resulting in a significant stretching of the midplane.

To afford a numerical comparison to the {1,2}-order theory, the corresponding correction factors for that theory are also computed and summarized in Table 4.4.

Case	k^2	k_{z0}	k_{z1}
A	1.0	1.0	1.0
B	0.97793	1.0	1.0
C	0.73262	1.0	1.0
D	0.37301	1.24326	1.76405
E	1.04737	1.14298	1.39621
F	0.41210	1.24326	1.76405

Table 4.4 {1,2} Theory Correction Factors

4.5 Results

Six test cases are investigated over a full range of span to thickness ratios. For each case defined in Table 4.2, thin, moderately thick, and very thick beams with the span to thickness ratios L/2h = { 100, 10, 4 } are analyzed. A unit beam width is assumed. The displacement, stress, and strain distributions through the thickness of the beam are

calculated at the locations where the quantities are maximum. These locations are depicted in Figure 4.2.

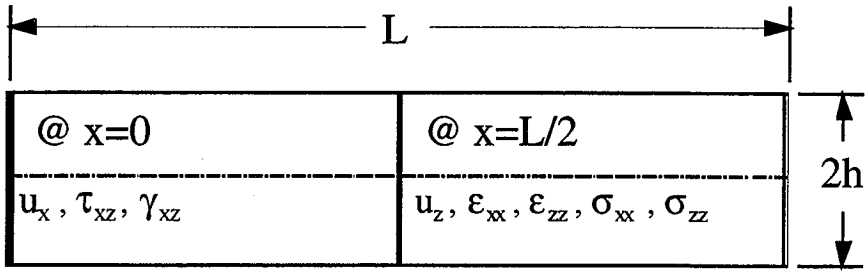

Figure 4.2 Locations for Displacement, Strain, and Stress Computations

Because the axial strain ε_{xx} is simply the derivative of the axial displacement u_x, their maximum values are proportional according to the equation $\varepsilon_{xx}(L/2) = -\frac{\pi}{L}u_x(0)$. The shear strain γ_{xz} is not shown in the graphical results since it is directly proportional to the shear stress τ_{xz}, as per equation (3.8). While the strains are dimensionless, it is also desirable to have the transverse displacement and stresses expressed in terms of non-dimensional quantities for a more general comparison of results. The transverse displacements are normalized with respect to the exact deflection at the midplane $u_z(\zeta = 0)_{exact}$. This normalization will also emphasize the nonlinear distribution of the transverse displacement for thick beams. The stresses are normalized with respect to the applied normal traction q, which at mid-span of the beam is equal to unity.

For each span to thickness ratio, six plots are presented to compare the present higher-order theory to the exact solution. For the smallest aspect ratio, L/2h = 4, the present {3,2} theory is also compared to the {1,2} theory. As the span to thickness ratio approaches the thin regime, the {1,2} theory results are expected to approach those obtained by the present theory, so a {1,2} comparison is not shown for span to thickness ratios greater than 4. For the test cases, the following notation is used for graphical comparison of the theories: **Exact** stands for the exact elasticity solution, **HOT** denotes the present {3,2}-order theory, and **{1,2}** represents the results of the {1,2}-order theory.

4.5.1 Homogeneous Beams

Case A assesses the accuracy of the theory for analysis of homogeneous materials. As demonstrated in Figures 4.3 - 4.5, the displacements, strains, and stresses, for both the {3,2} and {1,2} theories, produce excellent correlation with exact elasticity solutions. This is accomplished without the use of shear or transverse correction factors. Notice that as the span to thickness ratio decreases, the transverse deflection takes on a parabolic distribution through the thickness. For very thick beams (L/2h = 4), this deflection varies up to 3% of the nominal midplane deflection. The axial displacement, strain, and stress, as well as the transverse strain all take on linear distributions through the thickness regardless of the span to thickness ratio. At this point, the present {3,2} displacement theory does not provide any benefit over the {1,2} theory, but the results shown here are presented to demonstrate the accuracy of these theories for commonly used homogeneous materials.

The results in Figures 4.3 - 4.5 are expected since the exact normal strain and shear strain distributions are closely approximated by linear and parabolic distributions, respectively. These distributions are easily captured with only a linear axial displacement assumption and a quadratic transverse displacement. Note that both {3,2} and {1,2} theories have a unique advantage over previous higher-order shear deformation theories: they satisfy the traction-free boundary conditions without the need to integrate the equilibrium equations of elasticity. Many of the higher-order deformation theories do not satisfy the traction-free boundary conditions and cannot produce accurate shear stress results without integrating the equilibrium equations of elasticity theory. Though not shown, results of similar accuracy can be obtained for homogeneous orthotropic beams without the use of correction factors, i.e., $k^2 = k_{z0} = k_{z1} = 1.0$.

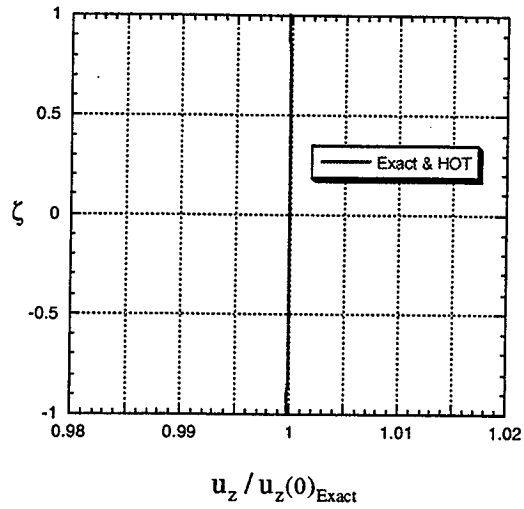

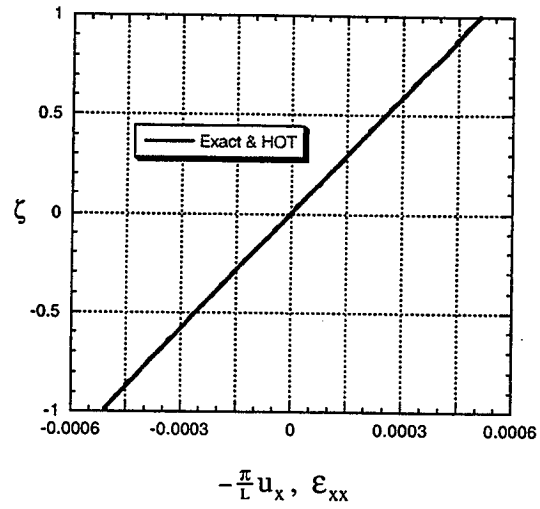

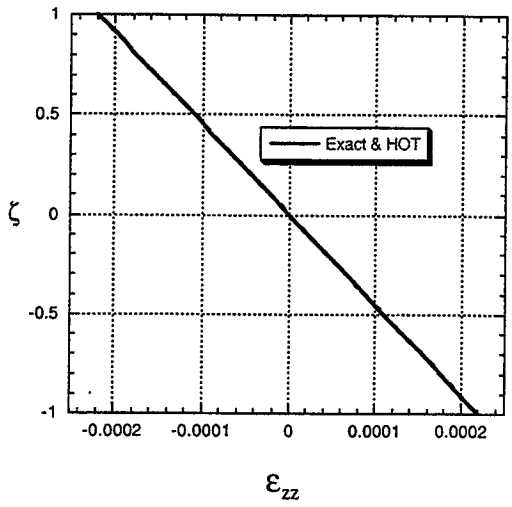

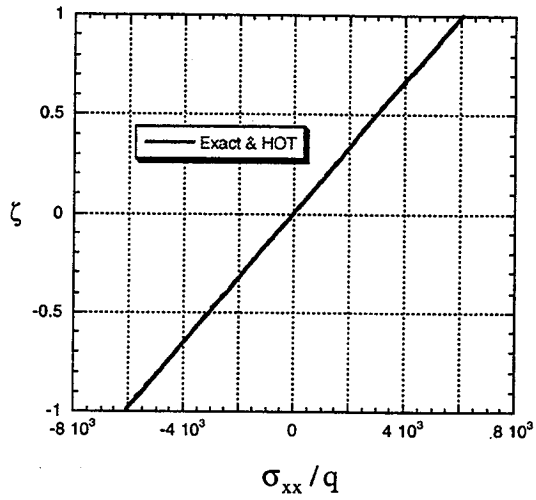

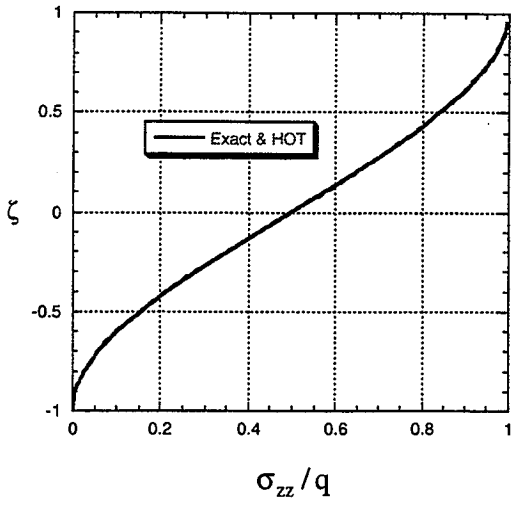

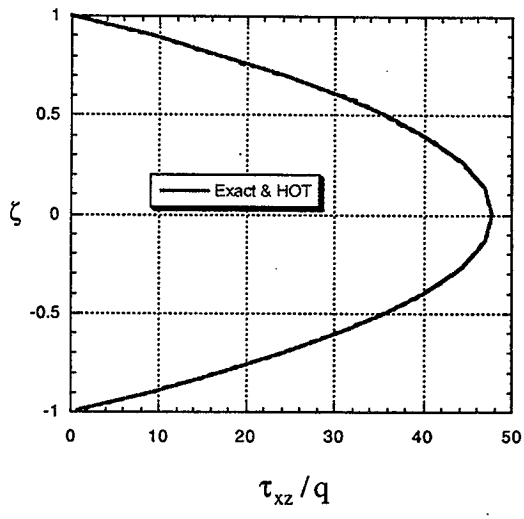

Figure 4.3 Case A: Aluminum, L/2h = 100

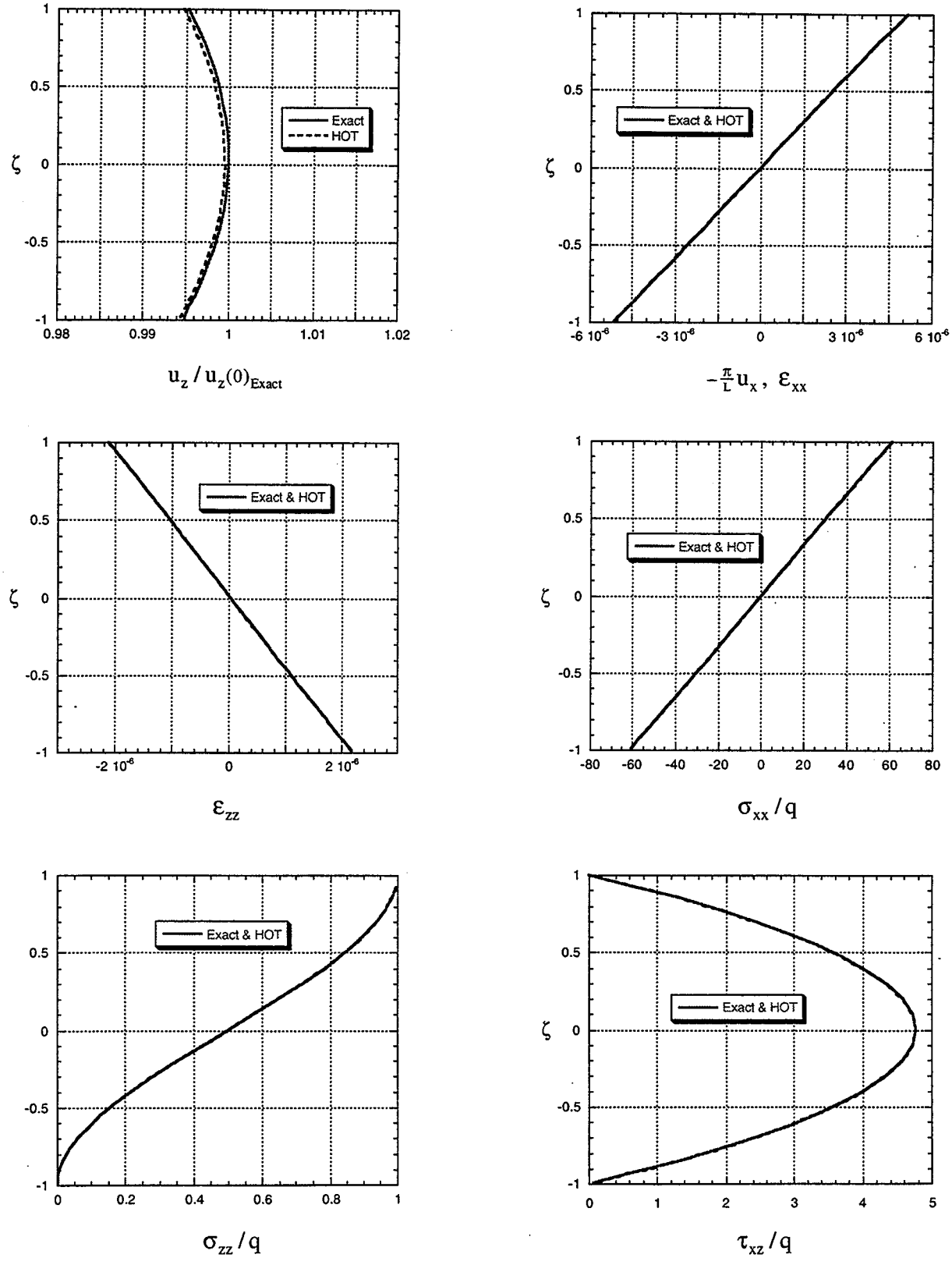

Figure 4.4 Case A: Aluminum, L/2h = 10

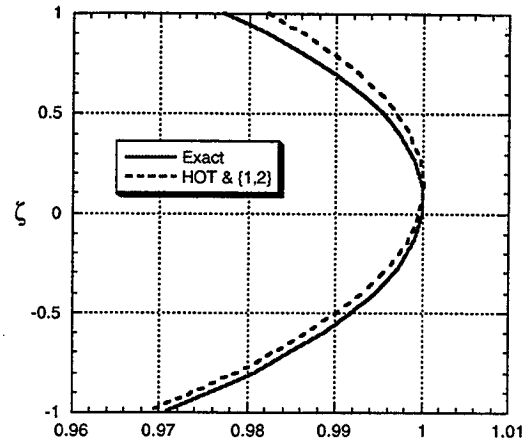

$u_z / u_z(0)_{Exact}$

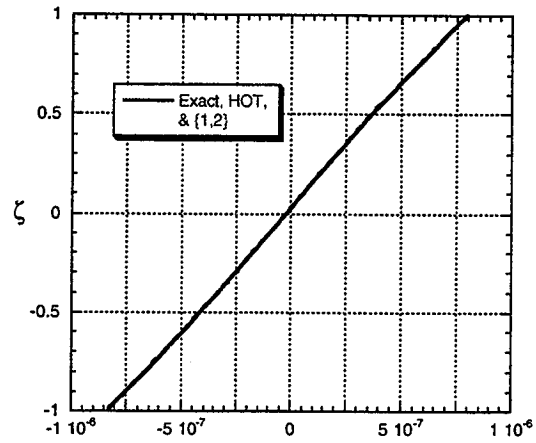

$-\frac{\pi}{L}u_x$, ε_{xx}

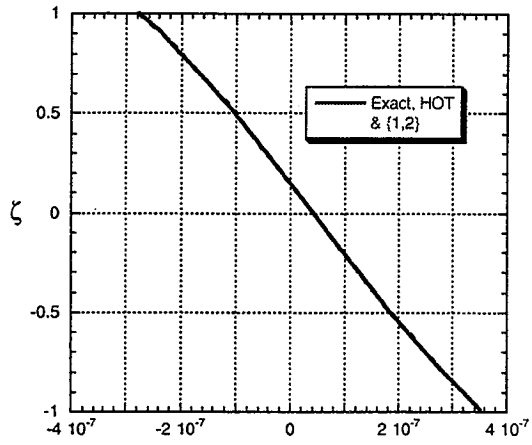

ε_{zz}

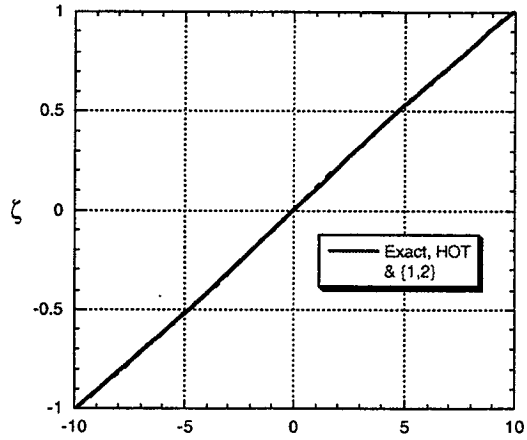

σ_{xx} / q

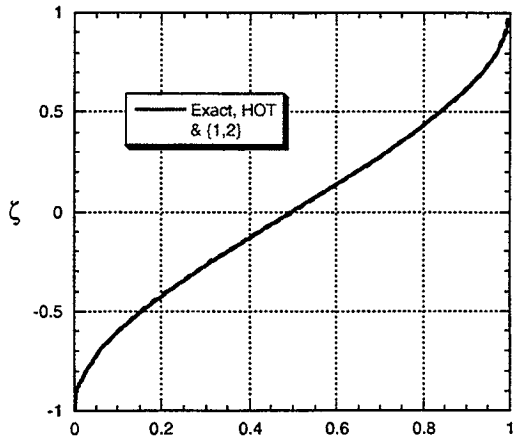

σ_{zz} / q

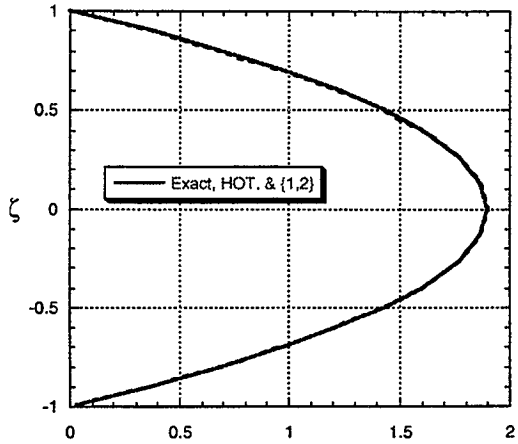

τ_{xz} / q

Figure 4.5 Case A: Aluminum, L/2h = 4

4.5.2 Laminated Composite Beams

Figures 4.6 - 4.8 depict through the thickness distributions of displacements, strains, and stresses for very thin (L/2h = 100), moderately thick (L/2h = 10), and very thick (L/2h = 4) symmetrically laminated composite beams. The material system is that identified in Table 4.2 as Case B. Similar distributions for an unsymmetric laminate, Case C in Table 4.2, are shown in Figures 4.9 - 4.11.

Figure 4.6 depicts displacement, strain, and stress results for a symmetrically laminated, thin beam. The {3,2} results are in excellent agreement with the exact solutions. While the transverse normal stress varies slightly from the exact curve through the thickness, the midplane stress and surface tractions are all accurately recovered. In Figure 4.7, the thickness distributions for the moderately thick case remain in close agreement with the elasticity solution. Figure 4.8 compares the results of the {1,2}, {3,2}, and exact solutions in the very thick regime. At the midplane, the transverse displacement is within 1% of the exact solution for both approximations, whereas at the top surface the difference is about 6%. The {3,2} cubic approximation of the axial strain, ε_{xx}, produces accurate maximum values at the top and bottom surfaces, whereas the {1,2} linear distribution underestimates these maximum values. This results a 20% underestimation for σ_{xx} when the {1,2}-order theory is used. This discrepancy is especially significant when designing a laminate according to the maximum stress criterion.

For the case of an unsymmetric laminate, the midplane exhibits straining due to the axial and transverse strains and the coupling between the two stretching modes. In Figure 4.9, a tensile ε_{xx} and a compressive ε_{zz} are observed at the midplane. In Figures 4.9 and 4.10, close agreement is shown for the through the thickness distributions, with the exception of the transverse normal stress σ_{zz}. The midplane stretching results in a σ_{zz} thickness variation that is not captured by the higher-order theory. In Figure 4.11, the {3,2} theory shows improvements over the {1,2} theory for very thick beams, although the polynomial distributions are unable to capture the piece-wise smooth, exact solution.

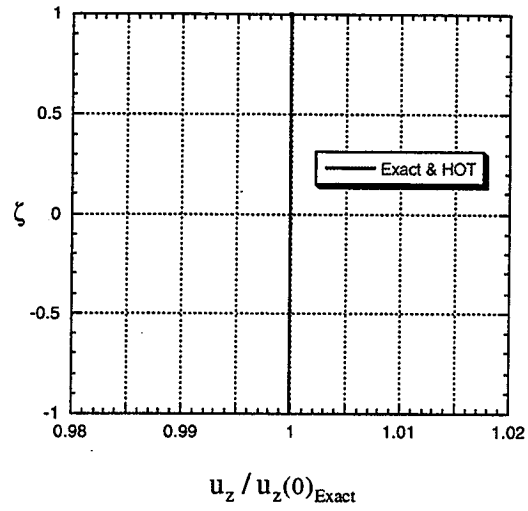

$u_z / u_z(0)_{Exact}$

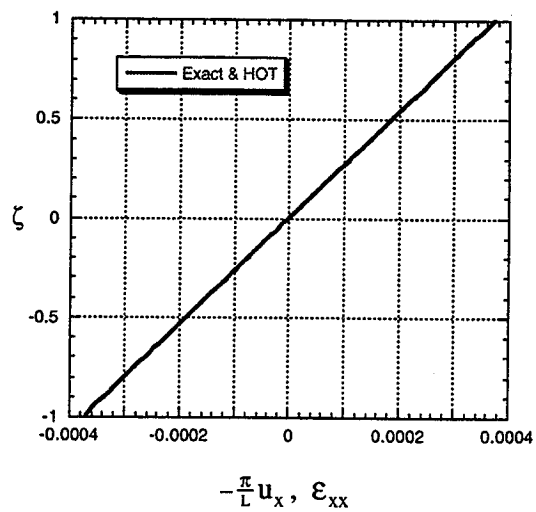

$-\frac{\pi}{L}u_x$, ε_{xx}

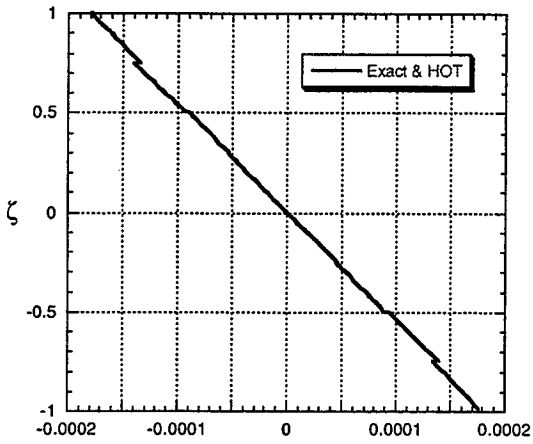

ε_{zz}

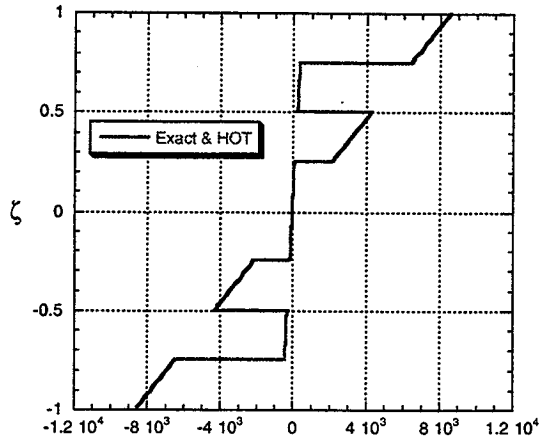

σ_{xx} / q

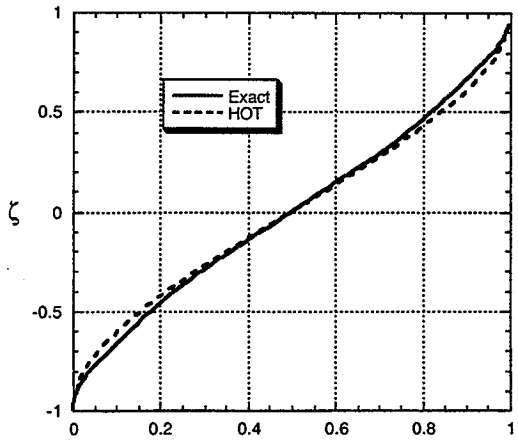

σ_{zz} / q

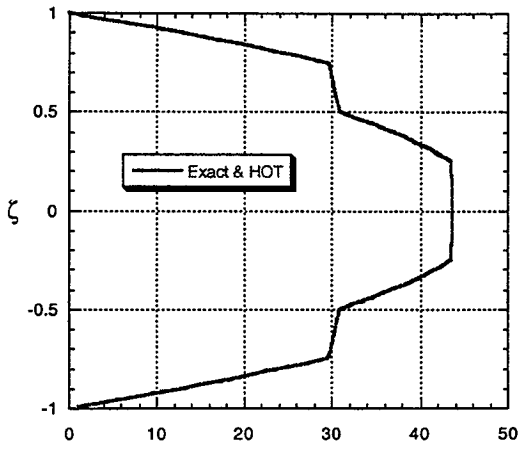

τ_{xz} / q

Figure 4.6 Case B: Gr/Ep Symmetric Laminate, L/2h = 100

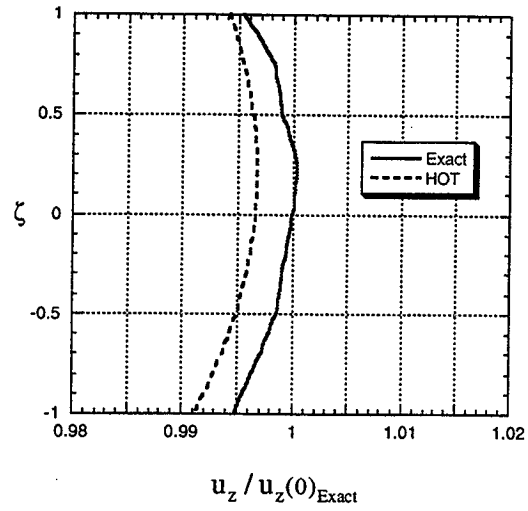

$u_z / u_z(0)_{Exact}$

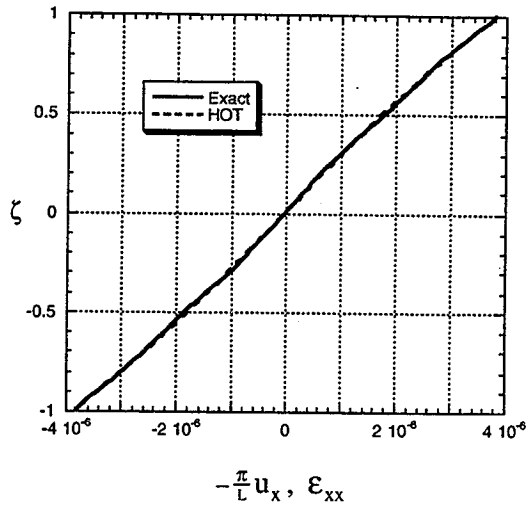

$-\frac{\pi}{L} u_x$, ε_{xx}

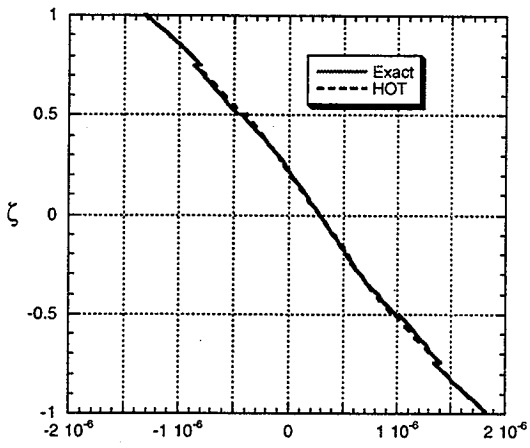

ε_{zz}

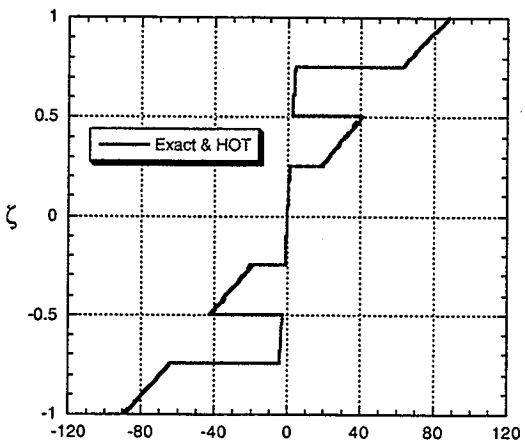

σ_{xx} / q

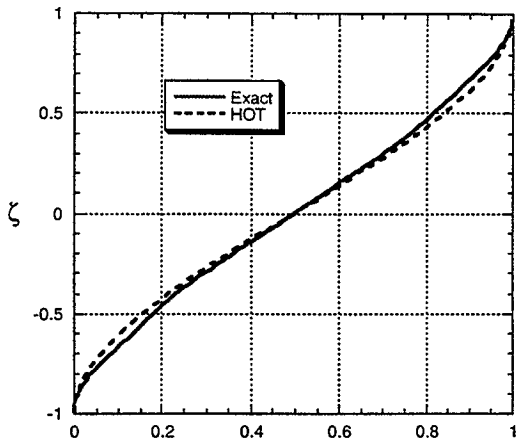

σ_{zz} / q

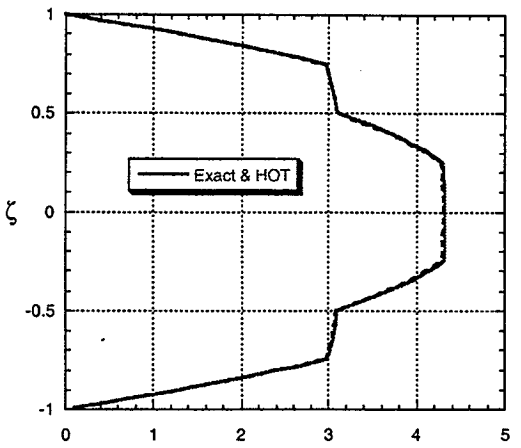

τ_{xz} / q

Figure 4.7 Case B: Gr/Ep Symmetric Laminate, L/2h = 10

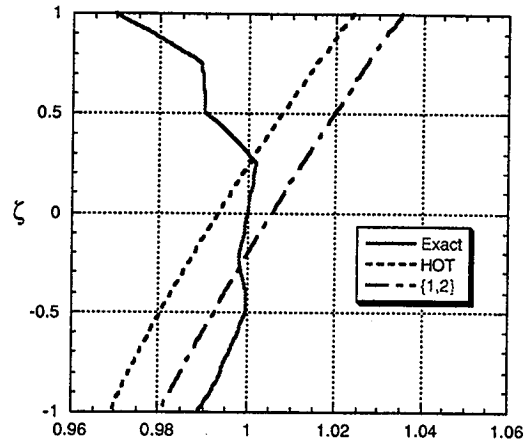

$u_z / u_z(0)_{Exact}$

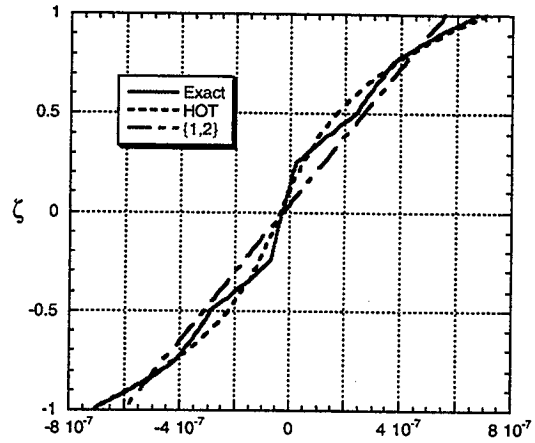

$-\frac{\pi}{L} u_x$, ε_{xx}

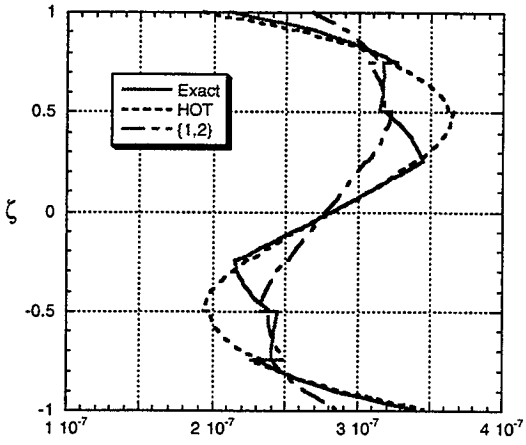

ε_{zz}

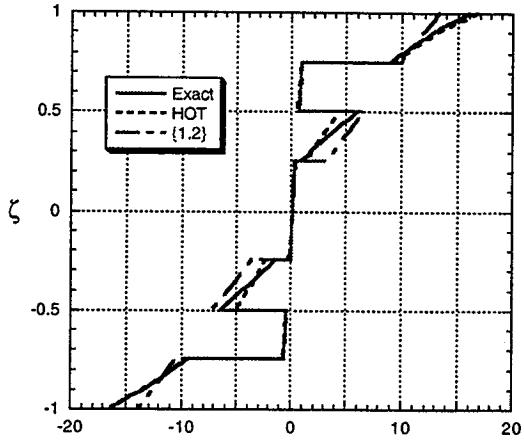

σ_{xx} / q

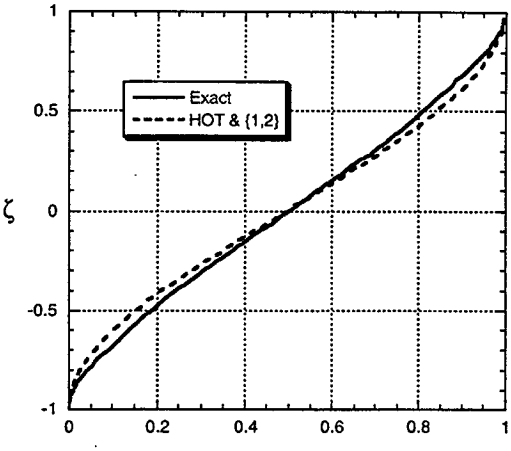

σ_{zz} / q

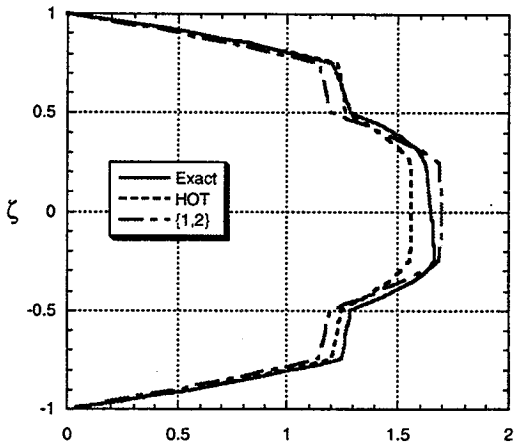

τ_{xz} / q

Figure 4.8 Case B: Gr/Ep Symmetric Laminate, L/2h = 4

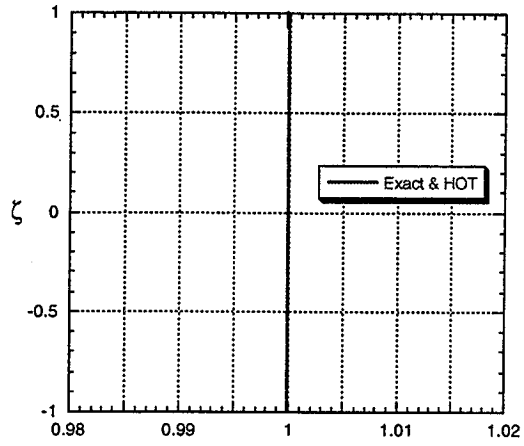

$u_z / u_z(0)_{Exact}$

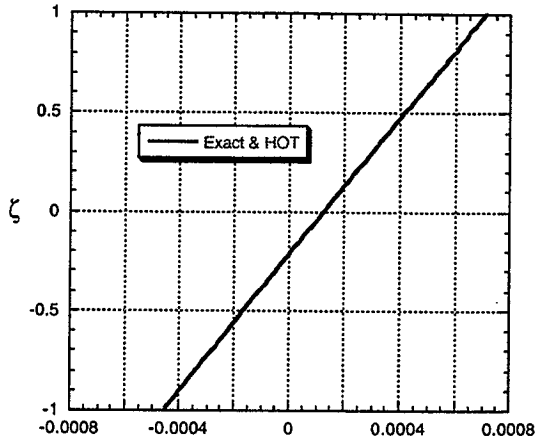

$-\frac{\pi}{L} u_x$, ε_{xx}

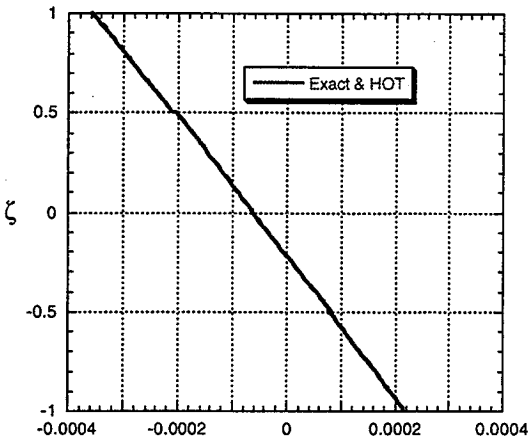

ε_{zz}

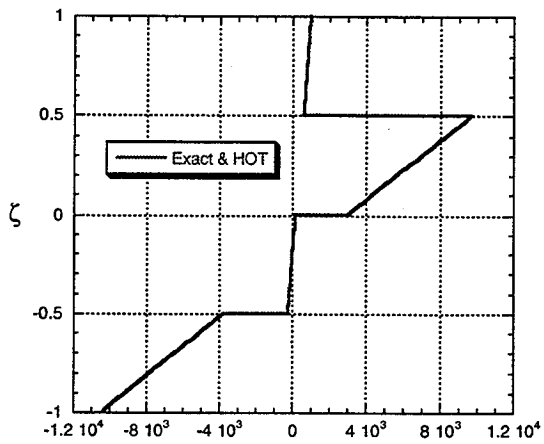

σ_{xx} / q

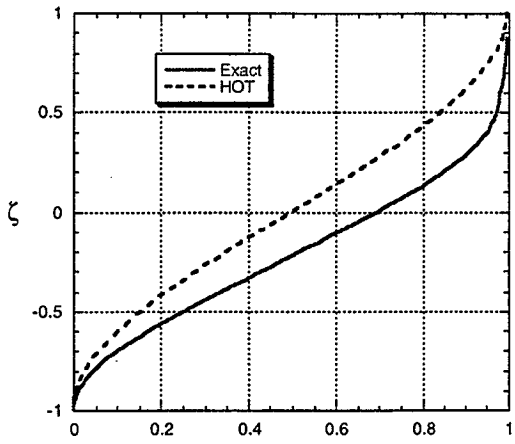

σ_{zz} / q

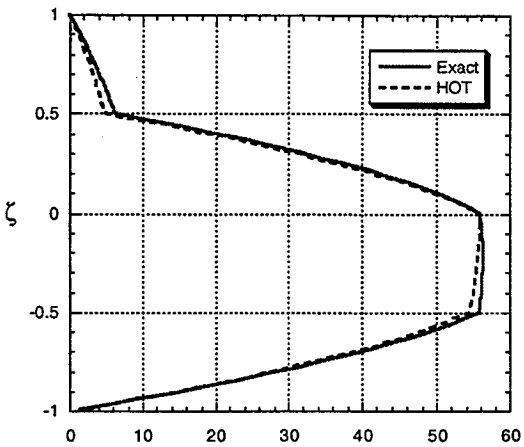

τ_{xz} / q

Figure 4.9 Case C: Gr/Ep Unsymmetric Laminate, L/2h = 100

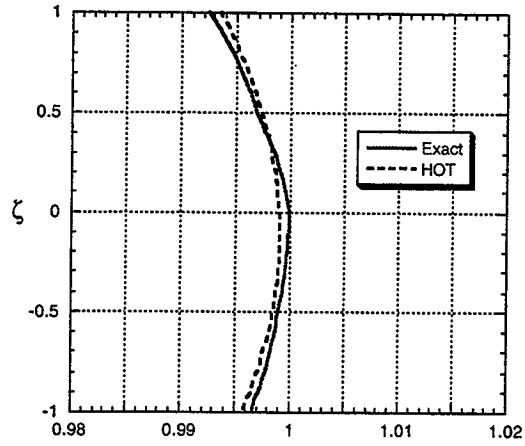

$u_z / u_z(0)_{Exact}$

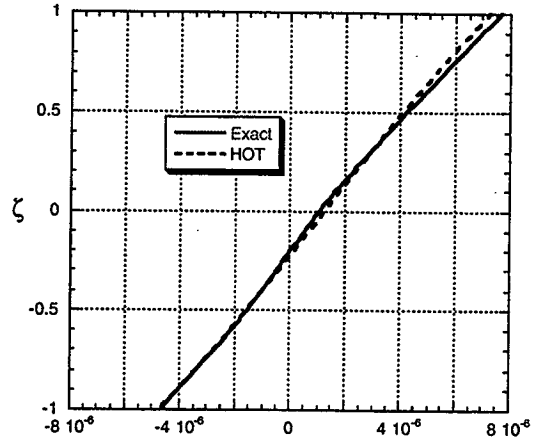

$-\frac{\pi}{L}u_x,\ \varepsilon_{xx}$

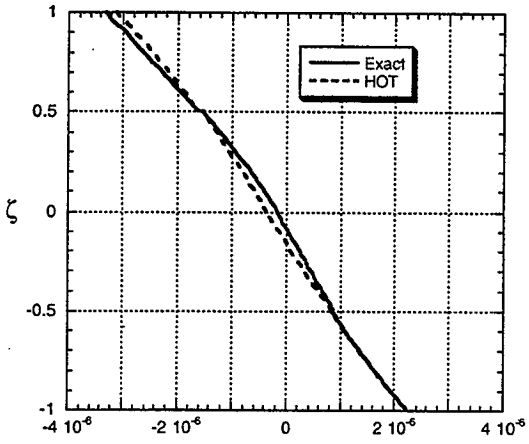

ε_{zz}

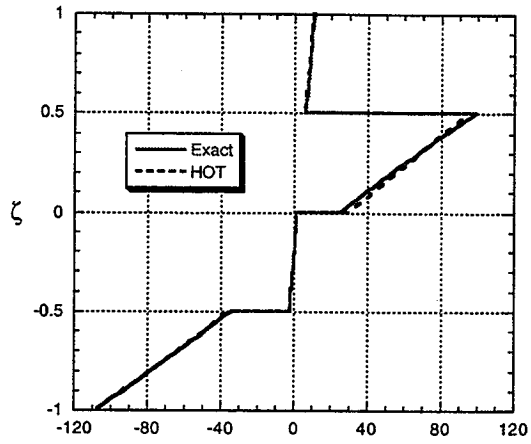

σ_{xx} / q

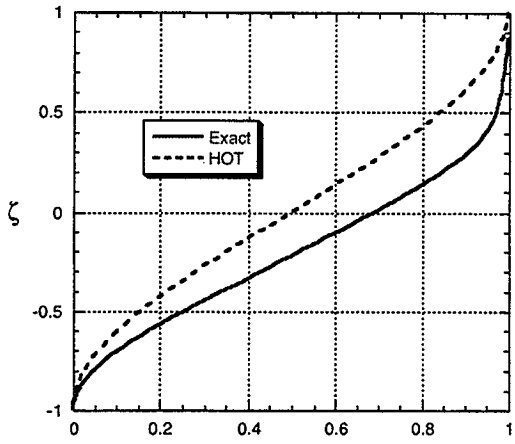

σ_{zz} / q

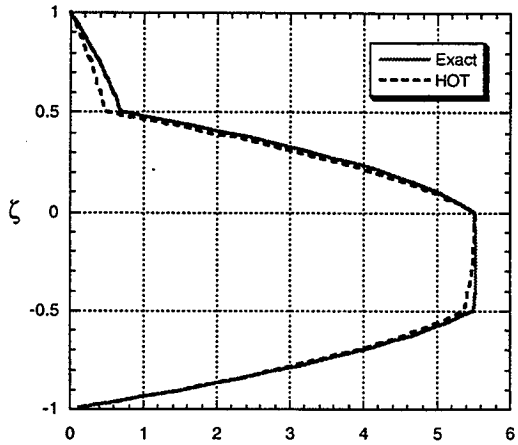

τ_{xz} / q

Figure 4.10 Case C: Gr/Ep Unsymmetric Laminate, L/2h = 10

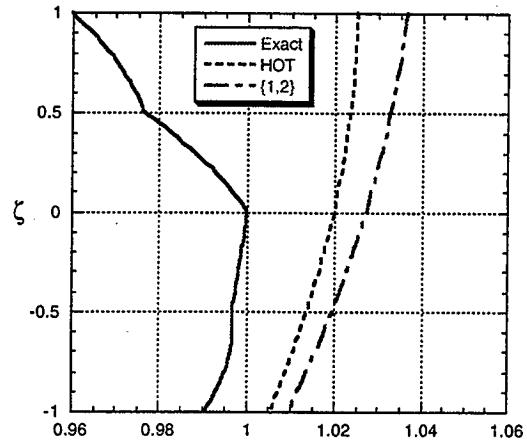

$u_z / u_z(0)_{Exact}$

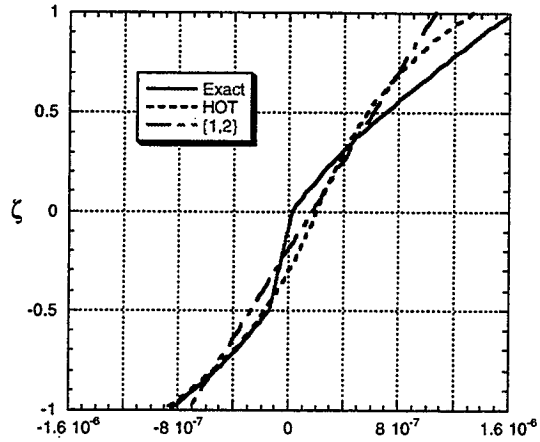

$-\frac{\pi}{L} u_x$, ε_{xx}

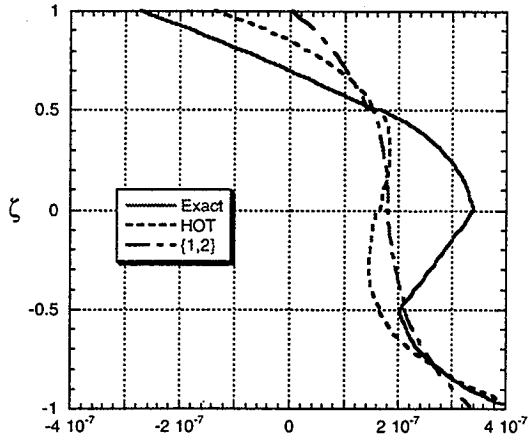

ε_{zz}

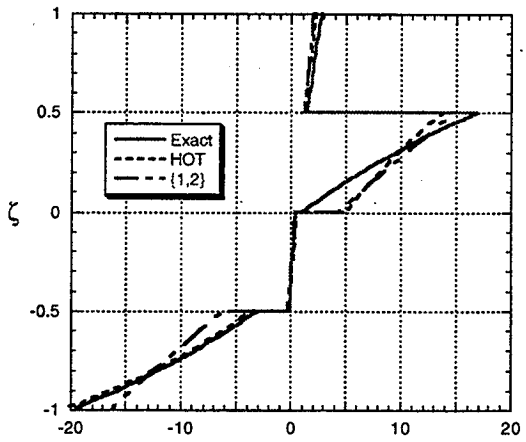

σ_{xx} / q

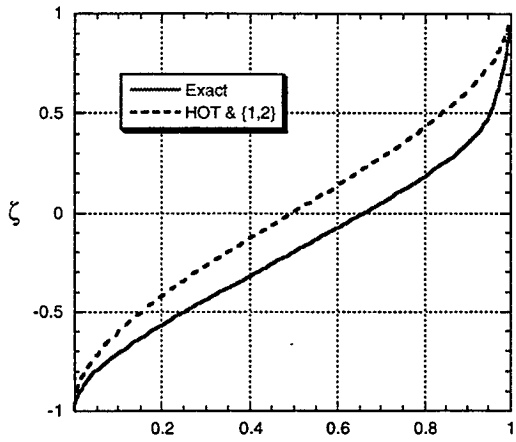

σ_{zz} / q

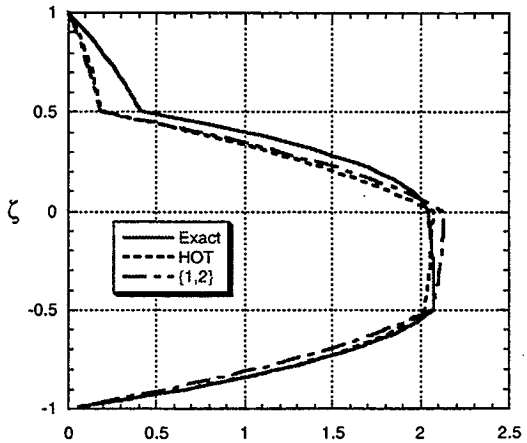

τ_{xz} / q

Figure 4.11 Case C: Gr/Ep Unsymmetric Laminate, L/2h = 4

4.5.3 Sandwich Beams

Cases D, E, and F address the analysis of symmetric and unsymmetric sandwich composite beams. Sandwich beams present a unique challenge to the theory owing to the drastic change in the material properties through the thickness. The face sheets of a sandwich are stiff in the axial direction to carry the axial stress while the core material may be considerably less stiff. This is possible because the magnitude of the transverse shear load is usually much less than the axial load. As a result, the core can be made of a lightweight, compliant material, reducing the weight of the structure. Typical thickness dimensions for the components of a sandwich beam are illustrated in Figure 4.12

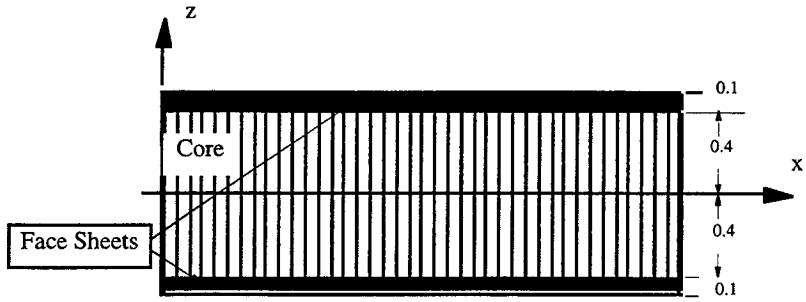

Figure 4.12 Sandwich Composite Beam

Figure 4.13 shows the results for Case D in the thin regime. Note how the axial stress σ_{xx} is carried by the Gr/Ep face sheets on the top and bottom faces of the beam while the transverse shear stress τ_{xz} is almost exclusively carried by the PVC core. For the thin sandwich, the {3,2}-order theory almost exactly matches the exact elasticity solution, while for the thicker case, shown in Figure 4.14, the limitations in the theory are more evident. The transverse displacement prediction is about 2% in error. The stresses and strain on the top and bottom faces, where these quantities are usually the largest, are accurately predicted by the theory. For the thick regime, Figure 4.15, the transverse displacement is overestimated by both the {3,2} and {1,2} theories, with errors ranging from 12% to 37%. Notice that the linear approximation for the axial displacement in the {1,2} theory underestimates the axial strain, resulting in a significant underestimation of

the axial stress. The {3,2}-order theory captures σ_{xx} at the top and bottom surfaces adequately, while the same stress for the {1,2} theory is 85% in error. The quality of these results suggests that the span to thickness ratio of L/2h = 4 may constitute a practical limit of application of this theory for sandwich beams.

In Case E, the sandwich core is made of titanium honeycomb. Because of the orthotropic stiffness properties of the honeycomb, the axial stiffness is very low compared to the relatively high transverse stiffness. The sandwich core acts as a shear web, resisting the transverse stresses only. The titanium honeycomb serves as an efficient core material, providing a large transverse stiffness with a minimal weight penalty. Figures 4.16 through 4.18 depict the results for the sandwich beam with a titanium honeycomb core. Note that the nonlinear axial effects are present until the beam approaches the thick regime (L/2h = 4). Comparing these results to those for the PVC core shows that the axial displacement and strain are already nonlinear at L/2h = 10. The axial quantities become increasingly nonlinear as the differences between the transverse stiffness through the thickness of the laminate increase. This is evident with the larger discrepancy between the {3,2} and {1,2} results for the sandwich beam with a PVC core. As a result, the higher-order terms in the {3,2} theory do not provide as much benefit over the {1,2} theory for Case E with a titanium honeycomb core.

In Case F, an unsymmetric sandwich beam with a PVC core is analyzed. This particular sandwich presents the greatest challenge to the beam theory because of the axial-bending coupling and the low stiffness of the PVC core. Figures 4.19 through 4.21 depict accurate correlations with the exact solution. In Figure 4.21, the benefits of the higher-order axial displacement over the linear axial displacement are evident. While the deflection predicted by the {3,2} theory differs from the exact solution by about 8%, the {1,2} theory prediction is in error by 22%. The axial strain exhibits a highly nonlinear distribution through the thickness, with the boundary conditions accurately modeled with the {3,2} theory. Although not particularly evident from Figure 4.21, the axial compressive stress for the {1,2} theory is underestimated on the bottom surface by 83%.

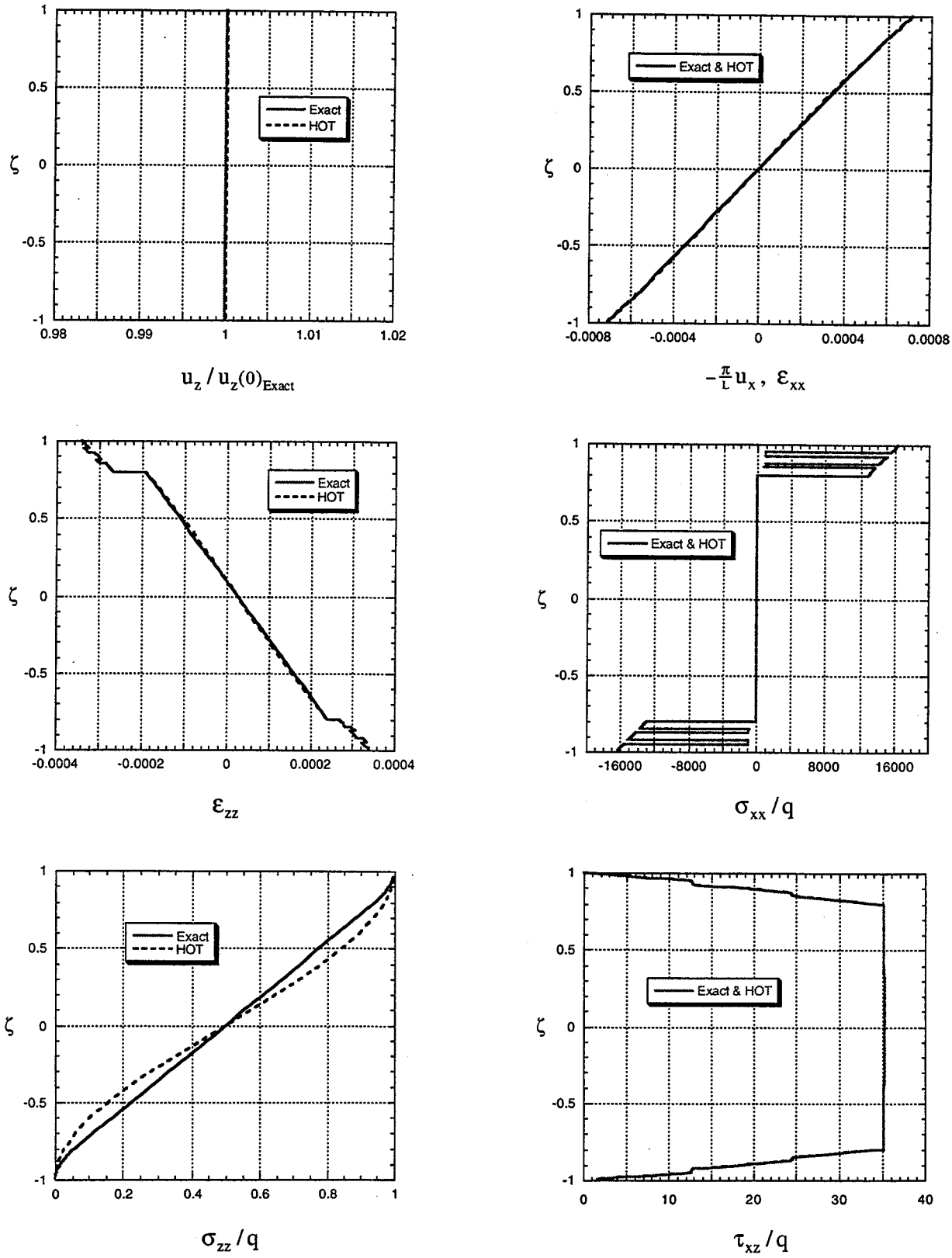

Figure 4.13 Case D: Gr/Ep-PVC Symmetric Sandwich, L/2h = 100

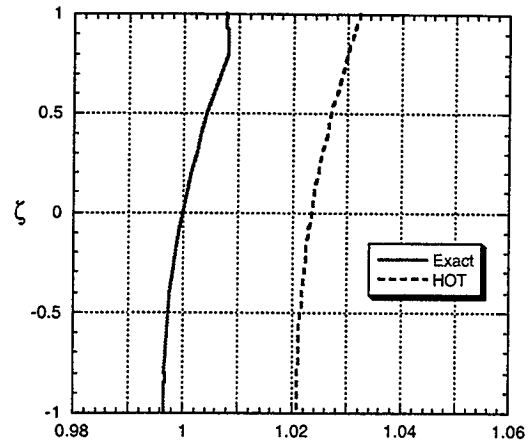

$u_z / u_z(0)_{Exact}$

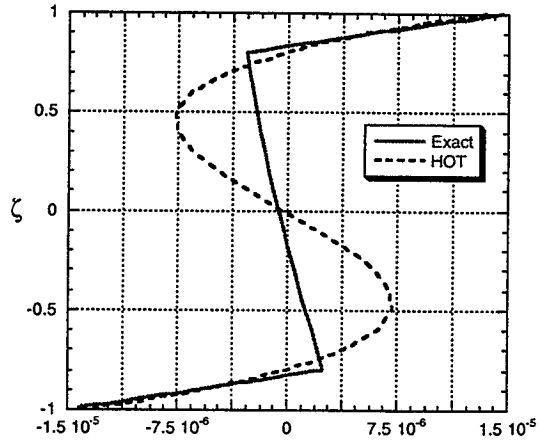

$-\frac{\pi}{L} u_x$, ε_{xx}

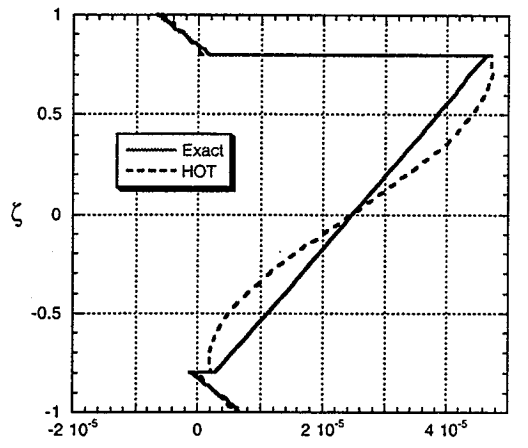

ε_{zz}

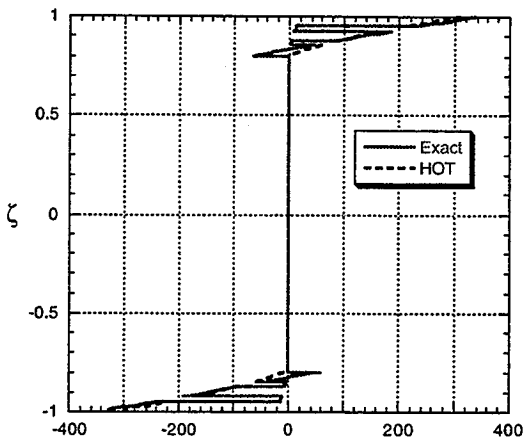

σ_{xx} / q

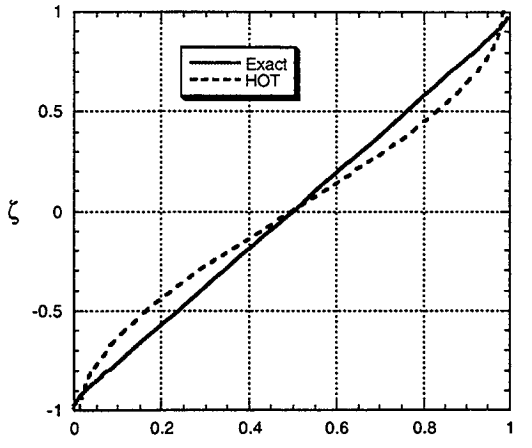

σ_{zz} / q

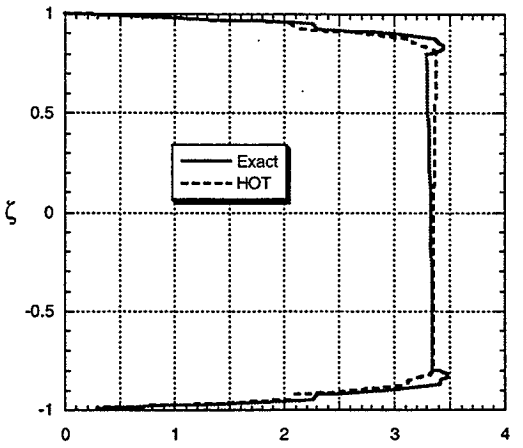

τ_{xz} / q

Figure 4.14 Case D: Gr/Ep-PVC Symmetric Sandwich, L/2h = 10

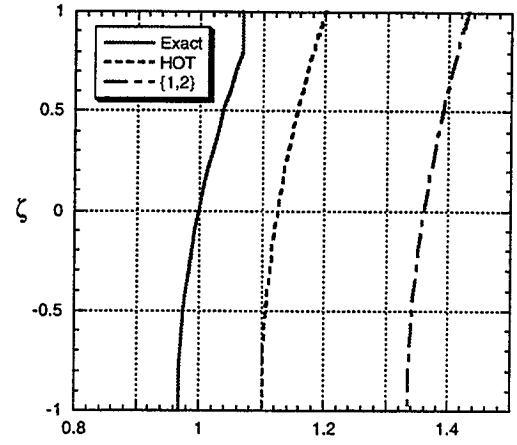

$u_z / u_z(0)_{Exact}$

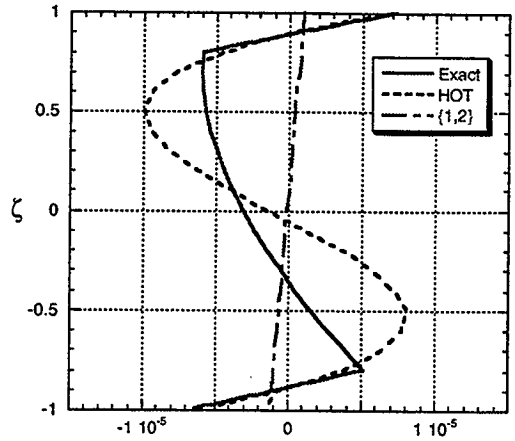

$-\frac{\pi}{L} u_x$, ε_{xx}

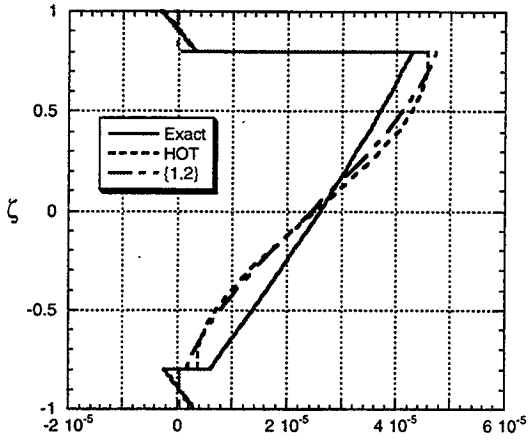

ε_{zz}

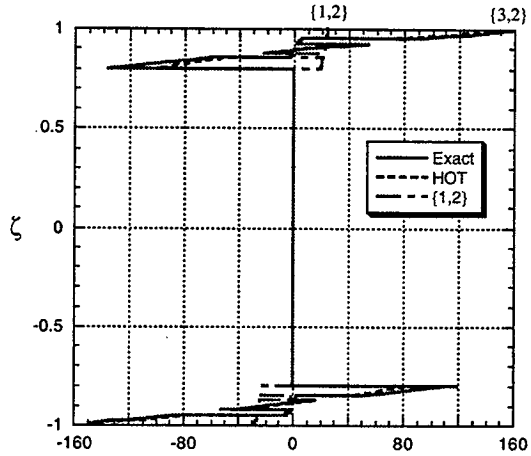

σ_{xx} / q

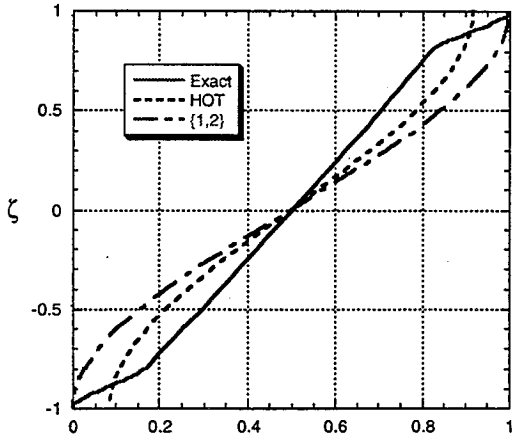

σ_{zz} / q

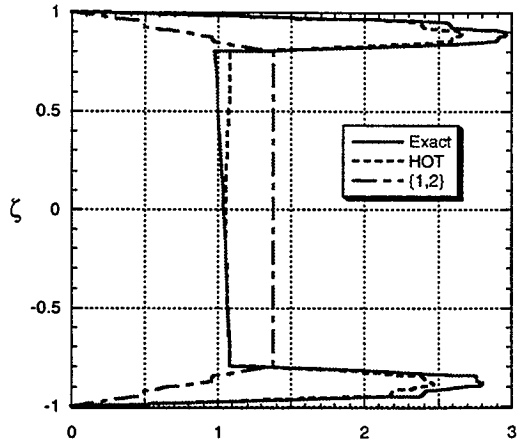

τ_{xz} / q

Figure 4.15 Case D: Gr/Ep-PVC Symmetric Sandwich, L/2h = 4

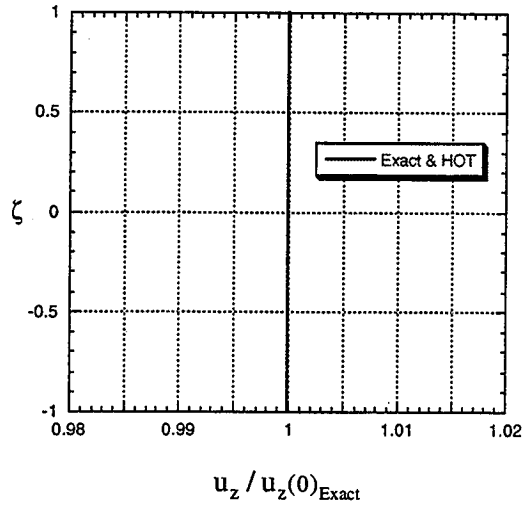

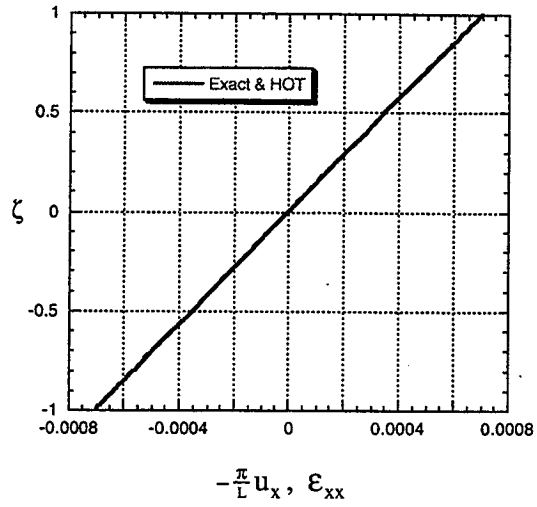

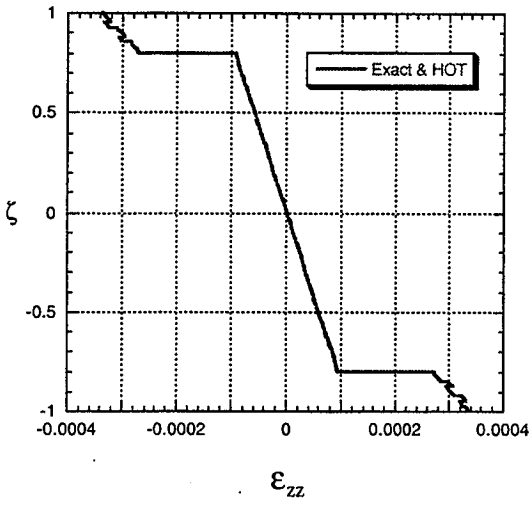

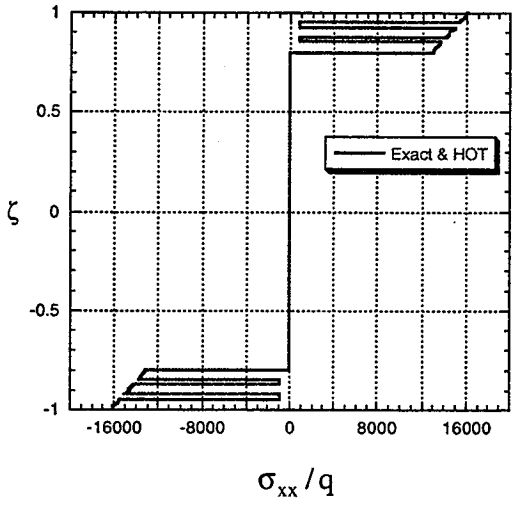

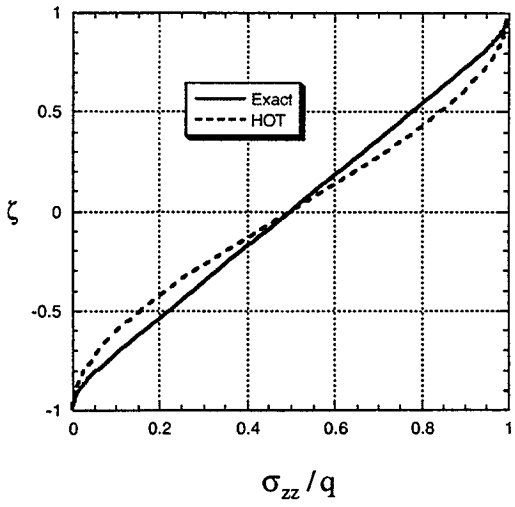

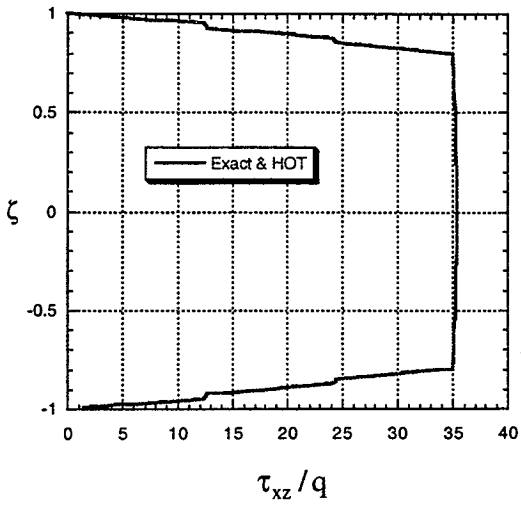

Figure 4.16 Case E: Gr/Ep-Ti Symmetric Sandwich, L/2h = 100

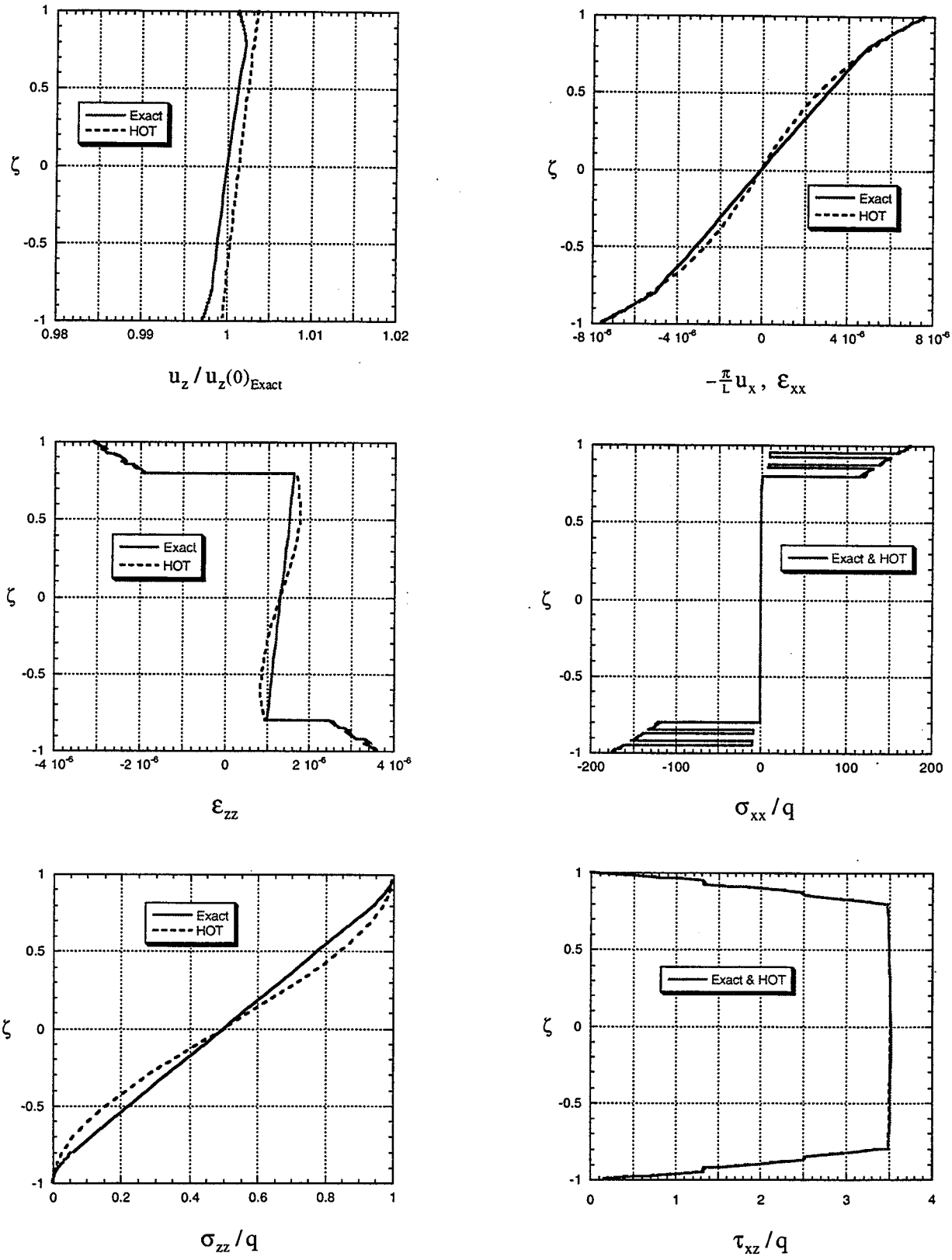

Figure 4.17 Case E: Gr/Ep-Ti Symmetric Sandwich, L/2h = 10

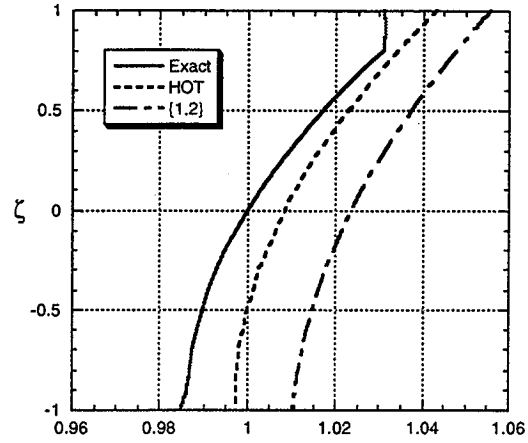

$u_z / u_z(0)_{Exact}$

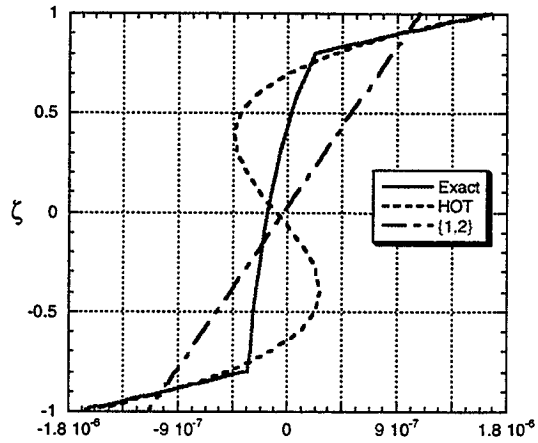

$-\frac{\pi}{L} u_x$, ε_{xx}

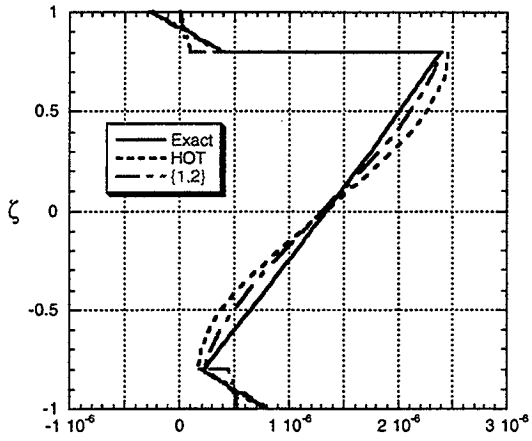

ε_{zz}

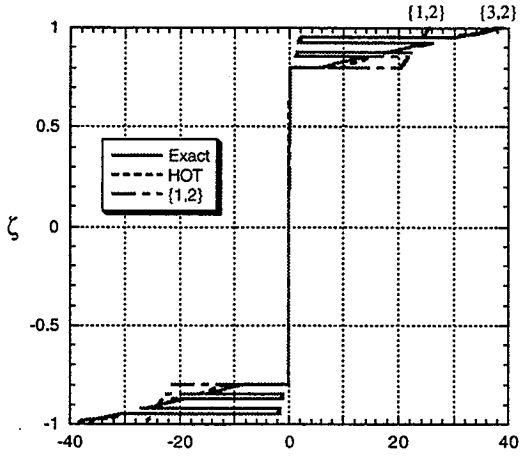

σ_{xx} / q

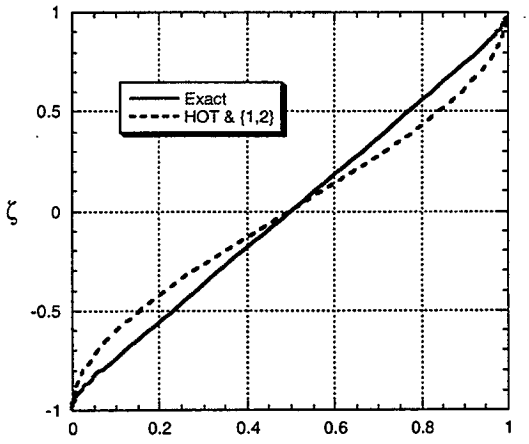

σ_{zz} / q

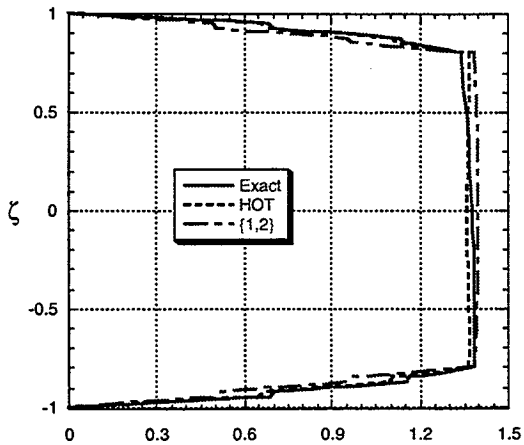

τ_{xz} / q

Figure 4.18 Case E: Gr/Ep-Ti Symmetric Sandwich, L/2h = 4

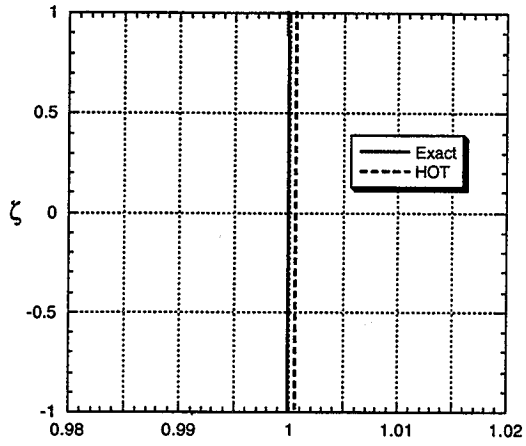

$u_z / u_z(0)_{Exact}$

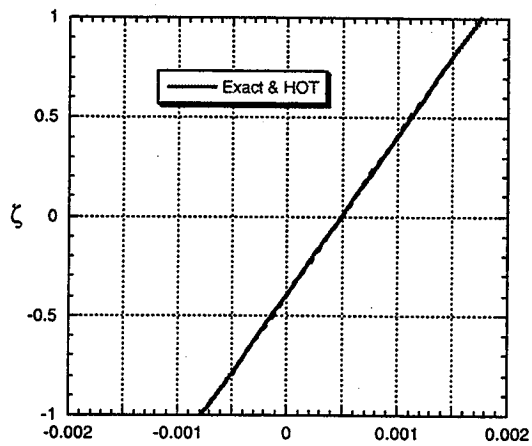

$-\frac{\pi}{L}u_x$, ε_{xx}

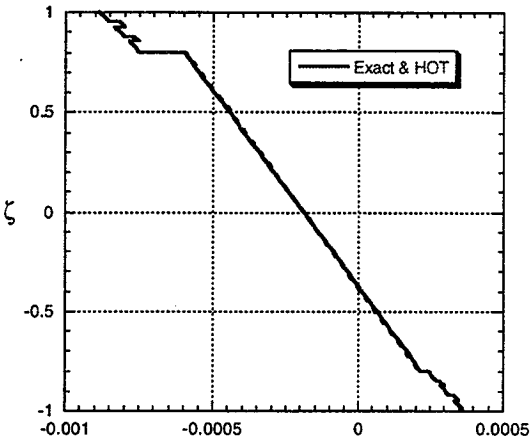

ε_{zz}

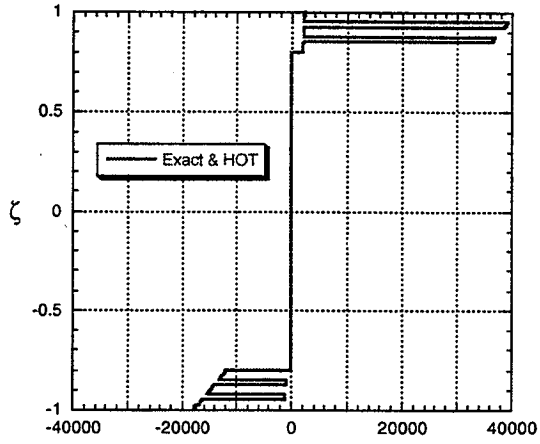

σ_{xx} / q

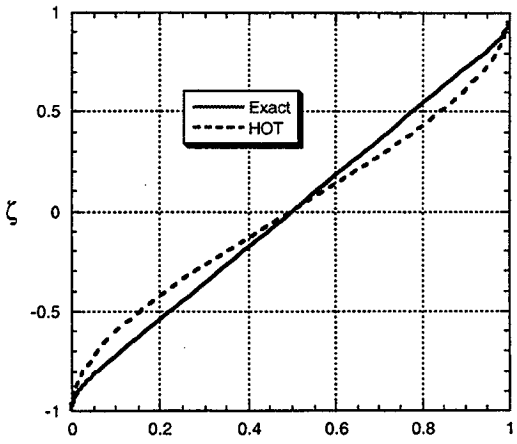

σ_{zz} / q

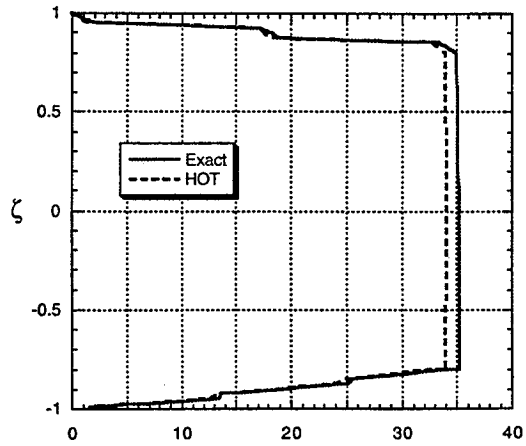

τ_{xz} / q

Figure 4.19 Case F: Gr/Ep-PVC Unsymmetric Sandwich , L/2h = 100

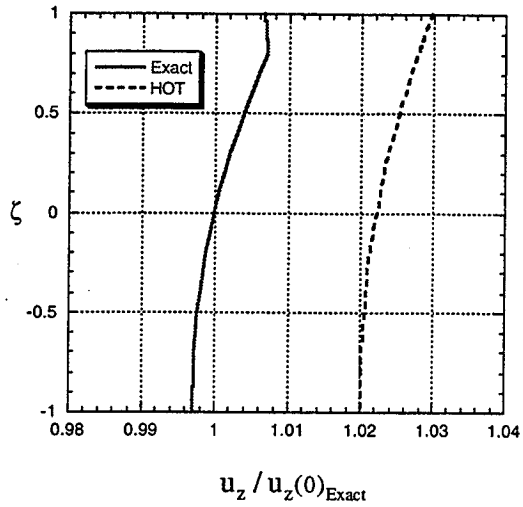

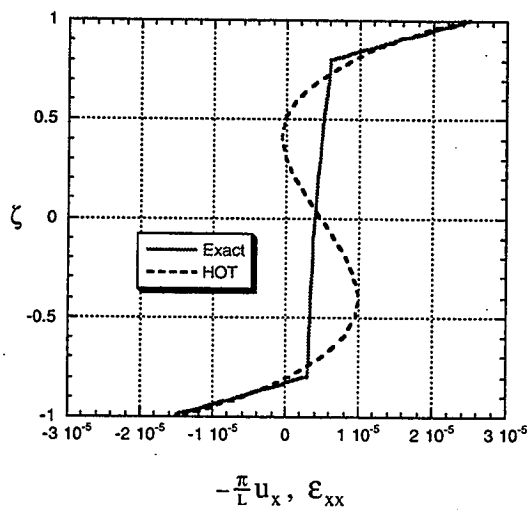

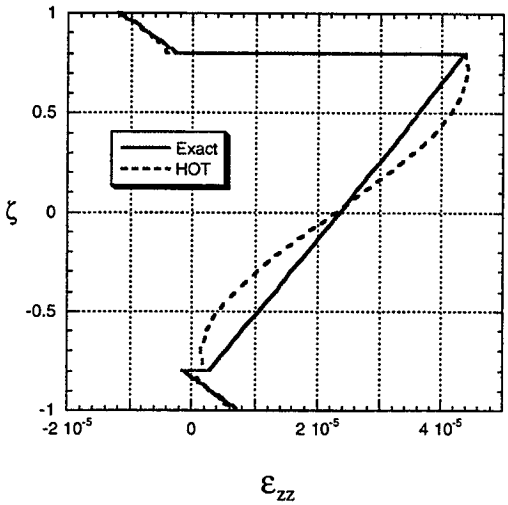

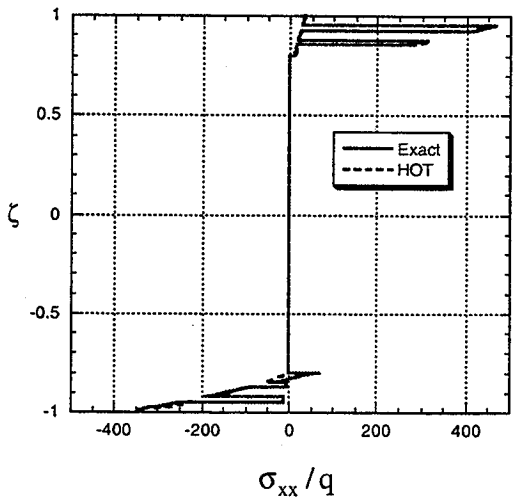

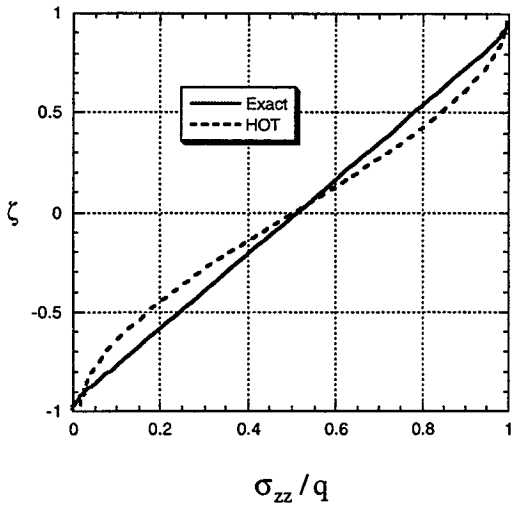

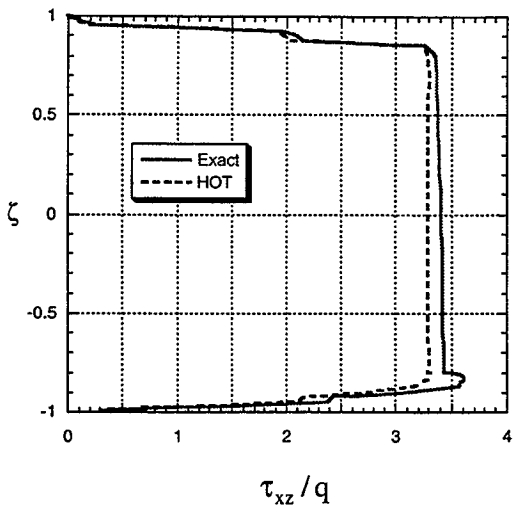

Figure 4.20 Case F: Gr/Ep-PVC Unsymmetric Sandwich , L/2h = 10

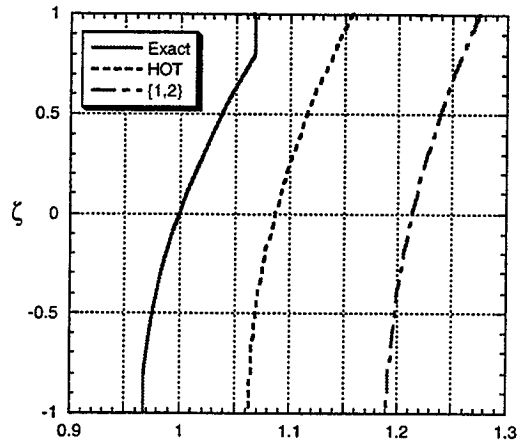

$u_z / u_z(0)_{Exact}$

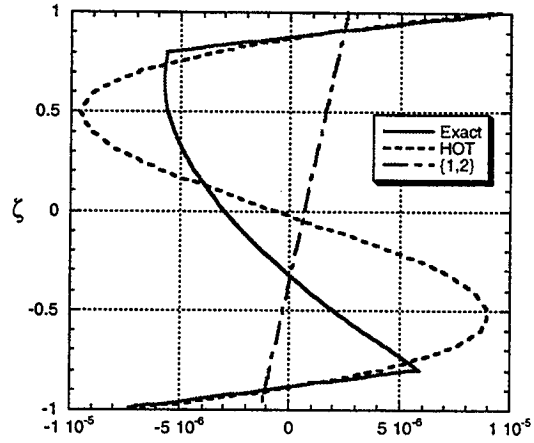

$-\frac{\pi}{L} u_x$, ε_{xx}

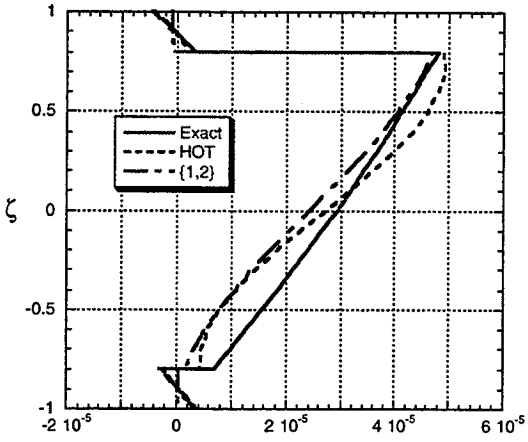

ε_{zz}

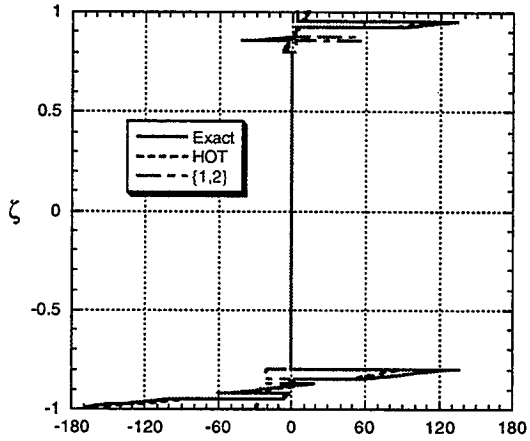

σ_{xx} / q

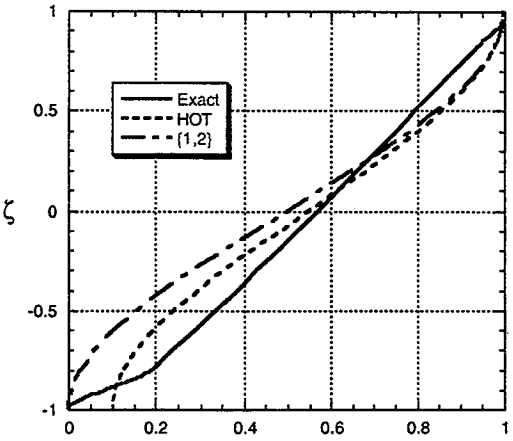

σ_{zz} / q

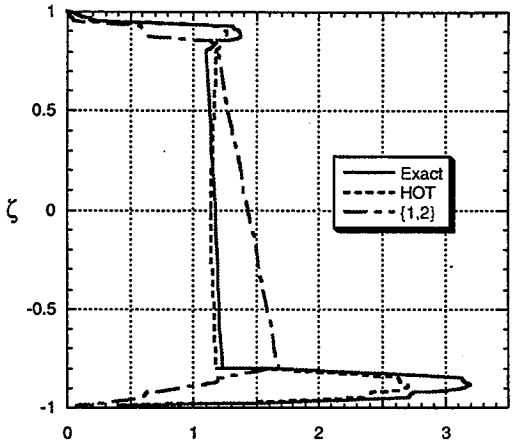

τ_{xz} / q

Figure 4.21 Case F: Gr/Ep-PVC Unsymmetric Sandwich , L/2h = 4

5. Guidelines for Finite Element Approximations

To enable the use of the present {3,2} theory on a wider range of applications, finite element approximations of the theory need to be undertaken. Tessler (1991) developed a computationally attractive two-node beam finite element based on the {1,2}-order theory. This element has the same number of degrees of freedom (dof) as a comparable Timoshenko beam element, yet is capable of recovering higher-order displacement and stress distributions through the thickness. While Timoshenko theory only accounts for transverse shear deformation, the {1,2}-theory element captures both the transverse shear and transverse normal deformations without any additional computational cost. The higher-order displacements w_1 and w_2 are statically condensed out at the element equilibrium level, leaving only u, θ, and w as kinematic degrees of freedom. Thus, the resulting element has only 6 dof, 3 dof for each node.

It is noted that thick composite and sandwich structures usually exhibit nonlinear axial displacement, strain, and stress distributions. For such structures, application of finite elements derived from the {1,2} theory may result in somewhat inadequate predictions. Instead, finite elements based upon the {3,2} theory can be used to model regions where the beam is particularly thick. This will allow the higher-order stress effects to be accurately modeled while keeping the simplicity of the beam element. Also, the basic kinematic variables u, θ, and w in the {3,2} theory are have the same physical meaning as in the {1,2} theory, ensuring proper compatibility between the elements.

Examining the highest order derivatives of the kinematic variables in the variational statement (2.31), necessary continuity requirements for the kinematic variables can be established (Hughes, 1987). While the shape functions within the finite element are always required to be continuous, the shape functions at the element interfaces, i.e. nodes, must satisfy minimum continuity requirements. For the kinematic variables which appear as first derivatives in the variational statement, i.e. $u_{,x}$ and $\theta_{,x}$, the shape functions must

be C^0 continuous, meaning they must be continuous at the element nodes. For kinematic variables which appear as second derivatives in the variational statement, i.e. $w_{,xx}$, $w_{1,xx}$, and $w_{2,xx}$, the shape functions must be C^1 continuous. This implies that both the function itself and its first derivative must be continuous. To accomplish this, degrees of freedom at each node must be associated with the variables:

$$u,\ \theta,\ w,\ w_1,\ \text{and}\ w_2$$

$$w_{,x},\ w_{1,x},\ \text{and}\ w_{2,x}$$

The {1,2} theory enables the w_1 and w_2 higher-order variables to be condensed out at the equilibrium equation level, thus defining w_1 and w_2 in terms of u and θ, respectively. Since only u, θ, and w need to be computed at each node, this allows for a simple, two-node, 6 dof element. A two-node element based on the present {3,2} theory will have 16 dof, 8 dof at each node, and the number of degrees of freedom cannot be reduced.

Considering a relatively large number of dof for a {3,2}-order beam finite element, a global-local computational strategy can be invoked. For example, the {1,2} beam elements would be sufficient to model the majority of beams, whereas the {3,2} elements would be used locally in thick regions of a beam where nonlinear effects are present. An example of this global-local modeling strategy would be a tapered laminated beam where the thickness increases linearly along the span. Figure 5.1 demonstrates the modeling of such a beam using both {1,2} and {3,2} elements.

It is noted that, as in the {3,2} analytic theory, the transverse shear and transverse normal correction factors are inherently present in the element stiffness matrix. Since the correction factors are only dependent on the material system, one set of factors is needed for the material layup used in the analysis. As previously discussed, the cylindrical bending problem provides a convenient means of computing the correction factors. The associated calculations are easily automated and computationally very efficient.

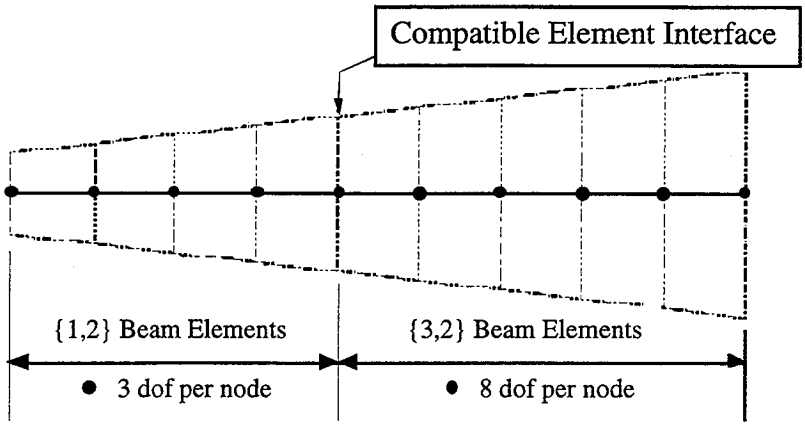

Figure 5.1 Finite Element Model of a Tapered Beam

6. Conclusions and Recommendations

A higher-order bending theory for laminated composite and sandwich beams has been successfully developed. Using a special cubic distribution for the axial displacement, the {1,2} theory has been extended to include higher-order axial effects without introducing additional kinematic variables. A special quadratic form of the transverse displacement is assumed such that the traction-free shear stress boundary conditions on the surface of the beam are satisfied. An independent expansion is also assumed for the transverse normal stress, notably improving the transverse strain and stress predictive capability of the theory. Appropriate shear correction factors have been used to adjust the shear stiffness based on energy considerations, thereby improving the transverse displacement response. A unique implementation of transverse correction factors has led to significant improvements in the transverse stretch response for laminated composite and sandwich beams. Accurate shear stresses for a wide range of laminates, including the challenging unsymmetric laminates and sandwich composites, have been obtained using an original integration scheme, which corrects for errors introduced due stretching of the midplane. A closed-form solution to the cylindrical bending problem has been derived, demonstrating excellent correlation to elasticity solutions for a wide range of beam aspect ratios and commonly used material systems. Results show that the axial response for thick sandwich beams has been improved over the {1,2} theory. To enable the use of the present {3,2} theory on a wider range of applications, guidelines for finite element approximations have been presented.

There are several possibilities for future work based on this theory. First, a straightforward extension of the present theory to plate theory should be possible, thereby enabling the analysis of laminated composite and sandwich plates. Second, a finite element formulation could be implemented to assess the accuracy of {3,2}-order beam elements. Although the kinematics of the {3,2} theory would require more nodal degrees of freedom than traditional finite elements, the higher-order beam elements may

provide improved accuracy previously attained only by complex three-dimensional finite elements.

Since the analytical theory and corresponding finite element approximation are more complex than the those of the {1,2} theory, it may be possible to employ a more efficient computational strategy while retaining the accuracy of the {3,2} theory. One possibility would be to determine the five kinematic variables from the {1,2} theory and then substitute these variables into the {3,2} equations to obtain displacement, strain, and stress distributions. Since the kinematic variables have the same meaning in each theory, these variables should be comparable in magnitude. This concept has been proposed by Tessler (1993b) with promising results for thick laminates, demonstrating significant improvement in the predictive capability of the {1,2} theory using the {3,2}-order recovery.

Acknowledgments

The author would like to thank foremost Dr. Alexander Tessler of the Computational Structures Branch, NASA Langley Research Center, for his direction and guidance during this research. His expertise and patience are greatly appreciated. Also deserving of recognition are: Dr. W. S. Burton, Center for Computational Structures Technology, University of Virginia, for providing sandwich material properties and the code for the elasticity solutions presented herein, Dr. A. R. Johnson, Army Research Laboratory, for his mathematical insight and suggestions, Dr. R. H. Tolson and the GWU/JIAFS personnel for their assistance, and the Computational Structures Branch at NASA Langley for supporting this research.

References

Burton, W. S., and Noor, A. K., 1994, "Three-Dimensional Solutions for Thermomechanical Stresses in Sandwich Panels and Shells," *Journal of Engineering Mechanics*, Vol. 120, No. 10, pp. 2044-2071.

Essenburg, F., 1975, "On the Significance of the Inclusion of the Effect of Transverse Normal Strain in Problems Involving Beams With Surface Constraints," *Journal of Applied Mechanics*, Vol. 42, pp. 127-132.

Hughes, T. J. R.,1987, *The Finite Element Method. Linear Static and Dynamic Finite Element Analysis*, Prentice-Hall, Englewood Cliffs, NJ.

Lo, K.H., Christensen, R. M., and Wu, E. M., 1977, "A Higher-Order Theory of Plate Deformation: Part 1. Homogeneous Plates; Part 2. Laminated Plates," *ASME Journal of Applied Mechanics*, Vol. 44, pp. 663-676.

Love, A. E. H., 1952, *A Treatise on the Mathematical Theory of Elasticity*, 4th ed., Cambridge University Press, Cambridge, England.

Mindlin, R. D., 1951, "Influence of Rotary Inertia and Shear on Flexural Motions of Isotropic, Elastic Plates," *Journal of Applied Mechanics*, Vol. 18, No. 1, pp. 31-38.

Mindlin, R. D., and Medick, M. A., 1958, "Extensional Vibrations of Elastic Plates," ONR Project NR-064-388, Technical Report No. 28.

Noor, A. K., and Burton, W. S., 1989, "Assessment of Shear Deformable Theories for Multilayered Composite Plates," *Applied Mechanics Review*, Vol. 42, pp. 1-12.

Pagano, N. J., 1969, "Exact Solutions for Composite Laminates in Cylindrical Bending," *Journal of Composite Materials*, Vol. 3, pp. 398-411.

Phan, N. D., and Reddy, J. N., 1985, "Analysis of Laminated Composite Plates Using a Higher-Order Shear Deformation Theory," *International Journal for Numerical Methods in Engineering*, Vol. 21, pp. 2201-2219.

Reddy, J. N., 1984, "A Simple Higher-Order Theory for Laminated Composite Plates," *Journal of Applied Mechanics*, Vol. 51, pp. 745-752.

Reddy, J. N., 1989, "On Refined Computational Models of Composite Laminates," *International Journal for Numerical Methods in Engineering*, Vol. 27, pp. 361-382.

Reddy, J. N., and Liu, C. F., 1987, "A Higher-Order Theory for Geometrically Nonlinear Analysis of Composite Laminates," NASA Contractor Report 4056.

Reissner, E., 1945, "The Effect of Transverse Shear Deformation on the Bending of Elastic Plates," *Journal of Applied Mechanics*, Vol. 12, No. 2, pp. A-69-77.

Reissner, E., 1985, "Reflections on the Theory of Elastic Plates," *Applied Mechanics Review*, Vol. 38, No. 11.

Schleicher, C. C., 1994, "Transverse Stress Effects for Laminated Composite Beams in Bending," Master's Report, Old Dominion University.

Stavsky, Y., 1959, "On the Theory of Heterogeneous Anisotropic Plates," Doctor's Report, M.I.T. Cambridge, Mass.

Tessler, A., 1991, "A Two-Node Beam Element Including Transverse Shear and Transverse Normal Deformations," *International Journal for Numerical Methods in Engineering*, 32, pp.1027-1039.

Tessler, A., 1993a, "An Improved Plate Theory of {1,2} Order for Thick Composite Laminates," *International Journal of Solids and Structures*, Vol. 30, No. 7, pp. 981-1000.

Tessler, A., 1993b, "Strain and Stress Computations in Thick Laminated Plates using Hierarchical Higher-Order Kinematics," Proceedings of the Second U.S. National Congress on Computational Mechanics, Washington, D.C., August 16-18.

Tessler, A., 1995, "Vibration of Thick Laminated Composite Plates," *Journal of Sound and Vibration*, Vol. 179, pp. 475-498.

Tessler, A., and Saether, E., 1991, "A Computationally Viable Higher-Order Theory for Laminated Composite Plates," *International Journal for Numerical Methods in Engineering*, Vol. 31, pp. 1069-1086.

Timoshenko, S. P., 1921, "On the Correction for Shear of the Differential Equation of Transverse Vibrations of Prismatic Bars," *Philosophical Magazine*, Vol. 41, pp. 744-746.

Timoshenko, S. P., 1934, *Theory of Elasticity*, First Edition, McGraw-Hill, pp. 32-42.

Whitney, J. M., 1972, "Stress Analysis of Thick Laminated Composite and Sandwich Plates," *Journal of Composite Materials*, Vol. 6, pp. 426-440.

Whitney, J. M., 1973, "Shear Correction Factors for Orthotropic Laminates Under Static Load," *Journal of Applied Mechanics*, Vol. 40, pp. 302-304.

Whitney, J. M., and Pagano, N. J., 1970, "Shear Deformation in Heterogeneous Anisotropic Plates," *Journal of Applied Mechanics*, pp. 1031-1036.

Whitney, J. M., and Sun, C. T., 1974, "A Refined Theory for Laminated Anisotropic, Cylindrical Shells," *Journal of Applied Mechanics*, Vol. 41, No. 2, pp. 471-476.

Vlachoutsis, S., 1992, "Shear Correction Factors for Plates and Shells," *International Journal for Numerical Methods in Engineering*, Vol. 33, pp. 1537-1552.

Yang, P. C., Norris, C. H., and Stavsky, Y., 1966, "Elastic Wave Propagation in Heterogeneous Plates," *International Journal of Solids and Structures*, Vol. 2, pp. 665-684.

Zenkert, D., 1995, *An Introduction to Sandwich Construction*, Engineering Materials Advisory Services, Ltd., pp. 22-24.

Appendix A: Transverse Normal Strain Coefficients

The shape functions for the transverse normal strain defined in equation (2.29) are defined as

$$\psi_1^{(k)} = \overline{S}_{33}^{(k)}\left(P_1 - R_1\phi_5 - \overline{C}_{13}^{(k)}\right) \qquad \psi_4^{(k)} = \overline{S}_{33}^{(k)}\left(P_4 - R_4\phi_5 - \overline{C}_{13}^{(k)}\phi_1\right)$$

$$\psi_2^{(k)} = \overline{S}_{33}^{(k)}\left(P_2 - R_2\phi_5\right) \qquad \psi_5^{(k)} = \overline{S}_{33}^{(k)}\left(P_5 - R_5\phi_5\right) \qquad \text{(A1)}$$

$$\psi_3^{(k)} = \overline{S}_{33}^{(k)}\left(P_3 - R_3\phi_5 - \overline{C}_{13}^{(k)}\phi_2\right) \qquad \psi_6^{(k)} = \overline{S}_{33}^{(k)}\left(P_6 - R_6\phi_5 - \overline{C}_{13}^{(k)}\phi_3\right)$$

where $\overline{S}_{33}^{(k)} = 1/\overline{C}_{33}^{(k)}$ and the constants P_i and R_i are defined as

$$P_i = \frac{p_8\left(p_7 r_i - p_i r_7\right)}{p_7\left(p_7 r_8 - p_8 r_7\right)} - \frac{p_i}{p_7} \qquad (i = 1,2,\ldots 6) \qquad \text{(A2)}$$

$$R_i = \frac{\left(p_7 r_i - p_i r_7\right)}{\left(p_7 r_8 - p_8 r_7\right)}$$

with the constants p_i defined as

$$p_1 = \sum_{k=1}^{N}\int_{h_{k-1}}^{h_k} \frac{-\overline{C}_{13}^{(k)}}{\overline{C}_{33}^{(k)^2}}dz, \qquad p_2 = \sum_{k=1}^{N}\int_{h_{k-1}}^{h_k} \frac{-1}{\overline{C}_{33}^{(k)}}dz,$$

$$p_3 = \sum_{k=1}^{N}\int_{h_{k-1}}^{h_k} \frac{-\overline{C}_{13}^{(k)}\phi_2}{\overline{C}_{33}^{(k)^2}}dz, \qquad p_4 = \sum_{k=1}^{N}\int_{h_{k-1}}^{h_k} \frac{-\overline{C}_{13}^{(k)}\phi_1}{\overline{C}_{33}^{(k)^2}}dz,$$

$$p_5 = \sum_{k=1}^{N} \int_{h_{k-1}}^{h_k} \frac{-2\phi_1}{\overline{C}_{33}^{(k)^2}} dz, \qquad p_6 = \sum_{k=1}^{N} \int_{h_{k-1}}^{h_k} \frac{-\overline{C}_{13}^{(k)} \phi_3}{\overline{C}_{33}^{(k)^2}} dz,$$

$$p_7 = \sum_{k=1}^{N} \int_{h_{k-1}}^{h_k} \frac{1}{\overline{C}_{33}^{(k)^2}} dz, \qquad p_8 = \sum_{k=1}^{N} \int_{h_{k-1}}^{h_k} \frac{\phi_5}{\overline{C}_{33}^{(k)^2}} dz \qquad \text{(A3)}$$

and the r_i constants are

$$r_1 = \sum_{k=1}^{N} \int_{h_{k-1}}^{h_k} \frac{-\overline{C}_{13}^{(k)} \phi_5}{\overline{C}_{33}^{(k)^2}} dz, \qquad r_2 = \sum_{k=1}^{N} \int_{h_{k-1}}^{h_k} \frac{-\phi_5}{\overline{C}_{33}^{(k)}} dz,$$

$$r_3 = \sum_{k=1}^{N} \int_{h_{k-1}}^{h_k} \frac{-\overline{C}_{13}^{(k)} \phi_2 \phi_5}{\overline{C}_{33}^{(k)^2}} dz, \qquad r_4 = \sum_{k=1}^{N} \int_{h_{k-1}}^{h_k} \frac{-\overline{C}_{13}^{(k)} \phi_1 \phi_5}{\overline{C}_{33}^{(k)^2}} dz,$$

$$r_5 = \sum_{k=1}^{N} \int_{h_{k-1}}^{h_k} \frac{-2\phi_1 \phi_5}{\overline{C}_{33}^{(k)^2}} dz, \qquad r_6 = \sum_{k=1}^{N} \int_{h_{k-1}}^{h_k} \frac{-\overline{C}_{13}^{(k)} \phi_3 \phi_5}{\overline{C}_{33}^{(k)^2}} dz, \qquad \text{(A3)}$$

$$r_7 = \sum_{k=1}^{N} \int_{h_{k-1}}^{h_k} \frac{\phi_5}{\overline{C}_{33}^{(k)^2}} dz, \qquad r_8 = \sum_{k=1}^{N} \int_{h_{k-1}}^{h_k} \frac{\phi_5^2}{\overline{C}_{33}^{(k)^2}} dz$$

Appendix B: Stress Resultants and Prescribed Tractions

Beam Stress Resultants:

$$N_x = b\sum_{k=1}^{N}\int_{h_{k-1}}^{h_k}\left(\sigma_{xx}^{(k)} + \sigma_{zz}\psi_1^{(k)}\right)dz \qquad M_x = b\sum_{k=1}^{N}\int_{h_{k-1}}^{h_k}\left(\sigma_{xx}^{(k)}\phi_1 + \sigma_{zz}\psi_4^{(k)}\right)dz$$

$$N_z = b\,k_{z0}\sum_{k=1}^{N}\int_{h_{k-1}}^{h_k}\left(\sigma_{zz}\psi_2^{(k)}\right)dz \qquad M_z = b\,k_{z1}\sum_{k=1}^{N}\int_{h_{k-1}}^{h_k}\left(\sigma_{zz}\psi_5^{(k)}\right)dz$$

$$N_H = b\sum_{k=1}^{N}\int_{h_{k-1}}^{h_k}\left(\sigma_{xx}^{(k)}\phi_2 + \sigma_{zz}\psi_3^{(k)}\right)dz \qquad M_H = b\sum_{k=1}^{N}\int_{h_{k-1}}^{h_k}\left(\sigma_{xx}^{(k)}\phi_3 + \sigma_{zz}\psi_6^{(k)}\right)dz$$

$$Q_x = b\sum_{k=1}^{N}\int_{h_{k-1}}^{h_k}\left(\tau_{xz}^{(k)}\phi_{xz}\right)dz \qquad \text{(B1)}$$

Prescribed Stress Resultants at Ends of Beam (@ x=0 & x=L) :

$$\overline{N}_{x0} = b\sum_{k=1}^{N}\int_{h_{k-1}}^{h_k}\left(T_{x0}\right)dz \qquad \overline{N}_{xL} = b\sum_{k=1}^{N}\int_{h_{k-1}}^{h_k}\left(T_{xL}\right)dz$$

$$\overline{M}_{x0} = b\sum_{k=1}^{N}\int_{h_{k-1}}^{h_k}\left(T_{x0}\,z\right)dz \qquad \overline{M}_{xL} = b\sum_{k=1}^{N}\int_{h_{k-1}}^{h_k}\left(T_{xL}\,z\right)dz$$

$$\overline{M}_{10} = b\,h\sum_{k=1}^{N}\int_{h_{k-1}}^{h_k}\left(T_{x0}\phi_2\right)dz \qquad \overline{M}_{1L} = bh\sum_{k=1}^{N}\int_{h_{k-1}}^{h_k}\left(T_{xL}\phi_2\right)dz$$

$$\overline{M}_{20} = b\sum_{k=1}^{N}\int_{h_{k-1}}^{h_k}\left(T_{x0}\phi_3\right)dz \qquad \overline{M}_{2L} = b\sum_{k=1}^{N}\int_{h_{k-1}}^{h_k}\left(T_{xL}\phi_3\right)dz$$

$$\overline{Q}_{x0} = b\sum_{k=1}^{N}\int_{h_{k-1}}^{h_k}\left(T_{z0}\right)dz \qquad \overline{Q}_{xL} = b\sum_{k=1}^{N}\int_{h_{k-1}}^{h_k}\left(T_{zL}\right)dz$$

$$\overline{Q}_{10} = b\sum_{k=1}^{N}\int_{h_{k-1}}^{h_k}\left(T_{z0}\,\zeta\right)dz \qquad \overline{Q}_{1L} = b\sum_{k=1}^{N}\int_{h_{k-1}}^{h_k}\left(T_{zL}\,\zeta\right)dz$$

$$\overline{Q}_{20} = b\sum_{k=1}^{N}\int_{h_{k-}}^{h_k} T_{z0}\left(\zeta^2 - \tfrac{1}{3}\right)dz \qquad \overline{Q}_{2L} = b\sum_{k=1}^{N}\int_{h_{k-}}^{h_k} T_{zL}\left(\zeta^2 - \tfrac{1}{3}\right)dz \qquad \text{(B2)}$$

Appendix C: Stiffness Coefficients for Beam Constitutive Matrix

A_{ij} Stiffness Coefficients:

$$A_{11} = b\sum_{k=1}^{N}\int_{h_{k-1}}^{h_k}\left(\overline{C}_{11}^{(k)} + 2\,\overline{C}_{13}^{(k)}\psi_1^{(k)} + \overline{C}_{33}^{(k)}\psi_1^{(k)^2}\right)dz$$

$$A_{12} = b\sum_{k=1}^{N}\int_{h_{k-1}}^{h_k}\left(\overline{C}_{13}^{(k)}\psi_2^{(k)} + \overline{C}_{33}^{(k)}\psi_1^{(k)}\psi_2^{(k)}\right)dz$$

$$A_{13} = b\sum_{k=1}^{N}\int_{h_{k-1}}^{h_k}\left(\overline{C}_{11}^{(k)}\phi_2 + \overline{C}_{13}^{(k)}\phi_2\psi_1^{(k)} + \overline{C}_{13}^{(k)}\psi_3^{(k)} + \overline{C}_{33}^{(k)}\psi_1^{(k)}\psi_3^{(k)}\right)dz$$

$$A_{22} = b\sum_{k=1}^{N}\int_{h_{k-1}}^{h_k}\left(\overline{C}_{33}^{(k)}\psi_2^{(k)^2}\right)dz$$

$$A_{23} = b\sum_{k=1}^{N}\int_{h_{k-1}}^{h_k}\left(\overline{C}_{13}^{(k)}\phi_2\psi_2^{(k)} + \overline{C}_{33}^{(k)}\psi_2^{(k)}\psi_3^{(k)}\right)dz \qquad \text{(C1)}$$

$$A_{33} = b\sum_{k=1}^{N}\int_{h_{k-1}}^{h_k}\left(\overline{C}_{11}^{(k)}\phi_2^2 + 2\,\overline{C}_{13}^{(k)}\phi_2\psi_3^{(k)} + \overline{C}_{33}^{(k)}\psi_3^{(k)^2}\right)dz$$

B_{ij} Stiffness Coefficients:

$$B_{11} = b\sum_{k=1}^{N}\int_{h_{k-1}}^{h_k}\left(\overline{C}_{11}^{(k)}\phi_1 + \overline{C}_{13}^{(k)}\phi_1\psi_1^{(k)} + \overline{C}_{13}^{(k)}\psi_4^{(k)} + \overline{C}_{33}^{(k)}\psi_1^{(k)}\psi_4^{(k)}\right)dz$$

$$B_{12} = b\sum_{k=1}^{N}\int_{h_{k-1}}^{h_k}\left(\overline{C}_{13}^{(k)}\psi_5^{(k)} + \overline{C}_{33}^{(k)}\psi_1^{(k)}\psi_5^{(k)}\right)dz$$

$$B_{13} = b\sum_{k=1}^{N}\int_{h_{k-1}}^{h_k}\left(\overline{C}_{11}^{(k)}\phi_3 + \overline{C}_{13}^{(k)}\phi_3\psi_1^{(k)} + \overline{C}_{13}^{(k)}\psi_6^{(k)} + \overline{C}_{33}^{(k)}\psi_1^{(k)}\psi_6^{(k)}\right)dz$$

$$B_{21} = b\sum_{k=1}^{N}\int_{h_{k-1}}^{h_k}\left(\overline{C}_{13}^{(k)}\phi_1\psi_2^{(k)} + \overline{C}_{33}^{(k)}\psi_2^{(k)}\psi_4^{(k)}\right)dz$$

$$B_{22} = b\sum_{k=1}^{N}\int_{h_{k-1}}^{h_k}\left(\overline{C}_{33}^{(k)}\psi_2^{(k)}\psi_5^{(k)}\right)dz$$

$$B_{23} = b\sum_{k=1}^{N}\int_{h_{k-1}}^{h_k}\left(\overline{C}_{13}^{(k)}\phi_3\psi_2^{(k)} + \overline{C}_{33}^{(k)}\psi_2^{(k)}\psi_6^{(k)}\right)dz$$

$$B_{31} = b\sum_{k=1}^{N}\int_{h_{k-1}}^{h_k}\left(\overline{C}_{11}^{(k)}\phi_1\phi_2 + \overline{C}_{13}^{(k)}\phi_1\psi_3^{(k)} + \overline{C}_{13}^{(k)}\phi_2\psi_4^{(k)} + \overline{C}_{33}^{(k)}\psi_3^{(k)}\psi_4^{(k)}\right)dz$$

$$B_{32} = b\sum_{k=1}^{N}\int_{h_{k-1}}^{h_k}\left(\overline{C}_{13}^{(k)}\phi_2\psi_5^{(k)} + \overline{C}_{33}^{(k)}\psi_3^{(k)}\psi_5^{(k)}\right)dz \qquad \text{(C2)}$$

$$B_{33} = b\sum_{k=1}^{N}\int_{h_{k-1}}^{h_k}\left(\overline{C}_{11}^{(k)}\phi_2\phi_3 + \overline{C}_{13}^{(k)}\phi_3\psi_3^{(k)} + \overline{C}_{13}^{(k)}\phi_2\psi_6^{(k)} + \overline{C}_{33}^{(k)}\psi_3^{(k)}\psi_6^{(k)}\right)dz$$

D_{ij} Stiffness Coefficients:

$$D_{11} = b\sum_{k=1}^{N}\int_{h_{k-1}}^{h_k}\left(\overline{C}_{11}^{(k)}\phi_1^2 + 2\,\overline{C}_{13}^{(k)}\phi_1\psi_4^{(k)} + \overline{C}_{33}^{(k)}\psi_4^{(k)^2}\right)dz$$

$$D_{12} = b\sum_{k=1}^{N}\int_{h_{k-1}}^{h_k}\left(\overline{C}_{13}^{(k)}\phi_1\psi_5^{(k)} + \overline{C}_{33}^{(k)}\psi_4^{(k)}\psi_5^{(k)}\right)dz$$

$$D_{13} = b\sum_{k=1}^{N}\int_{h_{k-1}}^{h_k}\left(\overline{C}_{11}^{(k)}\phi_1\phi_3 + \overline{C}_{13}^{(k)}\phi_3\psi_4^{(k)} + \overline{C}_{13}^{(k)}\phi_1\psi_6^{(k)} + \overline{C}_{33}^{(k)}\psi_4^{(k)}\psi_6^{(k)}\right)dz$$

$$D_{22} = b\sum_{k=1}^{N}\int_{h_{k-1}}^{h_k}\left(\overline{C}_{33}^{(k)}\psi_5^{(k)^2}\right)dz$$

$$D_{23} = b\sum_{k=1}^{N}\int_{h_{k-1}}^{h_k}\left(\overline{C}_{13}^{(k)}\phi_3\psi_5^{(k)} + \overline{C}_{33}^{(k)}\psi_5^{(k)}\psi_6^{(k)}\right)dz \qquad \text{(C3)}$$

$$D_{33} = b\sum_{k=1}^{N}\int_{h_{k-1}}^{h_k}\left(\overline{C}_{11}^{(k)}\psi_3^{(k)^2} + 2\,\overline{C}_{13}^{(k)}\phi_3\psi_6^{(k)} + \overline{C}_{33}^{(k)}\psi_6^{(k)^2}\right)dz$$

G Stiffness Coefficient:

$$G = b\sum_{k=1}^{N}\int_{h_{k-1}}^{h_k}\left(\overline{C}_{55}^{(k)}\phi_{xz}^2\right)dz \qquad \text{(C4)}$$

Appendix D: Derivation of Constitutive Relations

The stress-strain relations for a two-dimensional stress state are developed for plane strain and plane stress in the x-z plane (refer to coordinate system in Figure 2.1). Both constitutive relations are derived from the general three-dimensional state of stress and strain for an orthotropic ply. The constitutive relations for the k^{th} ply of a laminated orthotropic solid are defined as

$$\begin{Bmatrix} \varepsilon_1 \\ \varepsilon_2 \\ \varepsilon_3 \\ \gamma_{23} \\ \gamma_{13} \\ \gamma_{12} \end{Bmatrix}_m^{(k)} = \begin{bmatrix} S_{11} & S_{12} & S_{13} & 0 & 0 & 0 \\ S_{12} & S_{22} & S_{23} & 0 & 0 & 0 \\ S_{13} & S_{23} & S_{33} & 0 & 0 & 0 \\ 0 & 0 & 0 & S_{44} & 0 & 0 \\ 0 & 0 & 0 & 0 & S_{55} & 0 \\ 0 & 0 & 0 & 0 & 0 & S_{66} \end{bmatrix}_m^{(k)} \begin{Bmatrix} \sigma_1 \\ \sigma_2 \\ \sigma_3 \\ \tau_{23} \\ \tau_{13} \\ \tau_{12} \end{Bmatrix}_m^{(k)} \tag{D1}$$

which in condensed form are

$$\{\varepsilon_m\}^{(k)} = [S_m]^{(k)} \{\sigma_m\}^{(k)}$$

where the (k) superscript implies that the quantity is a function of the k^{th} ply; $[S_m]$ is the conventional orthotropic compliance matrix, and the m subscript identifies the lamina axes in the material coordinate system. The vectors $\{\sigma_m\}$ and $\{\varepsilon_m\}$ contain stresses and strains defined in the material reference frame.

The orthotropic plies of a laminated composite or sandwich may be of arbitrary orientation in the x-y plane of the beam. Since the constitutive relations are given with respect to the material coordinate system, the properties must be transformed into the beam coordinate system. The following matrices define the stress and strain transformations:

$$[T_\sigma]=\begin{bmatrix} c^2 & s^2 & 0 & 0 & 0 & 2cs \\ s^2 & c^2 & 0 & 0 & 0 & -2cs \\ 0 & 0 & 1 & 0 & 0 & 0 \\ 0 & 0 & 0 & c & -s & 0 \\ 0 & 0 & 0 & s & c & 0 \\ -cs & cs & 0 & 0 & 0 & c^2-s^2 \end{bmatrix} \quad , \quad [T_\varepsilon]=\begin{bmatrix} c^2 & s^2 & 0 & 0 & 0 & cs \\ s^2 & c^2 & 0 & 0 & 0 & -cs \\ 0 & 0 & 1 & 0 & 0 & 0 \\ 0 & 0 & 0 & c & -s & 0 \\ 0 & 0 & 0 & s & c & 0 \\ -2cs & 2cs & 0 & 0 & 0 & c^2-s^2 \end{bmatrix} \tag{D2}$$

with

$$c = \cos\beta \ , \quad s = \sin\beta$$

where β denotes the angle between the principal material direction of the ply and the x coordinate, as depicted in Figure D.1.

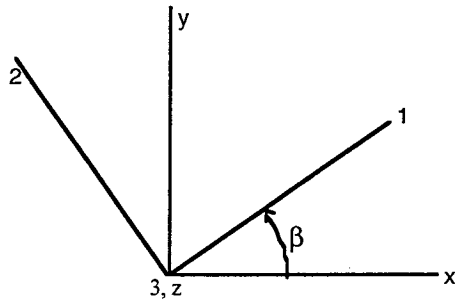

Figure D.1 Beam and Material Coordinate Frames

The stress and strain quantities for the material reference frame are expressed in terms of the global (x-y coordinate) stresses and strains using the transformation matrices defined in (D2):

$$\{\sigma_m\}^{(k)}=[T_\sigma]\{\sigma_g\}^{(k)} \ , \qquad \{\varepsilon_m\}^{(k)}=[T_\varepsilon]\{\varepsilon_g\}^{(k)} \tag{D3}$$

where the g subscript identifies quantities defined in the global coordinate system. The equations (D3) are substituted into (D1) to yield

$$[T_\varepsilon]\{\varepsilon_g\}^{(k)} = [S_m]^{(k)}[T_\sigma]\{\sigma_g\}^{(k)} \tag{D4}$$

Pre multiplication of both sides of the equation by the inverse of the strain transformation matrix results in the form

$$\{\varepsilon_g\}^{(k)} = [S_g]^{(k)}\{\sigma_g\}^{(k)} \tag{D5}$$

with the transformed compliance matrix defined as

$$[S_g]^{(k)} = [T_\varepsilon]^{-1}[S_m]^{(k)}[T_\sigma] \tag{D6}$$

Expressing equation (D5) in expanded form yields the transformed three-dimensional strain-stress relations in terms of global quantities:

$$\begin{Bmatrix} \varepsilon_x \\ \varepsilon_y \\ \varepsilon_z \\ \gamma_{yz} \\ \gamma_{xz} \\ \gamma_{xy} \end{Bmatrix}_g^{(k)} = \begin{bmatrix} S_{11} & S_{12} & S_{13} & 0 & 0 & S_{16} \\ S_{12} & S_{22} & S_{23} & 0 & 0 & S_{26} \\ S_{13} & S_{23} & S_{33} & 0 & 0 & S_{36} \\ 0 & 0 & 0 & S_{44} & S_{45} & 0 \\ 0 & 0 & 0 & S_{45} & S_{55} & 0 \\ S_{16} & S_{26} & S_{36} & 0 & 0 & S_{66} \end{bmatrix}_g^{(k)} \begin{Bmatrix} \sigma_x \\ \sigma_y \\ \sigma_z \\ \tau_{yz} \\ \tau_{xz} \\ \tau_{xy} \end{Bmatrix}_g^{(k)} \tag{D7}$$

Although the same notation is used, the S_{ij} coefficients shown in (D7) are not the same as those in (D1). The coefficients from equation (D7) are derived from the transformed compliance matrix defined in (D6) and are not expanded individually for this discussion.

Pre multiplication of equation (D7) by $[S_g]^{(k)^{-1}} = [C_g]^{(k)}$ results in the three-dimensional stress-strain relations:

$$\begin{Bmatrix} \sigma_x \\ \sigma_y \\ \sigma_z \\ \tau_{yz} \\ \tau_{xz} \\ \tau_{xy} \end{Bmatrix}^{(k)} = \begin{bmatrix} C_{11} & C_{12} & C_{13} & 0 & 0 & C_{16} \\ C_{12} & C_{22} & C_{23} & 0 & 0 & C_{26} \\ C_{13} & C_{23} & C_{33} & 0 & 0 & C_{36} \\ 0 & 0 & 0 & C_{44} & C_{45} & 0 \\ 0 & 0 & 0 & C_{45} & C_{55} & 0 \\ C_{16} & C_{26} & C_{36} & 0 & 0 & C_{66} \end{bmatrix}_g^{(k)} \begin{Bmatrix} \varepsilon_x \\ \varepsilon_y \\ \varepsilon_z \\ \gamma_{yz} \\ \gamma_{xz} \\ \gamma_{xy} \end{Bmatrix}^{(k)} \tag{D8}$$

where the stiffness matrix is defined as

$$[C_g]^{(k)} = [T_\sigma]^{-1} [C_m]^{(k)} [T_\varepsilon] \tag{D9}$$

Plane Strain

For the case of plane strain in the x-z plane, the strain components ε_y, γ_{yz}, and γ_{xy} are assumed to be negligible. By setting these strains equal to zero and solving equations (D7) simultaneously, the reduced constitutive relations for plane strain become

$$\begin{Bmatrix} \varepsilon_x \\ \varepsilon_z \\ \gamma_{xz} \end{Bmatrix}^{(k)} = \begin{bmatrix} \hat{S}_{11} & \hat{S}_{13} & 0 \\ \hat{S}_{13} & \hat{S}_{33} & 0 \\ 0 & 0 & \hat{S}_{55} \end{bmatrix}_g^{(k)} \begin{Bmatrix} \sigma_x \\ \sigma_z \\ \tau_{xz} \end{Bmatrix}^{(k)} \tag{D10}$$

where

$$\hat{S}_{11} = \frac{2S_{12}S_{16}S_{26} - S_{16}^{2}S_{22} - S_{11}S_{26}^{2} - S_{12}^{2}S_{66} + S_{11}S_{22}S_{66}}{S_{22}S_{66} - S_{26}^{2}}$$

$$\hat{S}_{13} = \frac{S_{16}S_{23}S_{26} - S_{26}^{2}S_{13} - S_{16}S_{22}S_{36} + S_{12}S_{26}S_{36} + S_{13}S_{22}S_{66} - S_{12}S_{23}S_{66}}{S_{22}S_{66} - S_{26}^{2}} \qquad \text{(D11)}$$

$$\hat{S}_{33} = \frac{2S_{23}S_{26}S_{36} - S_{26}^{2}S_{33} - S_{22}S_{36}^{2} - S_{23}^{2}S_{66} + S_{33}S_{22}S_{66}}{S_{22}S_{66} - S_{26}^{2}}$$

$$\hat{S}_{55} = S_{55} - \frac{S_{45}^{2}}{S_{44}}$$

The plane strain constitutive relations can be inverted to yield the stress-strain relations:

$$\begin{Bmatrix} \sigma_{xx} \\ \sigma_{zz} \\ \tau_{xz} \end{Bmatrix}_{g}^{(k)} = \begin{bmatrix} \hat{C}_{11} & \hat{C}_{13} & 0 \\ \hat{C}_{13} & \hat{C}_{33} & 0 \\ 0 & 0 & \hat{C}_{55} \end{bmatrix}_{g}^{(k)} \begin{Bmatrix} \varepsilon_{xx} \\ \varepsilon_{zz} \\ \gamma_{xz} \end{Bmatrix}_{g}^{(k)} \qquad \text{(D12)}$$

where

$$\hat{C}_{11} = \frac{\hat{S}_{33}}{\hat{S}_{11}\hat{S}_{33} - \hat{S}_{13}^{2}}, \qquad \hat{C}_{13} = \frac{-\hat{S}_{13}}{\hat{S}_{11}\hat{S}_{33} - \hat{S}_{13}^{2}}$$

$$\hat{C}_{33} = \frac{\hat{S}_{11}}{\hat{S}_{11}\hat{S}_{33} - \hat{S}_{13}^{2}}, \qquad \hat{C}_{55} = \frac{1}{\hat{S}_{55}} \qquad \text{(D13)}$$

Plane Stress

For a state of plane stress in the x-z plane, the stress components σ_y, τ_{yz}, and τ_{xy} in equation (D8) are set equal to zero. Solving the equations in terms of the stress components associated with x and z yields the two-dimensional constitutive relations for plane stress:

$$\begin{Bmatrix}\sigma_x\\ \sigma_z\\ \tau_{xz}\end{Bmatrix}_g^{(k)} = \begin{bmatrix}\tilde{C}_{11} & \tilde{C}_{13} & 0\\ \tilde{C}_{13} & \tilde{C}_{33} & 0\\ 0 & 0 & \tilde{C}_{55}\end{bmatrix}_g^{(k)} \begin{Bmatrix}\varepsilon_x\\ \varepsilon_z\\ \gamma_{xz}\end{Bmatrix}_g^{(k)} \tag{D14}$$

where

$$\tilde{C}_{11} = \frac{2C_{12}C_{16}C_{26} - C_{16}^{\,2}C_{22} - C_{11}C_{26}^{\,2} - C_{12}^{\,2}C_{66} + C_{11}C_{22}C_{66}}{C_{22}C_{66} - C_{26}^{\,2}}$$

$$\tilde{C}_{13} = \frac{C_{16}C_{23}C_{26} - C_{26}^{\,2}C_{13} - C_{16}C_{22}C_{36} + C_{12}C_{26}C_{36} + C_{13}C_{22}C_{66} - C_{12}C_{23}C_{66}}{C_{22}C_{66} - C_{26}^{\,2}} \tag{D15}$$

$$\tilde{C}_{33} = \frac{2C_{23}C_{26}C_{36} - C_{26}^{\,2}C_{33} - C_{22}C_{36}^{\,2} - C_{23}^{\,2}C_{66} + C_{33}C_{22}C_{66}}{C_{22}C_{66} - C_{26}^{\,2}}$$

$$\tilde{C}_{55} = C_{55} - \frac{C_{45}^{\,2}}{C_{44}}$$

REPORT DOCUMENTATION PAGE

Form Approved
OMB No. 0704-0188

1. AGENCY USE ONLY *(Leave blank)*	2. REPORT DATE	3. REPORT TYPE AND DATES COVERED
	March 1997	Contractor Report

4. TITLE AND SUBTITLE
A Higher-Order Bending Theory for Laminated Composite and Sandwich Beams

5. FUNDING NUMBERS
NCC1-208
537-06-21-09

6. AUTHOR(S)
Geoffrey M. Cook

7. PERFORMING ORGANIZATION NAME(S) AND ADDRESS(ES)
George Washington University
Joint Institute for Advancement of Flight Sciences
Hampton, VA 23681-0001

8. PERFORMING ORGANIZATION REPORT NUMBER

9. SPONSORING / MONITORING AGENCY NAME(S) AND ADDRESS(ES)
National Aeronautics and Space Administration
Langley Research Center
Hampton, VA 23681-0001

10. SPONSORING / MONITORING AGENCY REPORT NUMBER
NASA CR-201674

11. SUPPLEMENTARY NOTES
Langley Technical Monitor: Alex Tessler

12a. DISTRIBUTION / AVAILABILITY STATEMENT
Unclassified-Unlimited
Subject Category 39

12b. DISTRIBUTION CODE

13. ABSTRACT ***(Maximum 200 words)***

A higher-order bending theory is derived for laminated composite and sandwich beams. This is accomplished by assuming a special form for the axial and transverse displacement expansions. An independent expansion is also assumed for the transverse normal stress. Appropriate shear correction factors based on energy considerations are used to adjust the shear stiffness. A set of transverse normal correction factors is introduced, leading to significant improvements in the transverse normal strain and stress for laminated composite and sandwich beams. A closed-form solution to the cylindrical elasticity solutions for a wide range of beam aspect ratios and commonly used material systems. Accurate shear stresses for a wide range of laminates, including the challenging unsymmetric composite and sandwich laminates, are obtained using an original corrected integration scheme. For application of the theory to a wider range of problems, guidelines for finite element approximations are presented.

14. SUBJECT TERMS
Beam Theory; Laminated Beams; Sandwich Beams; Correction Factors; Cylindrical Bending; Interlaminar Stresses; Finite Elements; Virtual Work

15. NUMBER OF PAGES
88

16. PRICE CODE
A05

17. SECURITY CLASSIFICATION OF REPORT	18. SECURITY CLASSIFICATION OF THIS PAGE	19. SECURITY CLASSIFICATION OF ABSTRACT	20. LIMITATION OF ABSTRACT
Unclassified	Unclassified	Unclassified	Unlimited